Mechanistic Studies in Copper Catalysis

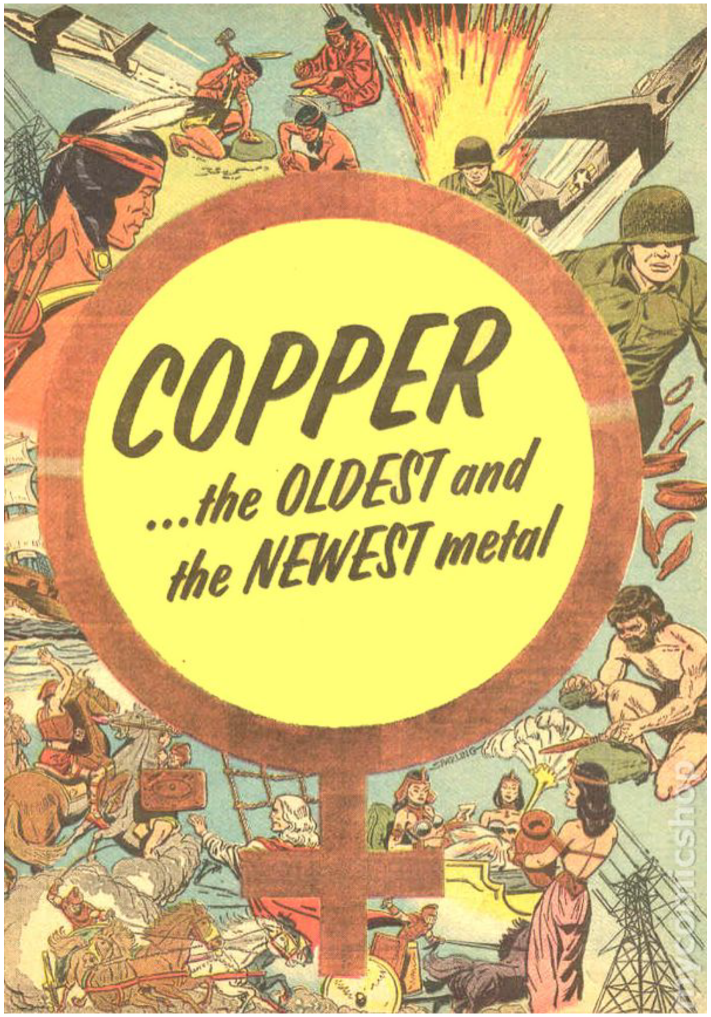

Jen Alleva

May 1st 2013

Timeline of Achievements in Copper Chemistry

General Historical Overview

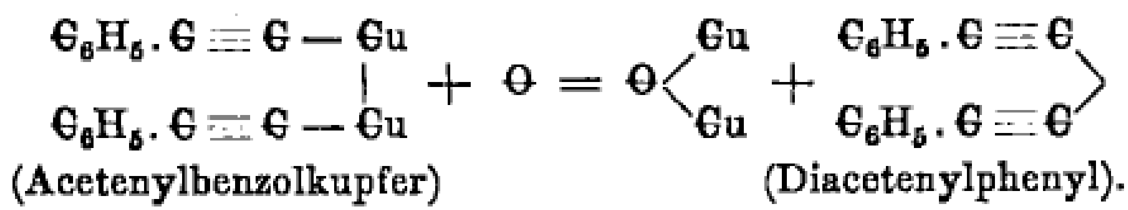

first cross-couplings

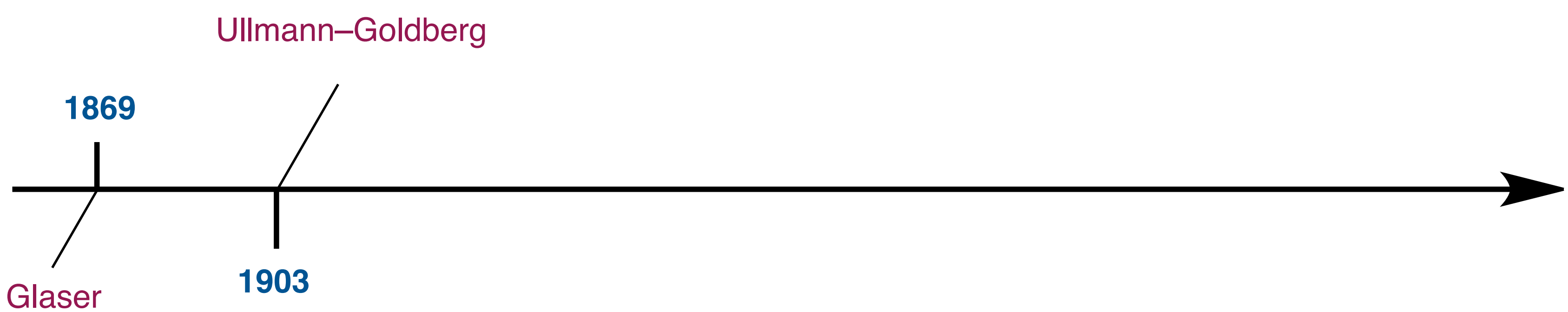

Glaser, C. *Ann. D. Chemie U. Pharm,* **1869**, *2*, 137–171

Timeline of Achievements in Copper Chemistry

General Historical Overview

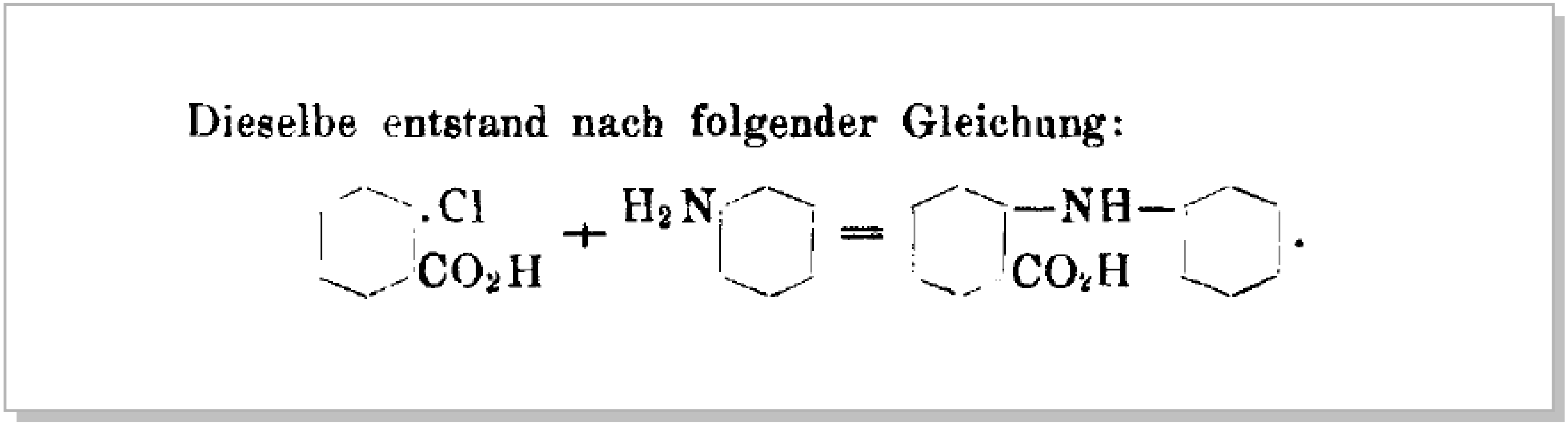

first cross-couplings

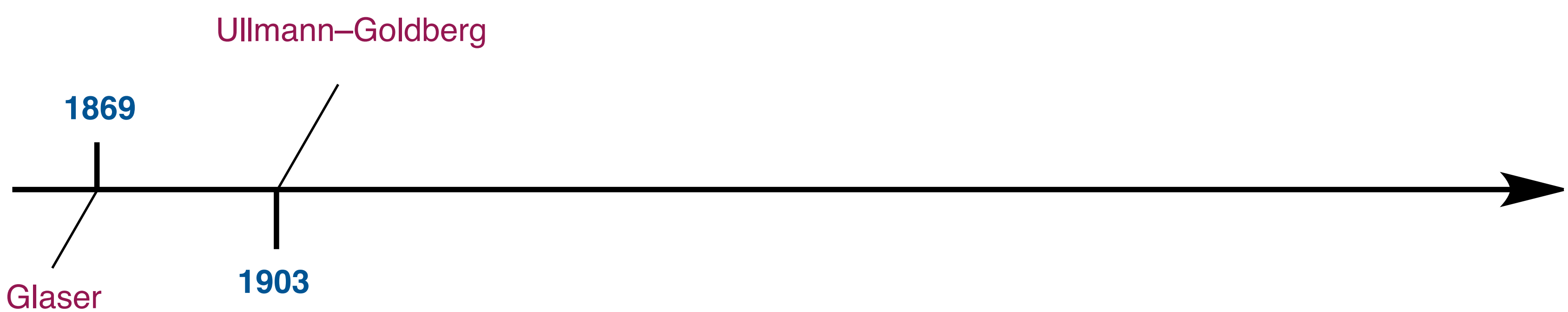

Ullman, F. *Ber.* **1903**, *36*, 2382–2384

Goldberg, I. *Ber.* **1906**, *39*, 1691–1692

Timeline of Achievements in Copper Chemistry

General Historical Overview

THE PREPARATION OF METHYLCOPPER AND SOME OBSERVATIONS ON THE DECOMPOSITION OF ORGANOCOPPER COMPOUNDS[1]

$$2\ CH_3Li + 2\ CuCl_2 \rightarrow C_2H_6 + Cu_2Cl_2 + 2\ LiCl$$
$$2\ CH_3Li + Cu_2Cl_2 \rightarrow 2[CH_3Cu] + 2\ LiCl$$

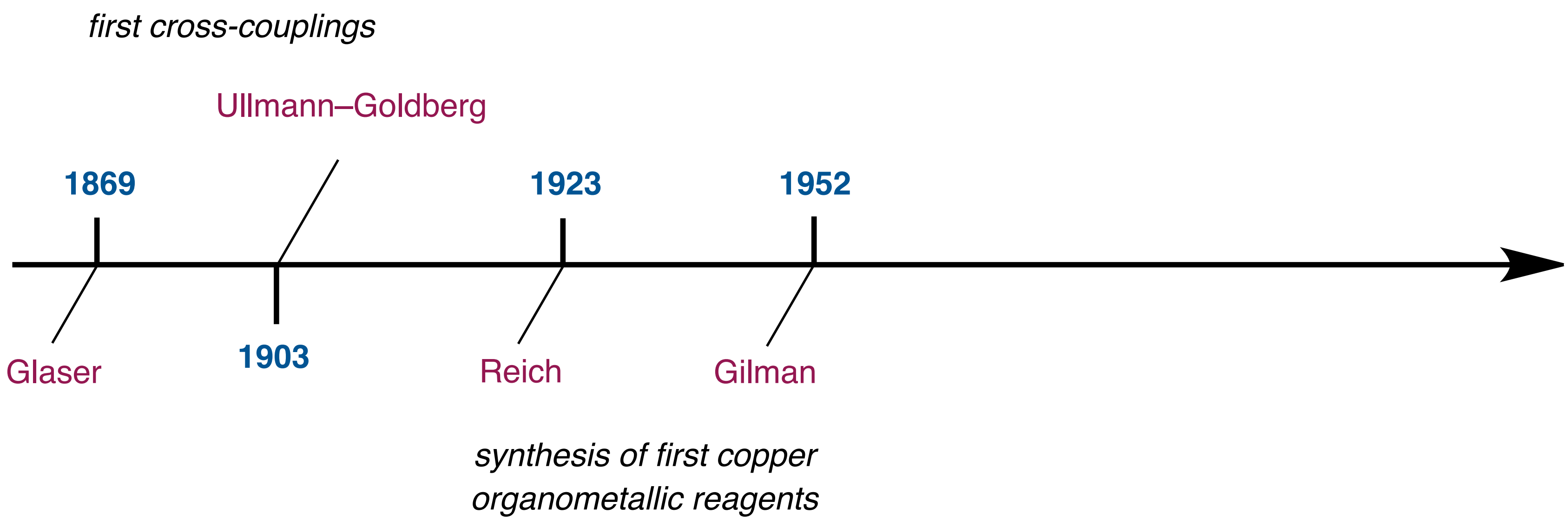

Gilman, H.; Jones, R. G.; Woods, L. A. *J. Org. Chem,* **1952**, *17*, 1630–1634

Timeline of Achievements in Copper Chemistry

General Historical Overview

1,3-Dipolar Cycloadditions

By Rolf Huisgen

(University of Munich, Germany)

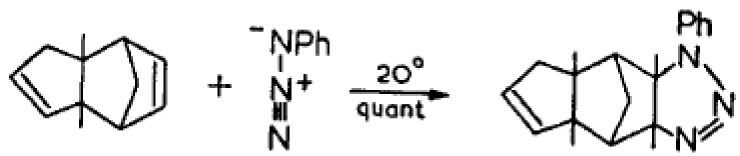

(I)

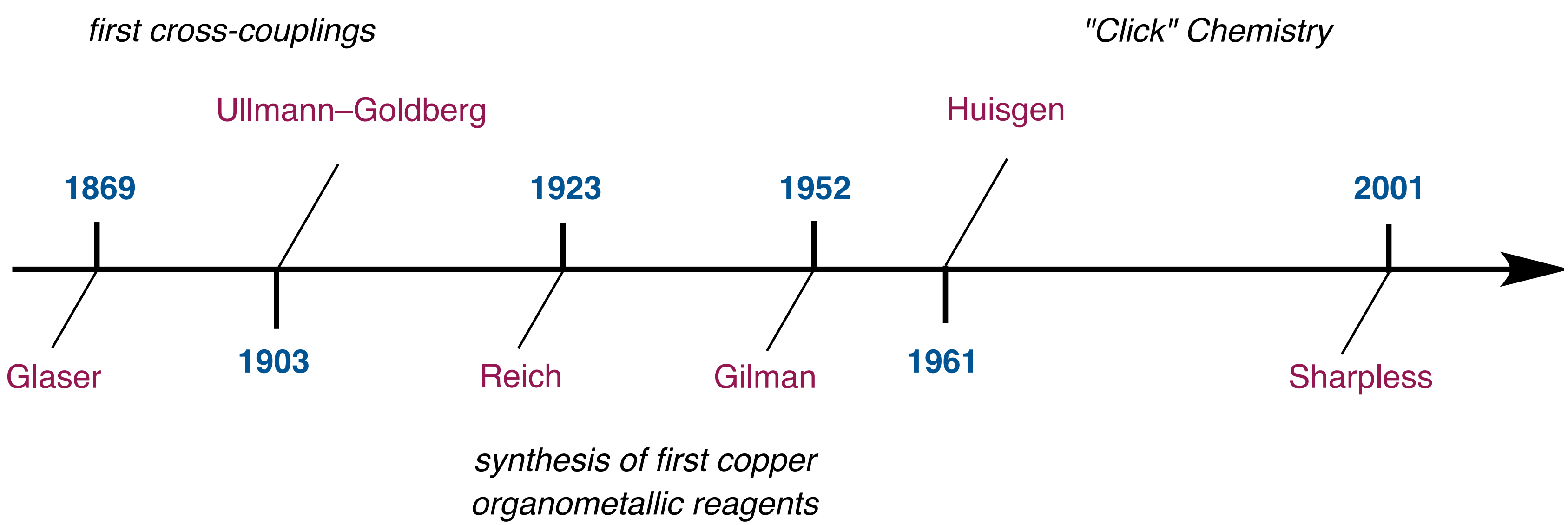

Huisgen, R. *Proc. Chem Soc.*, **1961**, 357–396

Timeline of Achievements in Copper Chemistry

General Historical Overview

1,3-Dipolar Cycloadditions

By Rolf Huisgen

(University of Munich, Germany)

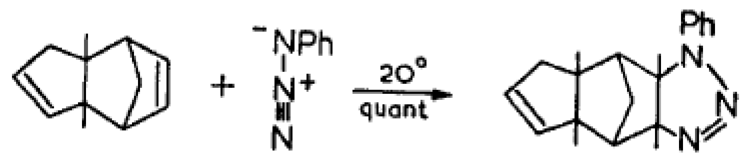

(I)

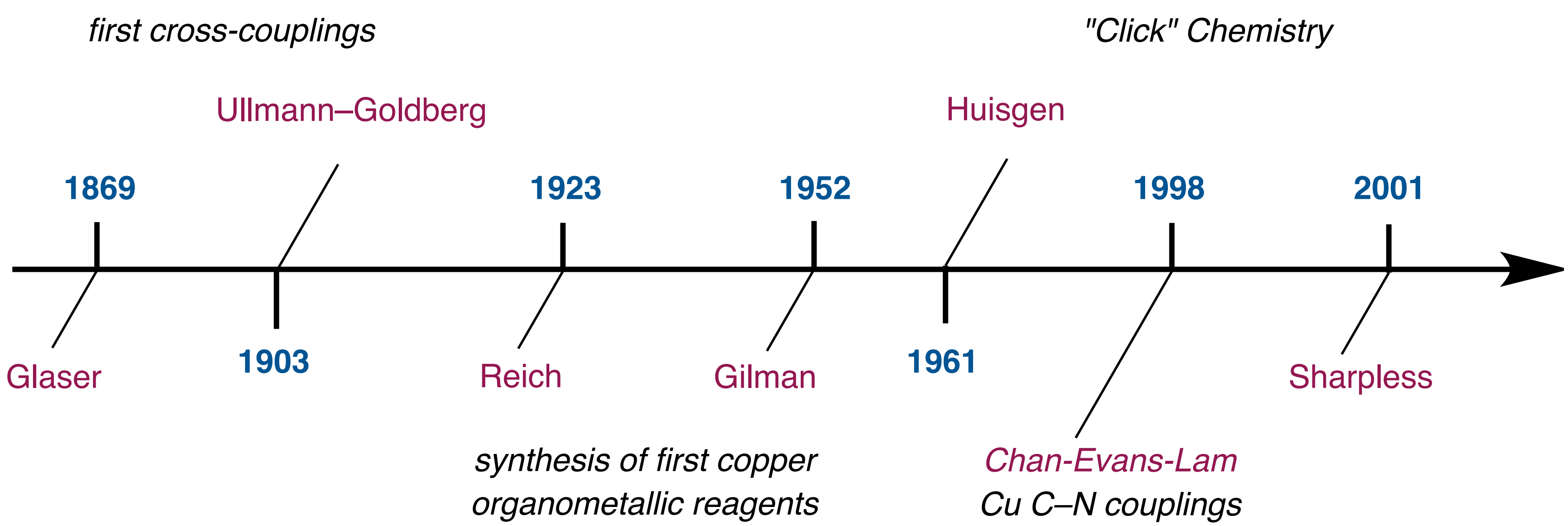

Huisgen, R. *Proc. Chem Soc.*, **1961**, 357–396

Copper in Cross-Coupling Reactions

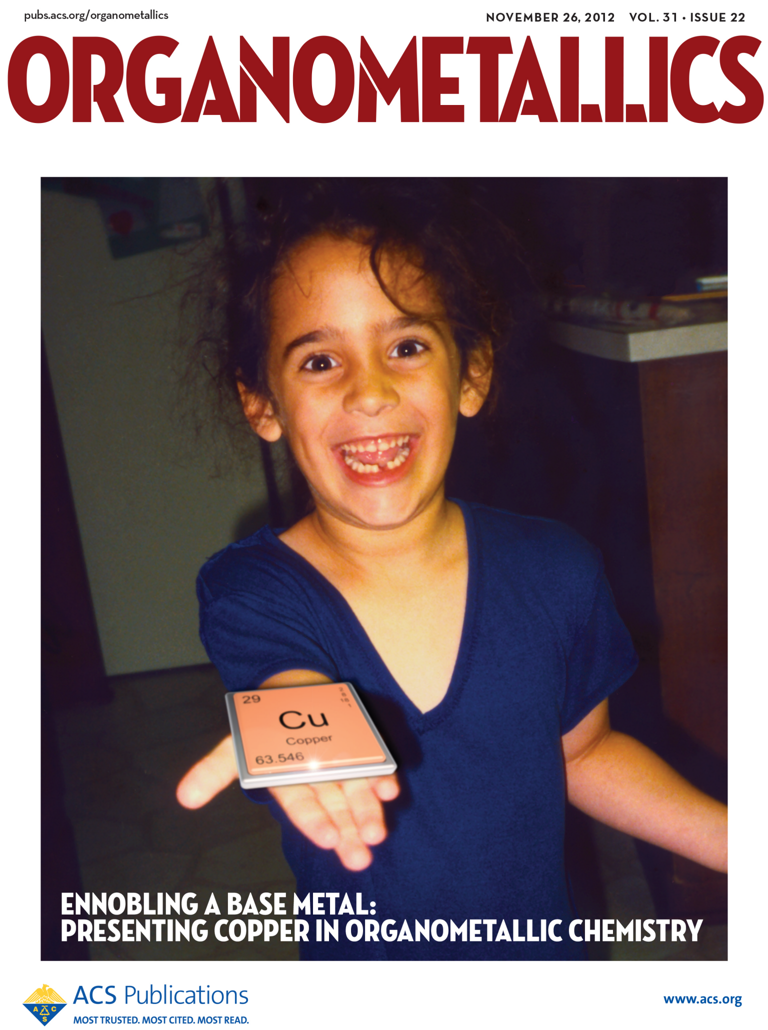

Copper in Cross-Coupling Reactions

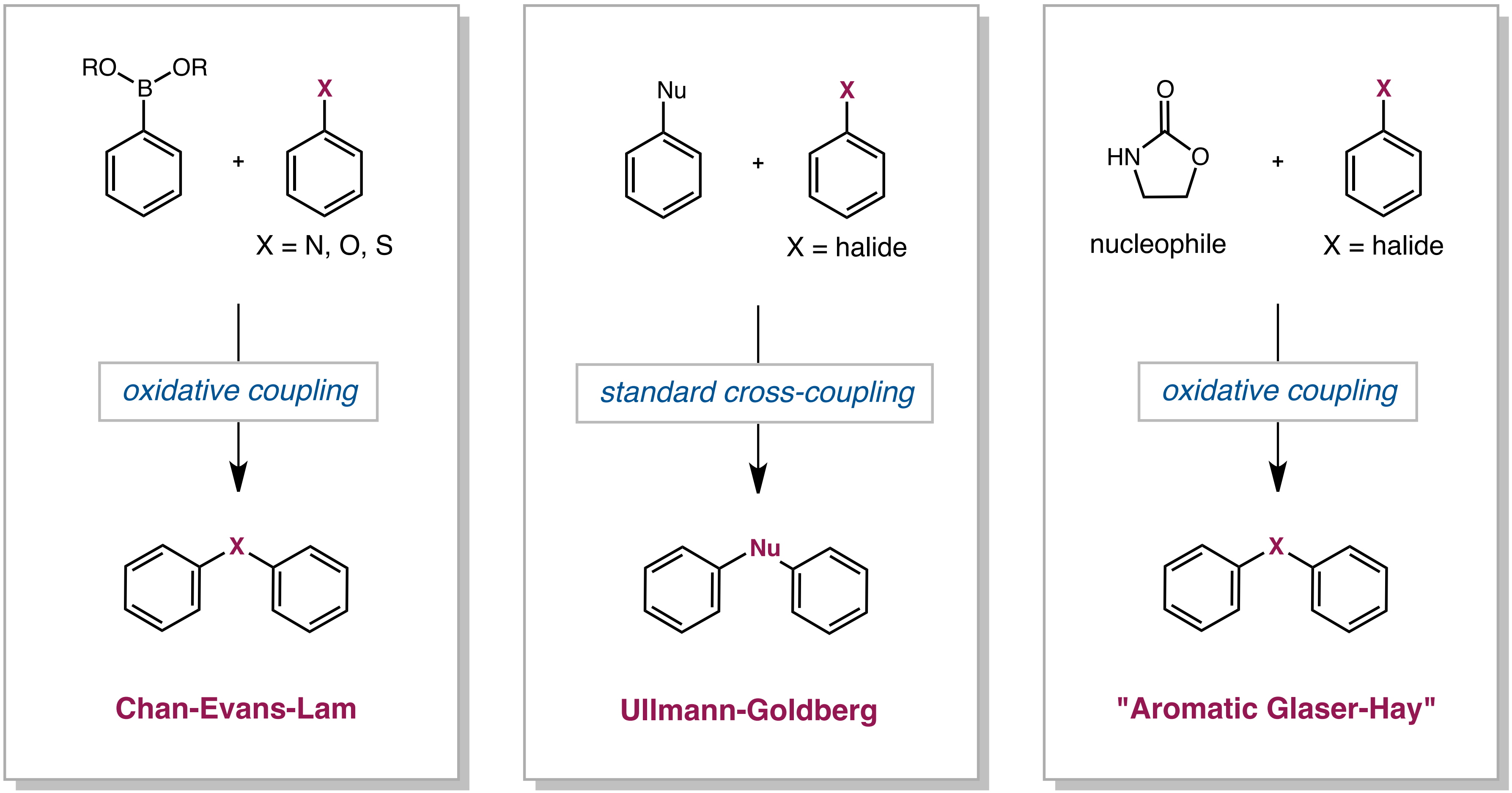

Electronic Properties of Copper

$Cu^{I} \xrightleftharpoons{E_{1/2}= 0.16V} Cu^{II} \xrightleftharpoons{E_{1/2}= 2.4V} Cu^{III}$

Cu^{I}	Cu^{II}	Cu^{III}
d^{10}	d^{9}	d^{8}, metal cation
isoelectronic with Ni(0)		isoelectronic with Pd(II)

* Vs. SCE in MeCN, Bratsch, S. G. *J. Phys. Chem. Ref. Data* **1989**, *18*, 1–21

Electronic Properties of Copper

Cu^{I}	$\underset{}{\overset{E_{1/2}= 0.16V}{\rightleftharpoons}}$	Cu^{II}	$\overset{E_{1/2}= 2.4V}{\rightleftharpoons}$	Cu^{III}
d^{10}		d^{9}		d^{8}, metal cation
isoelectronic with Ni(0)				isoelectronic with Pd(II)

- forms shorter bonds than Pd
- harder Lewis acidity than Pd
- higher affinity for O, N ligands
- smaller coordination shell can not accomodate large ancillary ligands

Beletskaya, I. P; Cheprakov, A. V. *Organometallics* **2012**, *31*, 7753–7808

* Vs. SCE in MeCN, Bratsch, S. G. *J. Phys. Chem. Ref. Data* **1989**, *18*, 1–21

Electronic Properties of Copper

Cu^{I}	$\underset{}{\overset{E_{1/2}= 0.16V}{\rightleftharpoons}}$	Cu^{II}	$\overset{E_{1/2}= 2.4V}{\rightleftharpoons}$	Cu^{III}
d^{10}		d^{9}		d^{8}, metal cation
isoelectronic with Ni(0)				isoelectronic with Pd(II)

- forms shorter bonds than Pd
- harder Lewis acidity than Pd
- higher affinity for O, N ligands
- smaller coordination shell can not accomodate large ancillary ligands

- highly electrophilic and unstable
- potent oxidizer
- requires highly stabilizing ligands

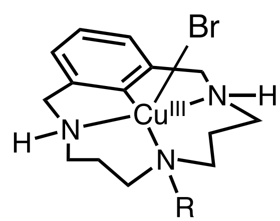

Beletskaya, I. P; Cheprakov, A. V. *Organometallics* **2012**, *31*, 7753–7808

* Vs. SCE in MeCN, Bratsch, S. G. *J. Phys. Chem. Ref. Data* **1989**, *18*, 1–21

Electronic Properties of Copper

$$Cu^{I} \underset{}{\overset{E_{1/2}= 0.16V}{\rightleftharpoons}} Cu^{II} \underset{}{\overset{E_{1/2}= 2.4V}{\rightleftharpoons}} Cu^{III}$$

d^{10} — d^{9} — d^{8}, metal cation

Cu(I): isoelectronic with Ni(0)

- forms shorter bonds than Pd
- harder Lewis acidity than Pd
- higher affinity for O, N ligands
- smaller coordination shell can not accomodate large ancillary ligands

Cu(III): isoelectronic with Pd(II)

- highly electrophilic and unstable
- potent oxidizer
- requires highly stabilizing ligands
- unstable towards the reverse reductive elimination
- can not take part in ligand exchange
- requires the nucleophile to be in the coordination sphere prior to oxidative addition

Beletskaya, I. P; Cheprakov, A. V. *Organometallics* **2012**, *31*, 7753–7808

* Vs. SCE in MeCN, Bratsch, S. G. *J. Phys. Chem. Ref. Data* **1989**, *18*, 1–21

Cross-Coupling Classifications

regular cross-coupling: transition metal mediated nucleophilic substitution

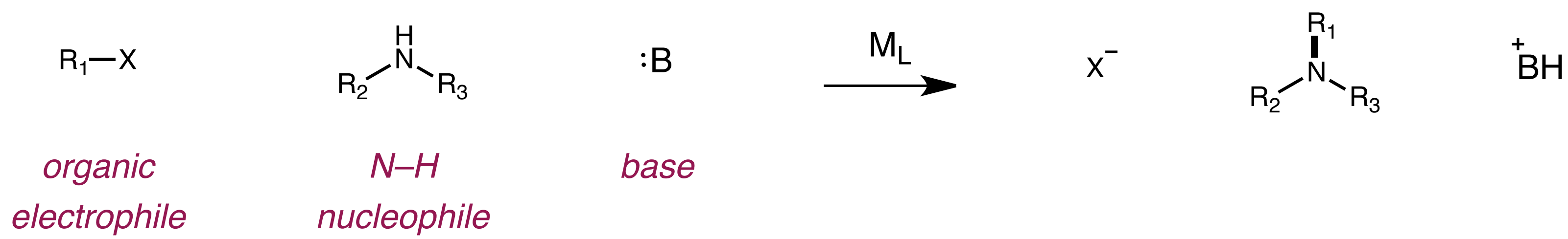

Cross-Coupling Classifications

regular cross-coupling: transition metal mediated nucleophilic substitution

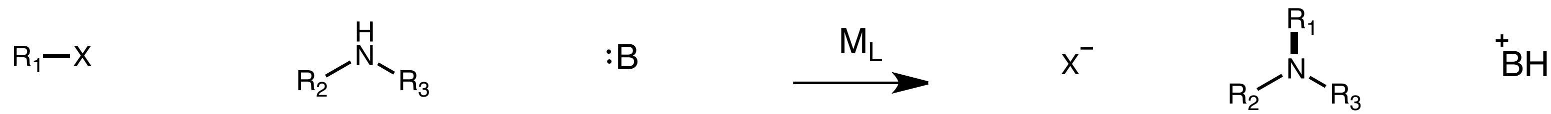

organic electrophile | *N–H nucleophile* | *base*

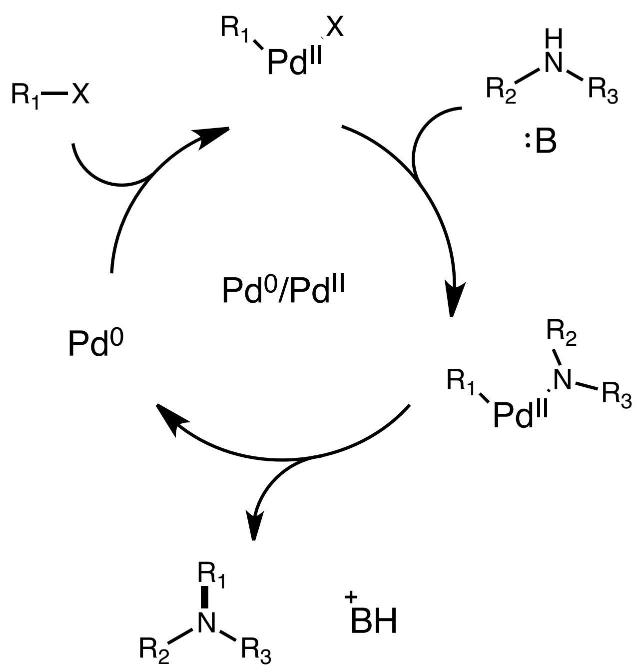

Cross-Coupling Classifications

regular cross-coupling: transition metal mediated nucleophilic substitution

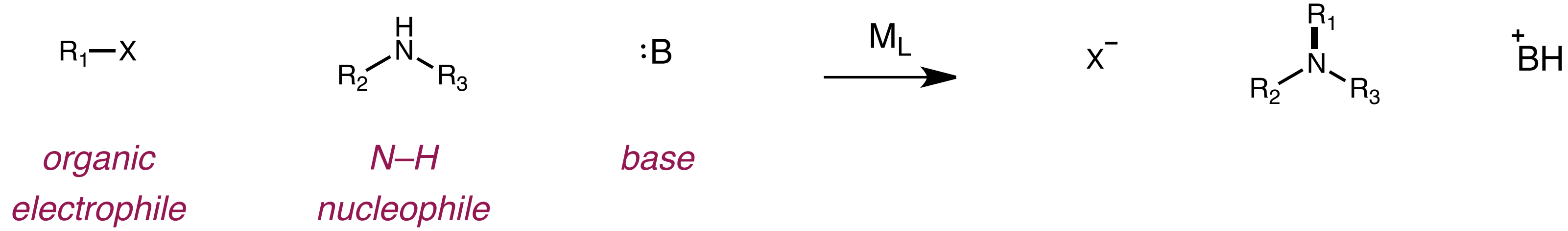

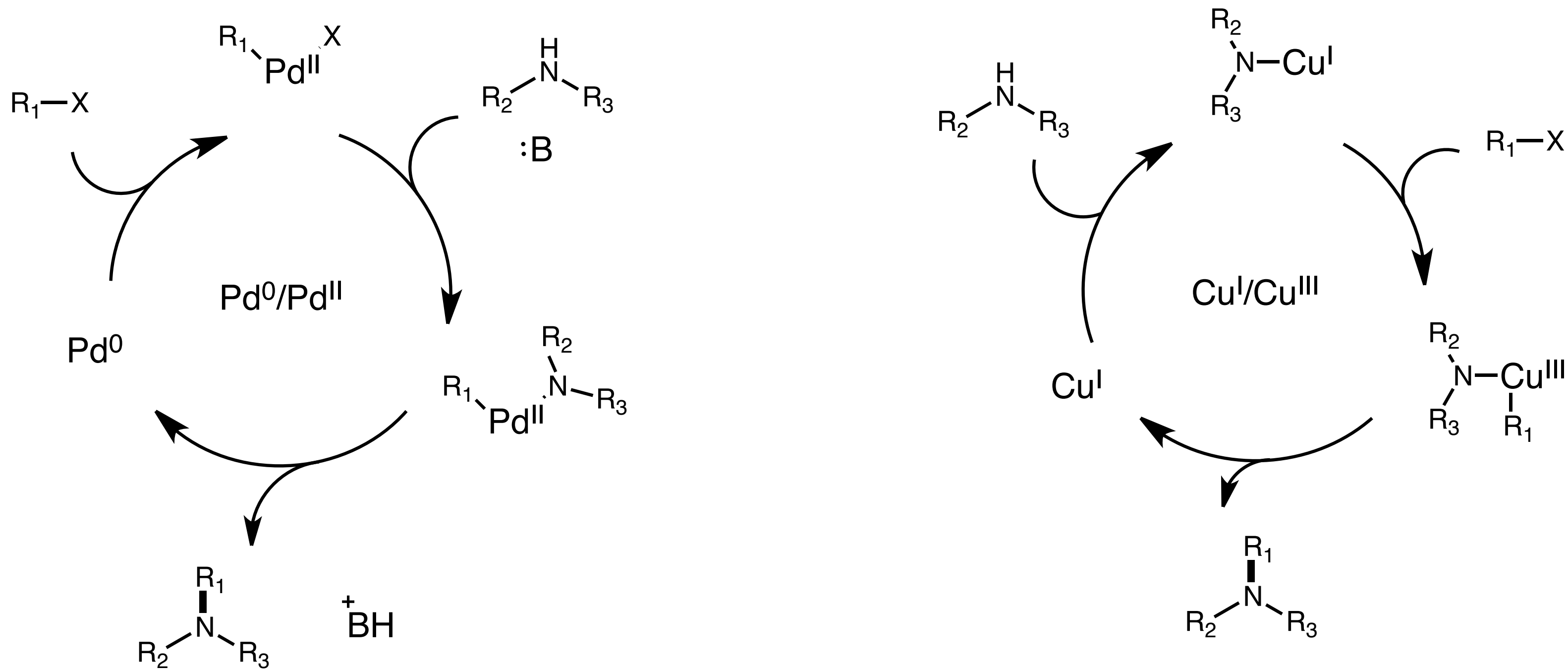

nucleophile plays the role of ancillary ligand in Cu^{I}/Cu^{III}

Cross-Coupling Classifications

oxidative cross-coupling: transition metal mediated coupling of two nucleophiles

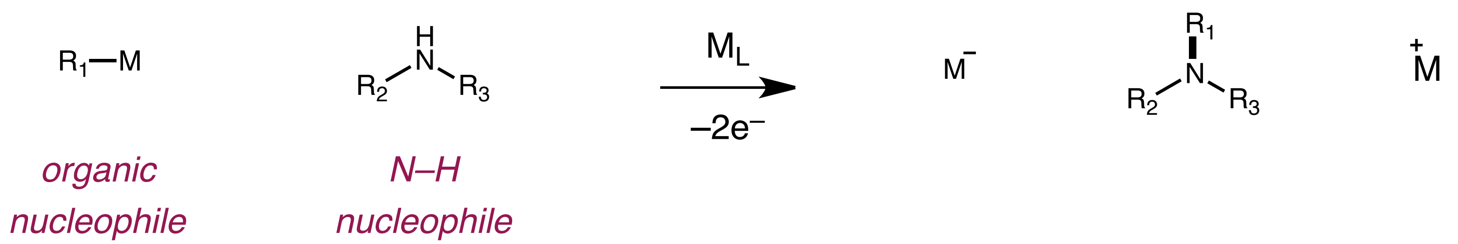

Cross-Coupling Classifications

oxidative cross-coupling: transition metal mediated coupling of two nucleophiles

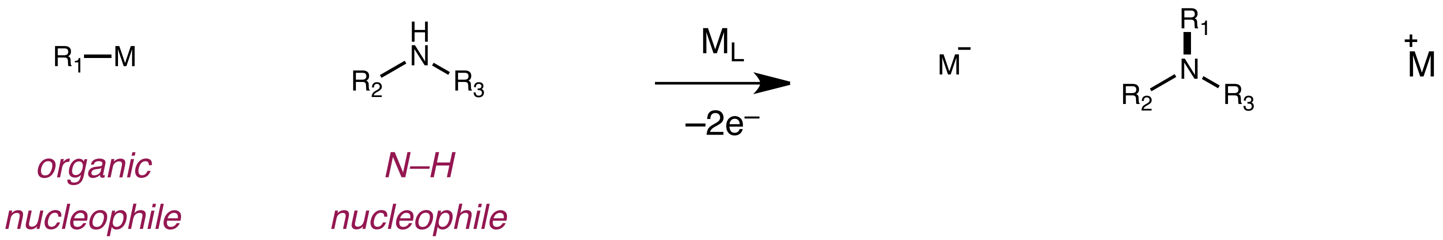

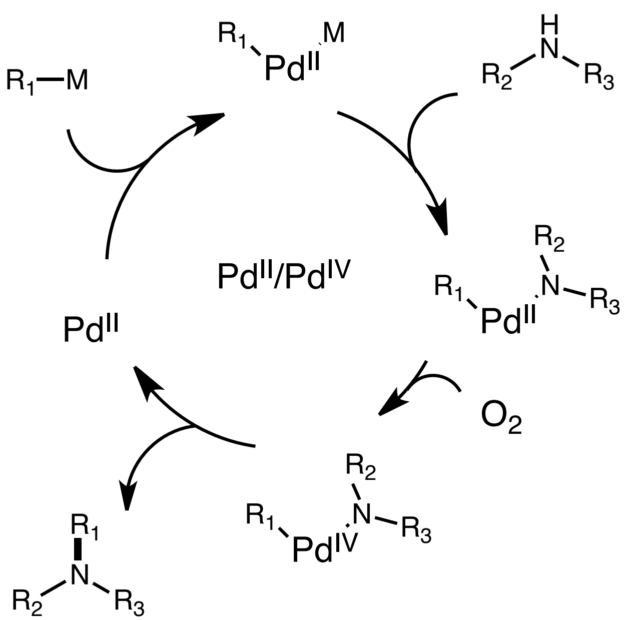

Cross-Coupling Classifications

oxidative cross-coupling: transition metal mediated coupling of two nucleophiles

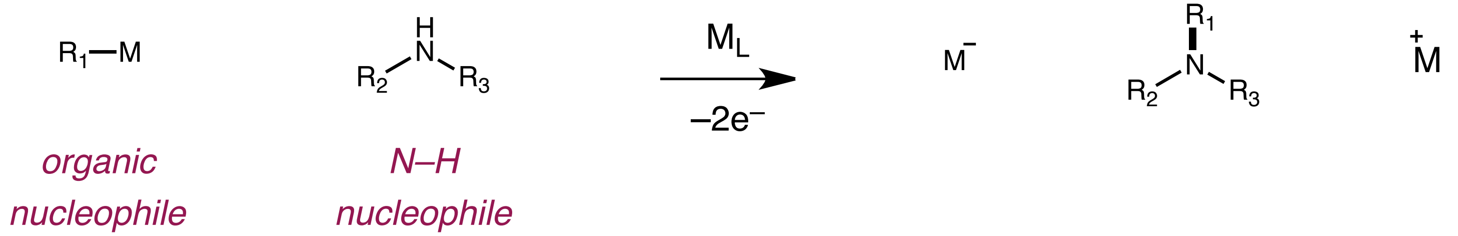

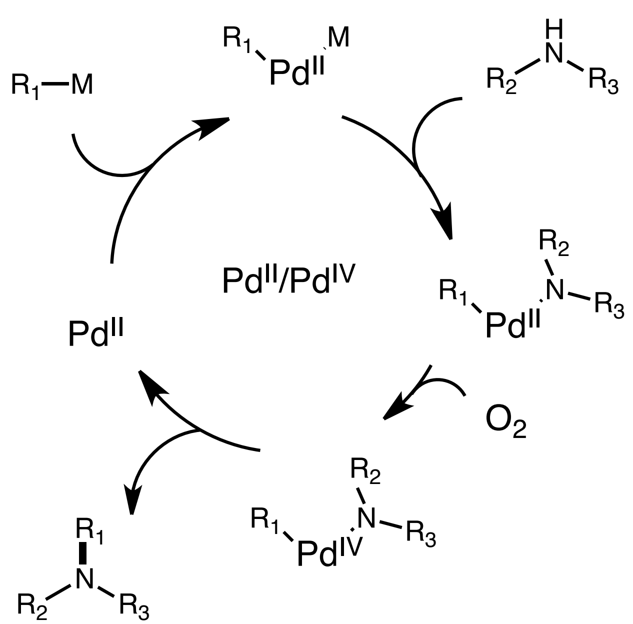

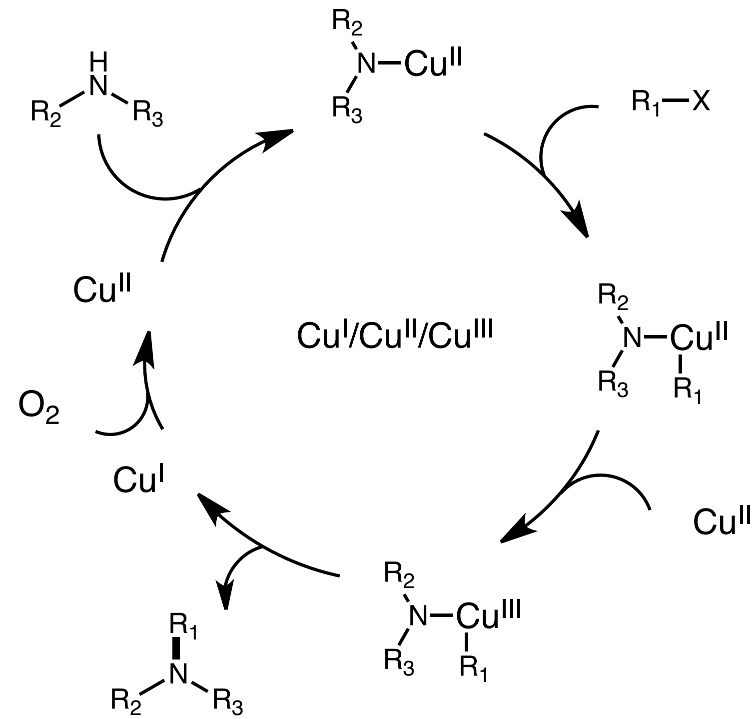

Cross-Coupling Classifications

inverse or Umpolung cross-coupling: transition metal mediated electrophilic substitution

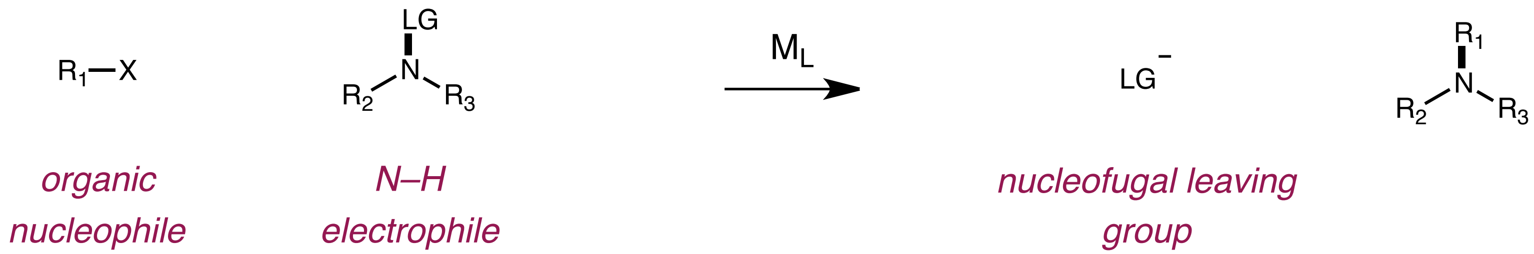

Cross-Coupling Classifications

inverse or Umpolung cross-coupling: transition metal mediated electrophilic substitution

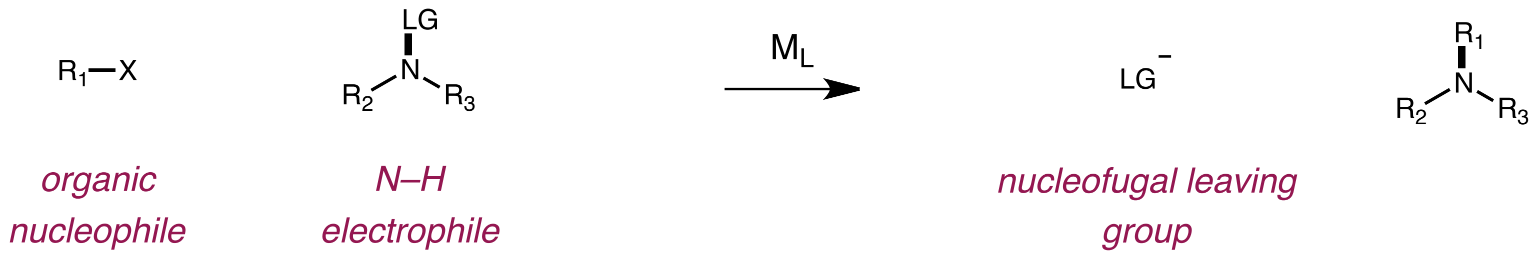

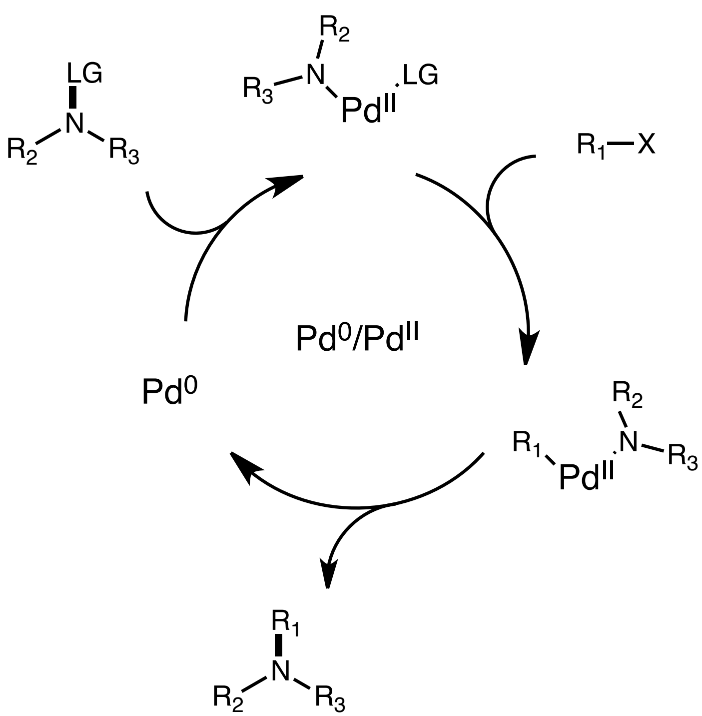

Cross-Coupling Classifications

inverse or Umpolung cross-coupling: transition metal mediated electrophilic substitution

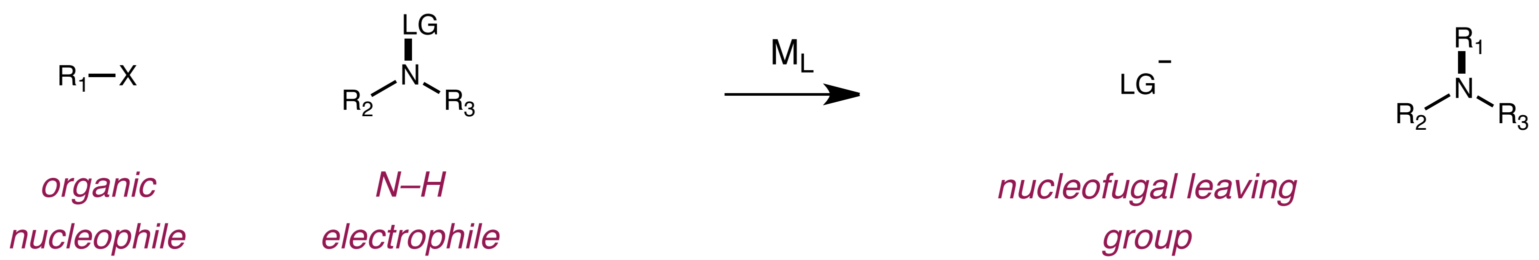

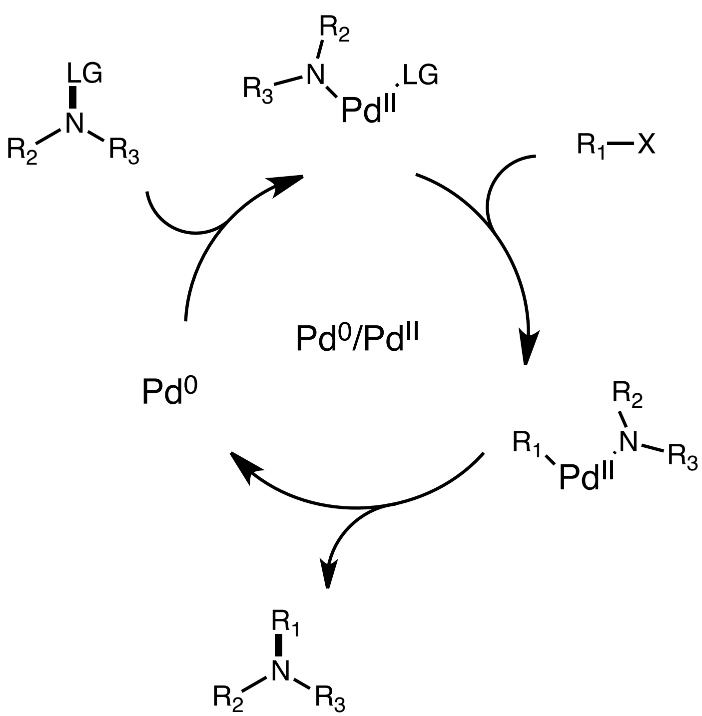

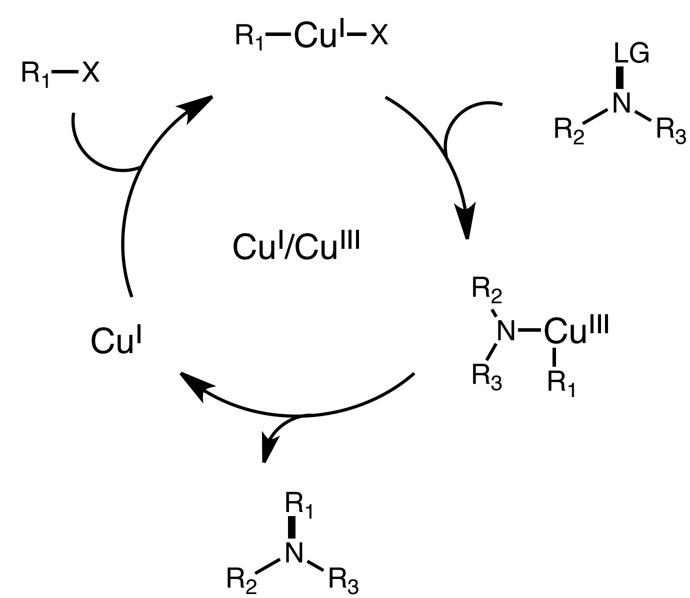

Copper in Cross-Coupling Reactions

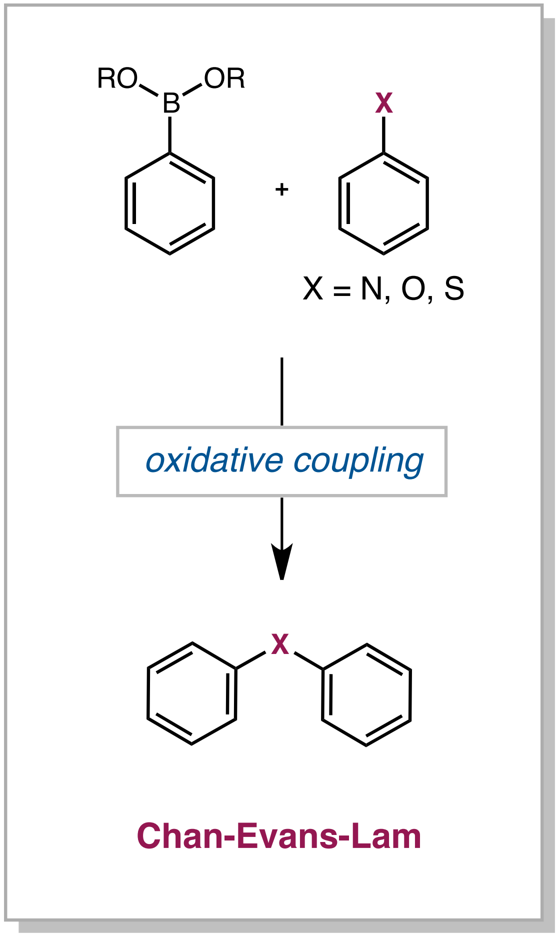

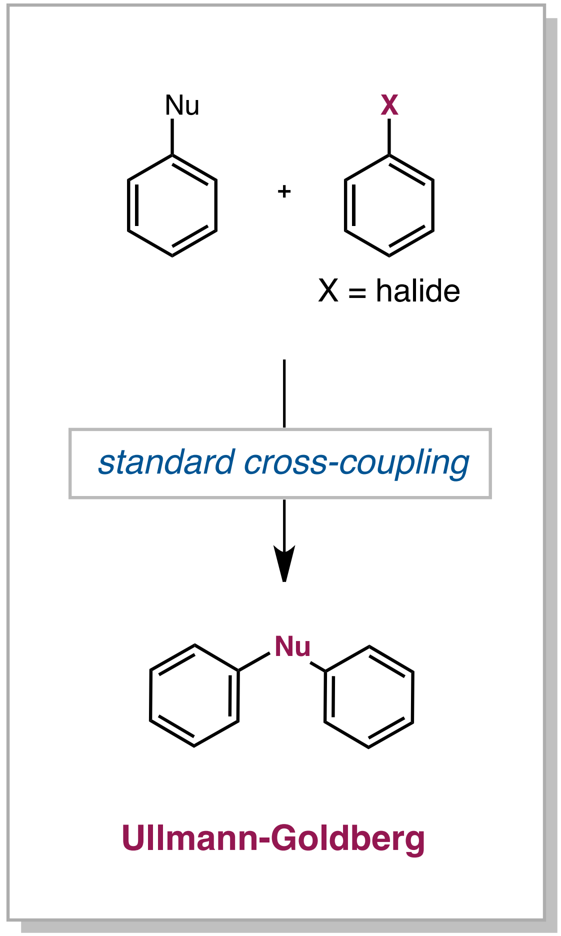

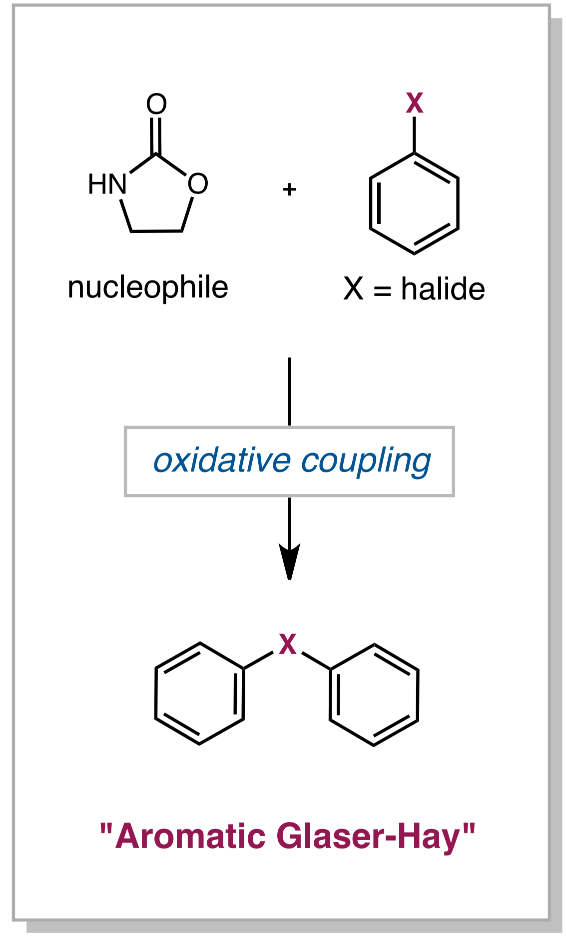

Mechanistic Studies in Copper Catalysis

Shannon Stahl

Xavi Ribas

Ted Cohen

Copper in Cross-Coupling Reactions

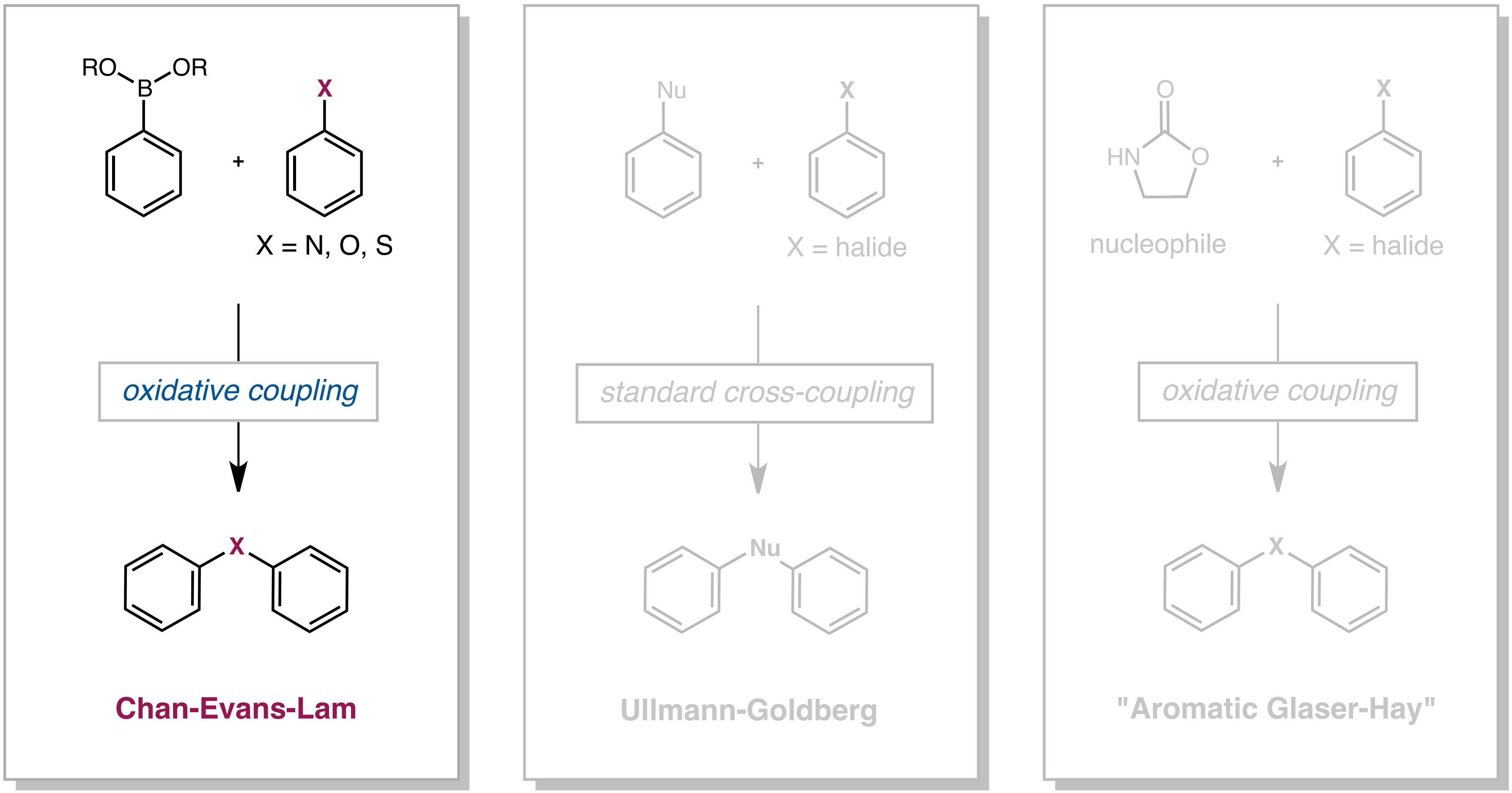

Chan-Evans-Lam Coupling

oxidative cross-coupling

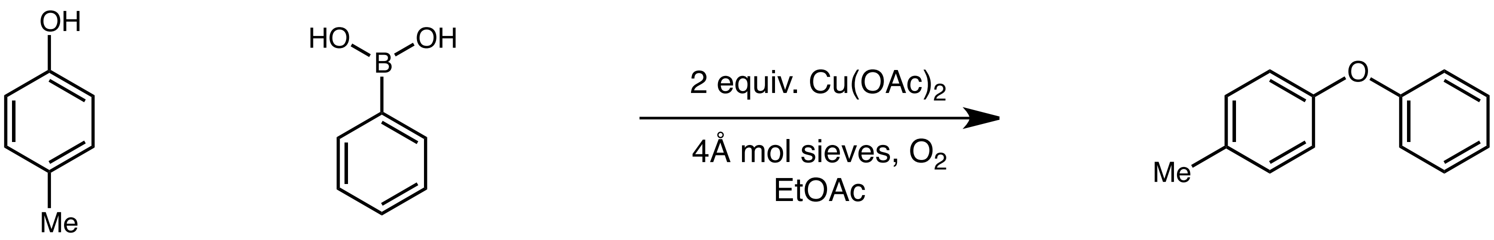

heteroatom nucleophile

boronic acid

diaryl ether

Chan D. M. T.; Monaco, K. L.; Wang, R.-P.; Winters, M. P. *Tetrahedron Lett.* **1998**, *39*, 2933.

Evans, D. A.; Katz, J. L.; West, T. R. *Tetrahedron Lett.* **1998**, *39*, 2937.

Lam, P. Y. S.; Clark, C. G.; Saubern, S.; Adams, J.; Winters, M. P.; Chan, D. T., Combs, A. *Tetrahedron Lett.* **1998**, *39*, 2941.

Chan-Evans-Lam Coupling

oxidative cross-coupling

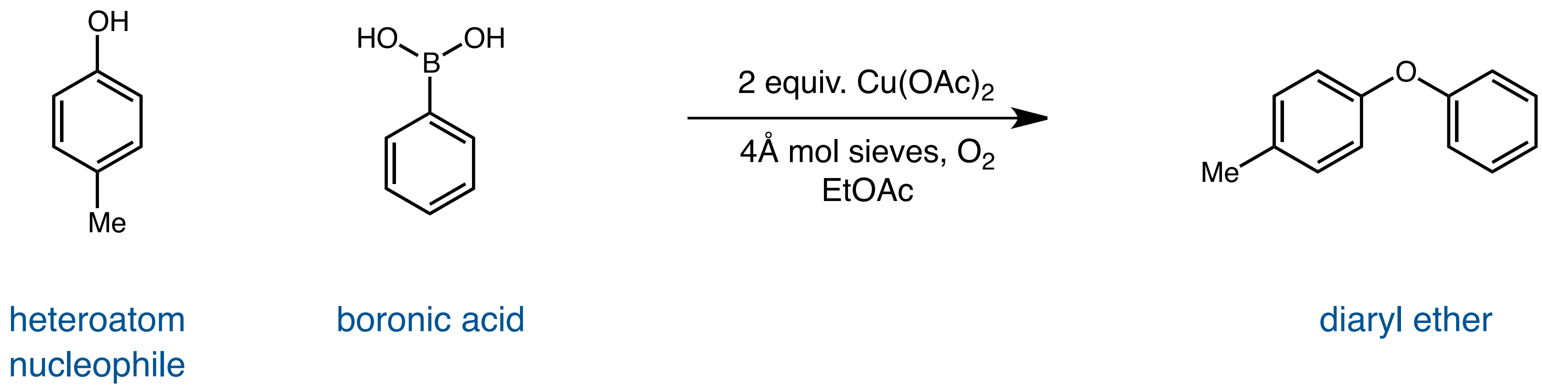

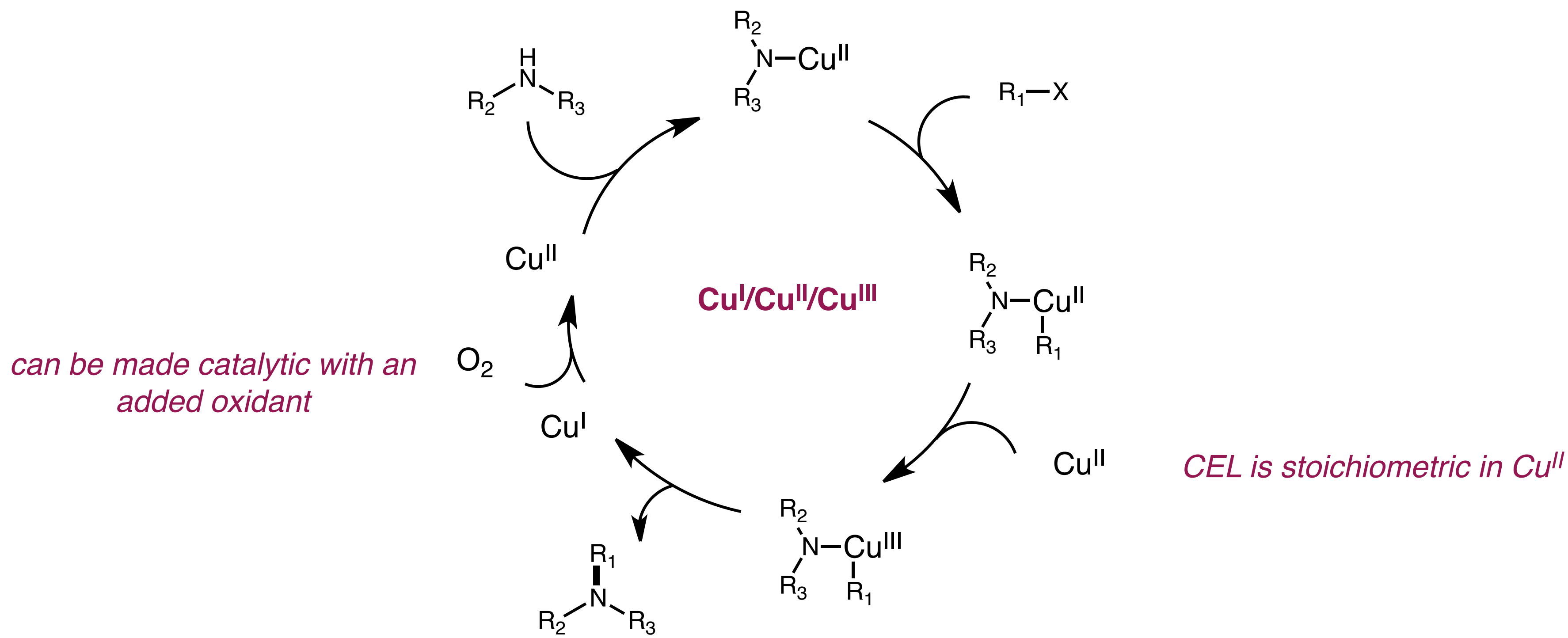

Chan-Evans-Lam Coupling

select catalytic methods

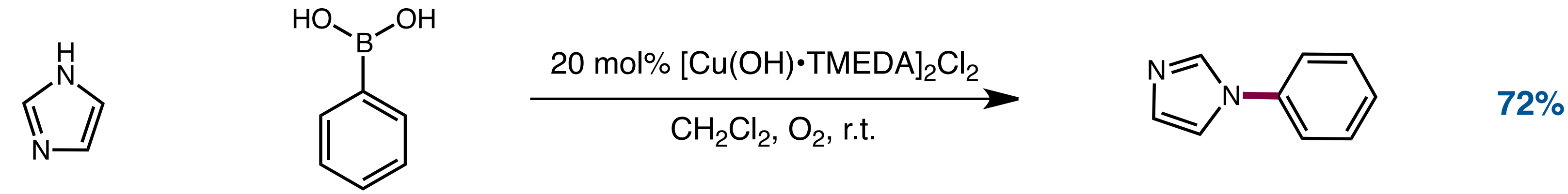

Collman, J. P.; Zhong, M. *Org. Lett.* **2000**, *2*, 1233–1236

Chan-Evans-Lam Coupling

select catalytic methods

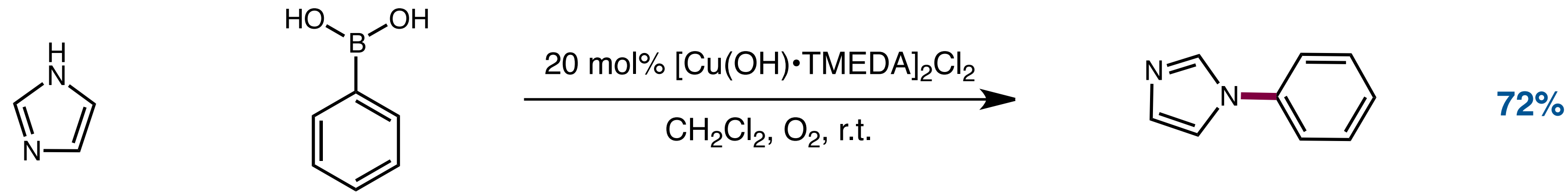

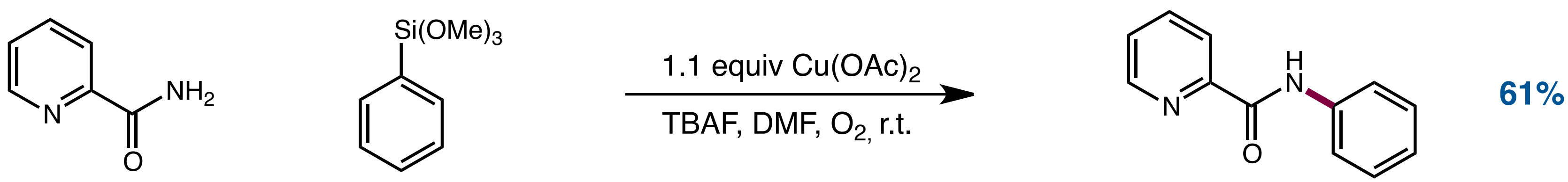

Lam, P. S.; Deudon, S.; Hauptman, E.; Clark, C. G. *Tetrahedron Lett.* **2001**, *42*, 2427–2429

Collman, J. P.; Zhong, M. *Org. Lett.* **2000**, *2*, 1233–1236

Chan-Evans-Lam Coupling

select catalytic methods

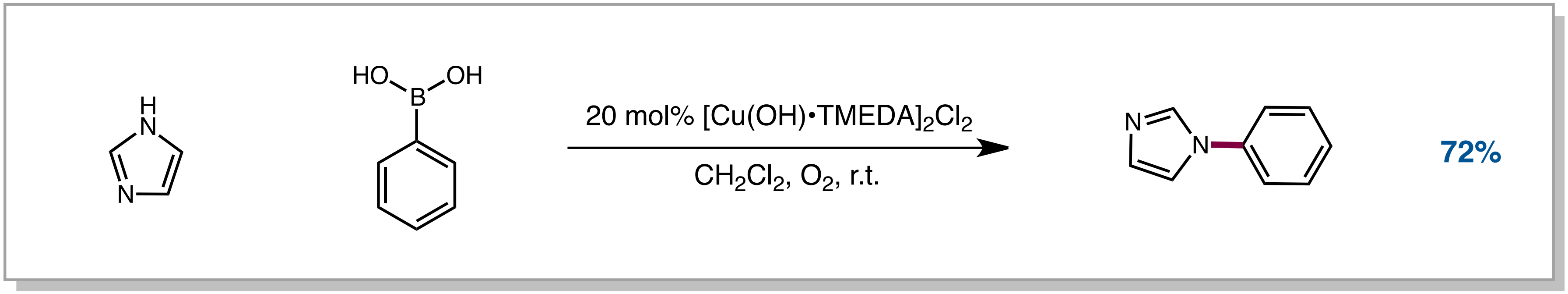

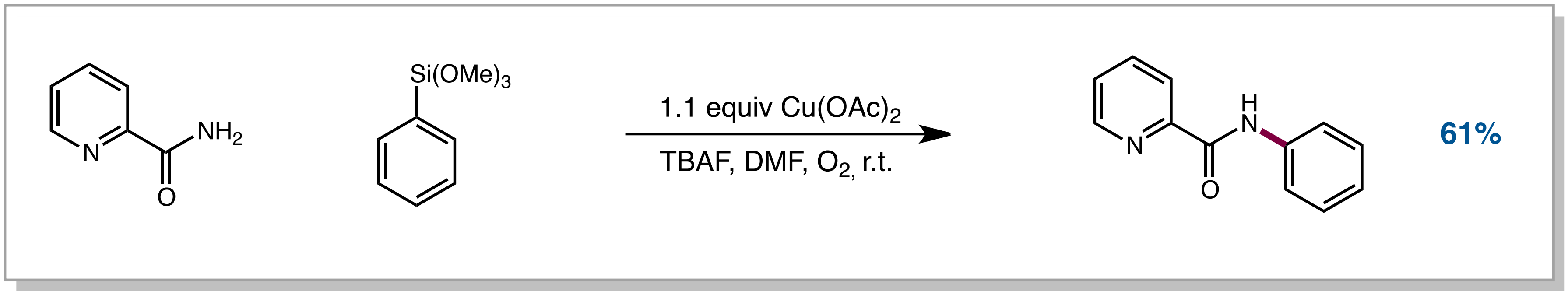

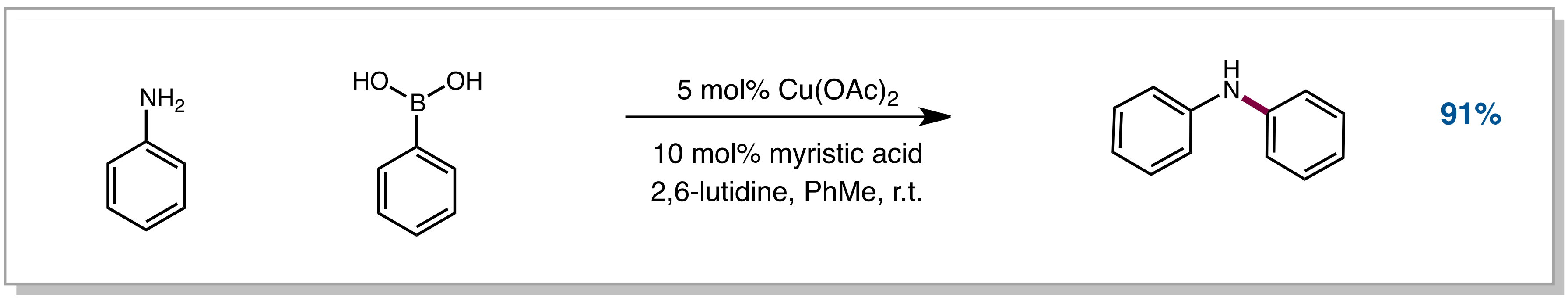

Antilla, J. C.; Buchwald, S. L. *Org Lett*, **2001**, *3*, 2077–2079

Lam, P. S.; Deudon, S.; Hauptman, E.; Clark, C. G. *Tetrahedron Lett.* **2001**, *42*, 2427–2429

Collman, J. P.; Zhong, M. *Org. Lett.* **2000**, *2*, 1233–1236

Chan-Evans-Lam Coupling

determining reaction stoichiometry

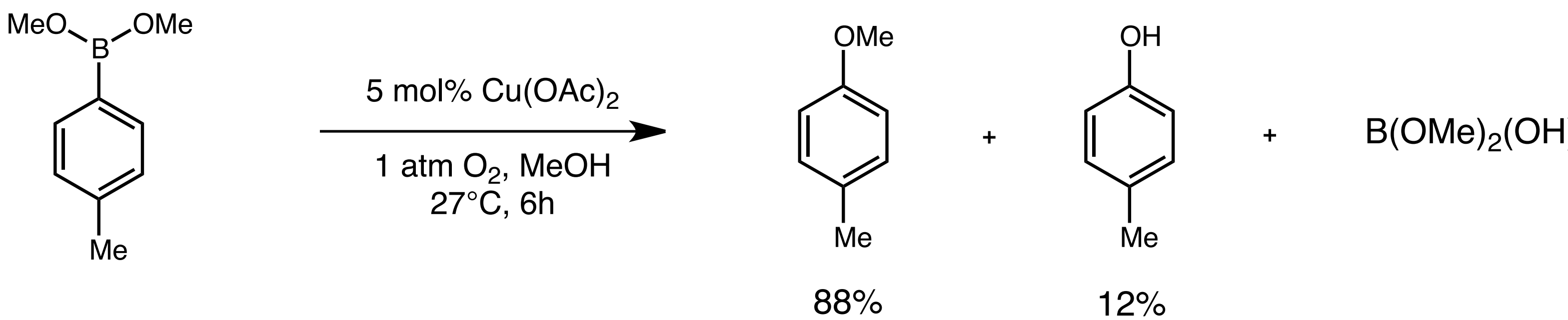

King, A. E.; Brunold, T. C.; Stahl. S. S. *J. Am. Chem. Soc.* **2009**, *131*, 5044–5045

Chan-Evans-Lam Coupling

determining reaction stoichiometry

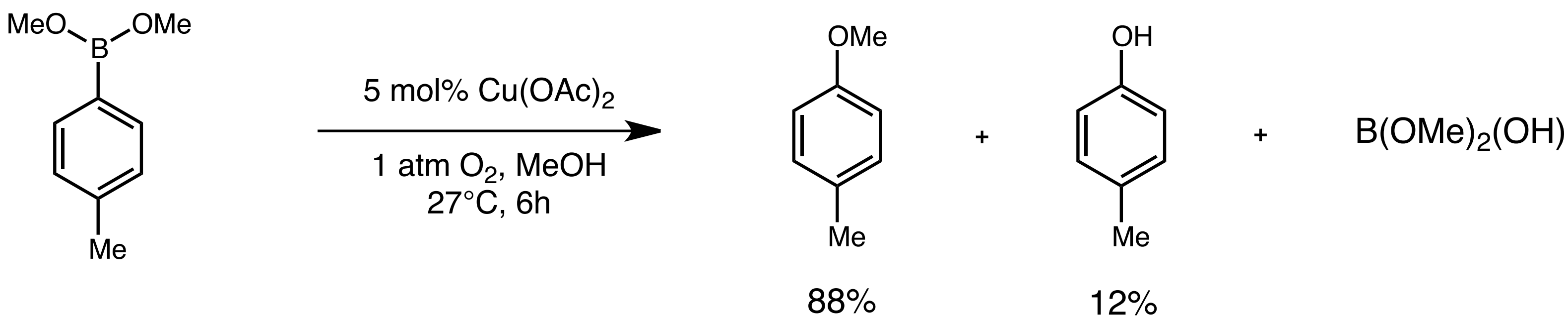

Cu and O_2 stoichiometry determined from anaerobic single-turnover experiment

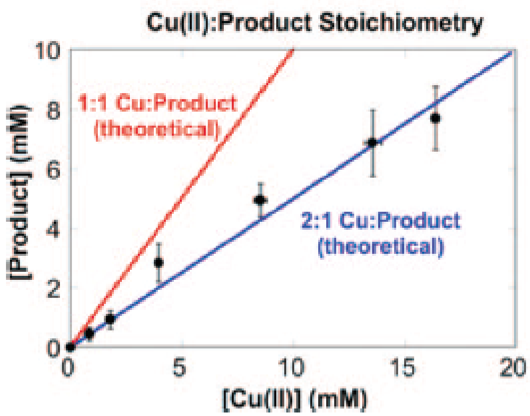

Cu^{II}/product ratio is 2:1

King, A. E.; Brunold, T. C.; Stahl. S. S. *J. Am. Chem. Soc.* **2009**, *131*, 5044–5045

Chan-Evans-Lam Coupling

determining reaction stoichiometry

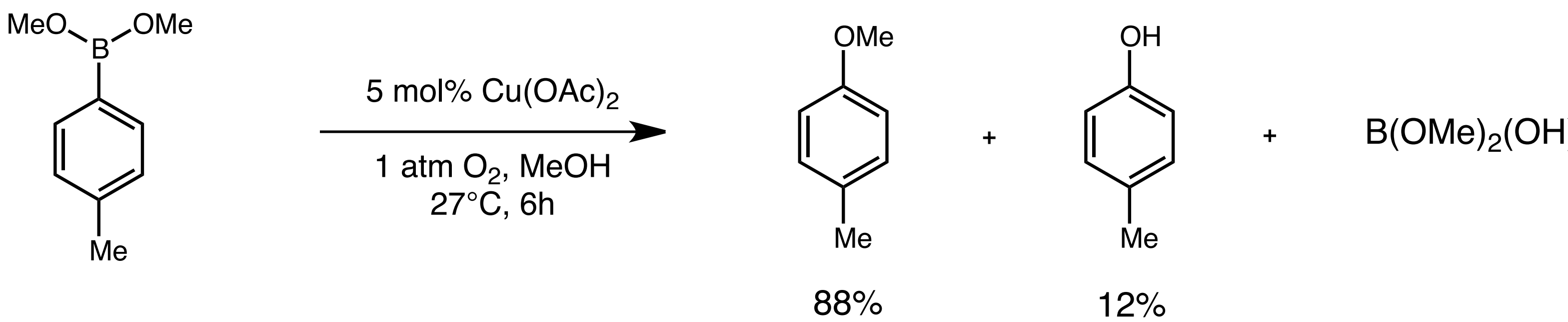

Cu and O_2 stoichiometry determined from anaerobic single-turnover experiment

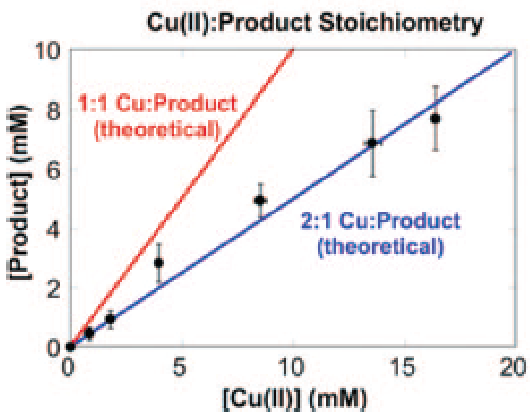

Cu^{II}/product ratio is 2:1

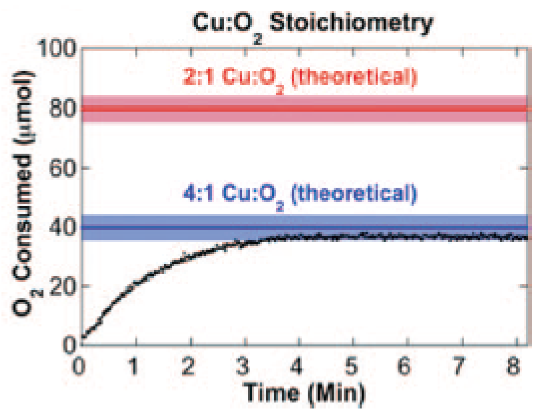

Cu^{I}/O_2 ratio is 4:1

result consistent with
Cu oxidase mechanism

King, A. E.; Brunold, T. C.; Stahl. S. S. *J. Am. Chem. Soc.* **2009**, *131*, 5044–5045

Chan-Evans-Lam Coupling

initial rates experiment reveals turnover-limiting step

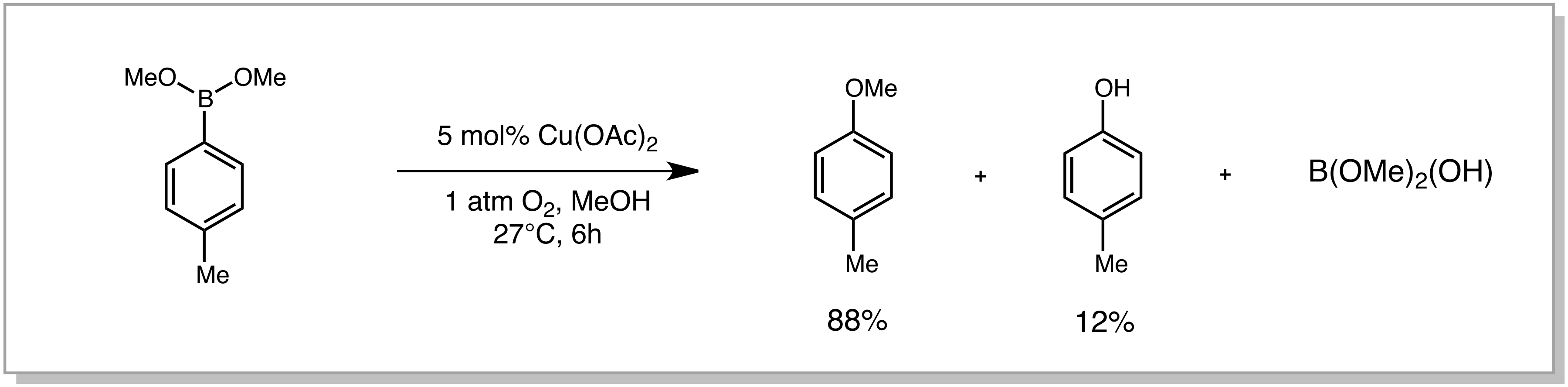

Initial rates experiment: suggest transmetalation as turnover-limiting

King, A. E.; Brunold, T. C.; Stahl. S. S. *J. Am. Chem. Soc.* **2009**, *131*, 5044–5045

Chan-Evans-Lam Coupling

initial rates experiment reveals turnover-limiting step

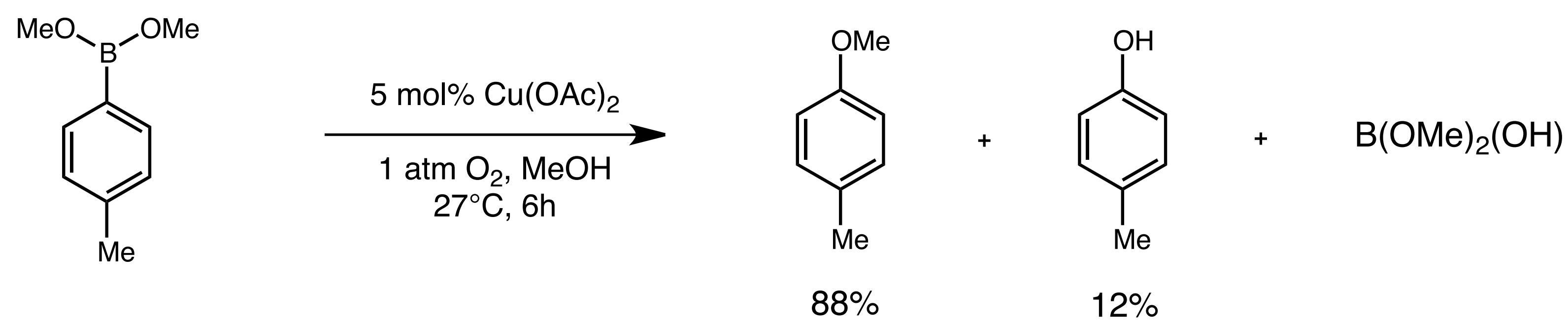

Initial rates experiment: suggest transmetalation as turnover-limiting

- 1st order dependence on $Cu(OAc)_2$
- saturation dependence on boronic ester

King, A. E.; Brunold, T. C.; Stahl. S. S. *J. Am. Chem. Soc.* **2009**, *131*, 5044–5045

Chan-Evans-Lam Coupling

initial rates experiment reveals turnover-limiting step

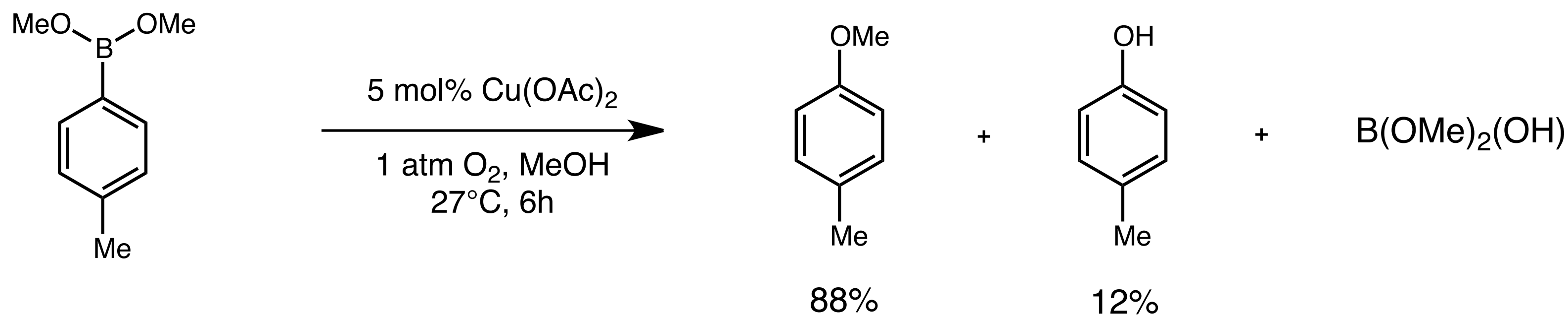

Initial rates experiment: suggest transmetalation as turnover-limiting

- 1^{st} order dependence on $Cu(OAc)_2$
- saturation dependence on boronic ester
- 0 order dependence on O_2

Cu^I oxidation is relatively fast compared to transmetalation →

King, A. E.; Brunold, T. C.; Stahl. S. S. *J. Am. Chem. Soc.* **2009**, *131*, 5044–5045

Electron Paramagnetic Resonance Spectroscopy

Cu^{II}: d^9, square planar

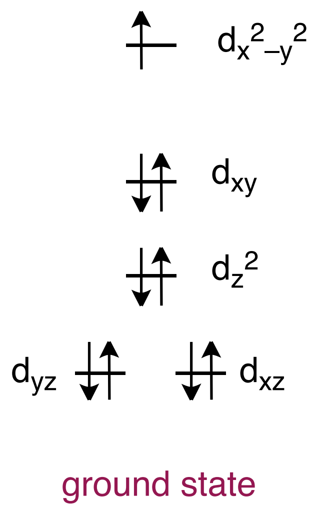

Electron Paramagnetic Resonance Spectroscopy

Cu^{II}: d^9, square planar

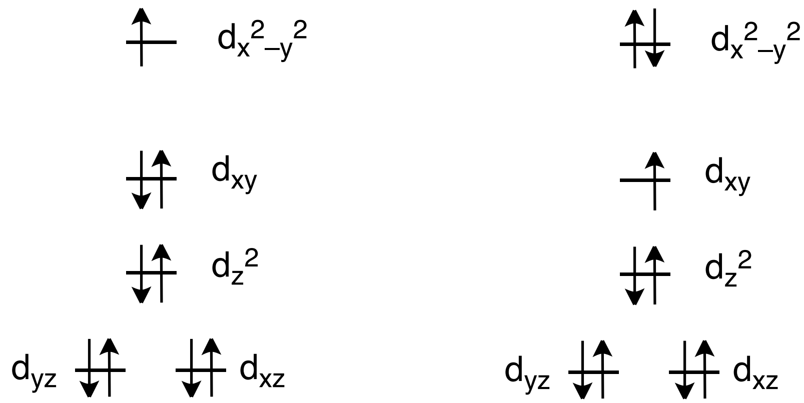

ground state

coupling excited state

Electron Paramagnetic Resonance Spectroscopy

Cu^{II}: d^9, square planar

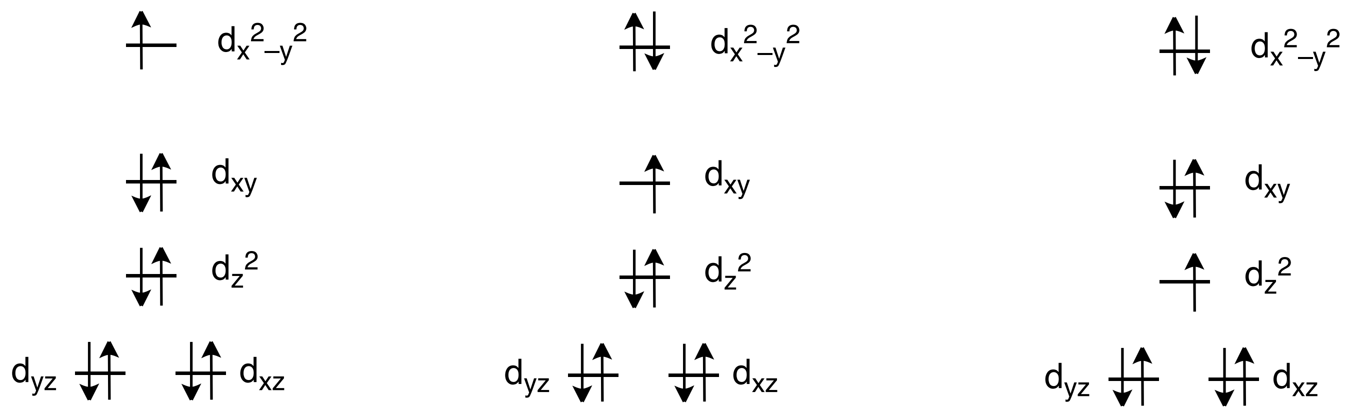

ground state

coupling excited state

d_{z^2} does not couple

orbitals have incorrect symmetry

Electron Paramagnetic Resonance Spectroscopy

Cu^{II}: d^9, square planar

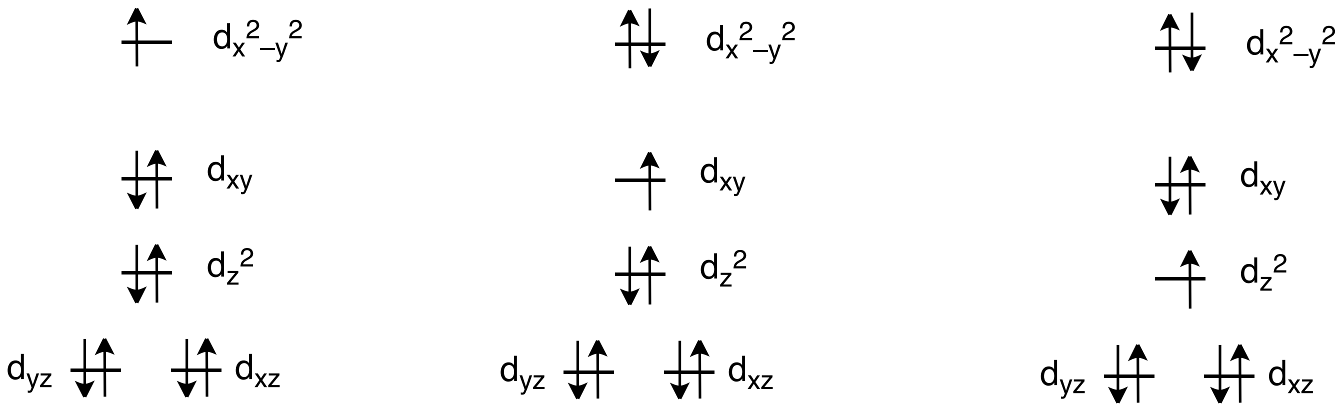

ground state

coupling excited state

d_{z^2} does not couple

orbitals have incorrect symmetry

$$g_{obs} = g_e - \frac{x\lambda}{\Delta E}$$

Electron Paramagnetic Resonance Spectroscopy

Cu^{II}: d^9, square planar

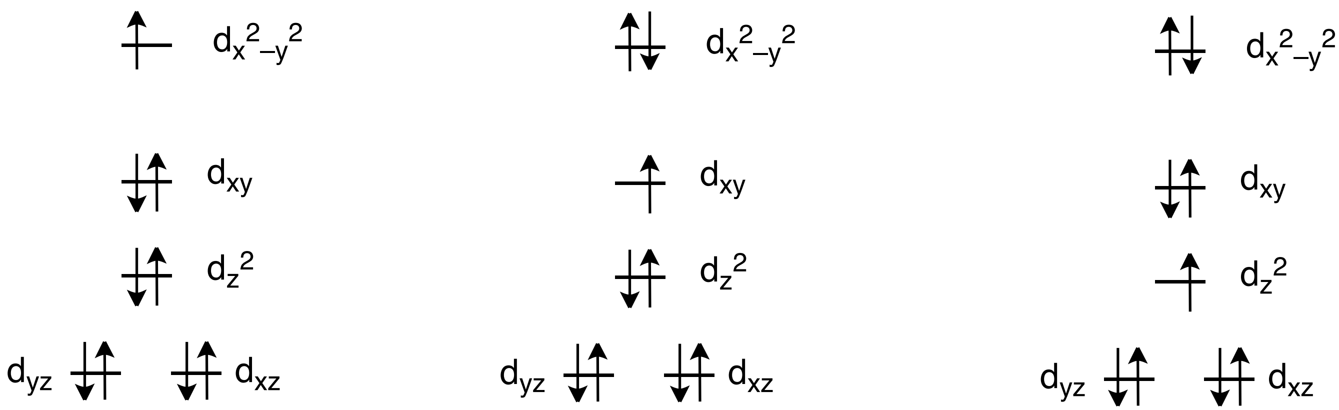

ground state

coupling excited state

d_{z^2} does not couple
orbitals have incorrect symmetry

$$g_{obs} = g_e - \frac{x\lambda}{\Delta E}$$

g_{obs}: empirical value from spectrum

g_e: energy of free electron (2.00023)

Electron Paramagnetic Resonance Spectroscopy

Cu^{II}: d^9, square planar

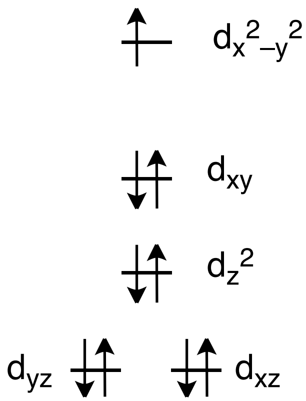

ground state

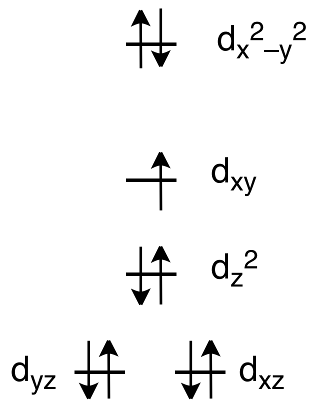

coupling excited state

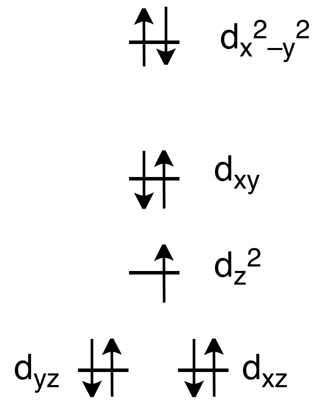

d_{z^2} does not couple

orbitals have incorrect symmetry

$$g_{obs} = g_e - \frac{x\lambda}{\Delta E}$$

g_{obs}: empirical value from spectrum

g_e: energy of free electron (2.00023)

x: modification factor of the free electron based on orbital mixing

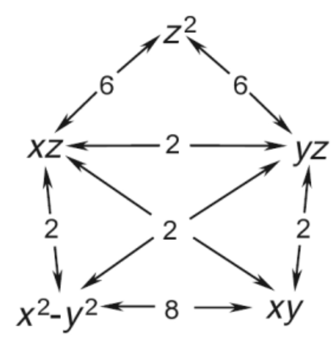

'Magic pentagon'

Electron Paramagnetic Resonance Spectroscopy

Cu^{II}: d^9, square planar

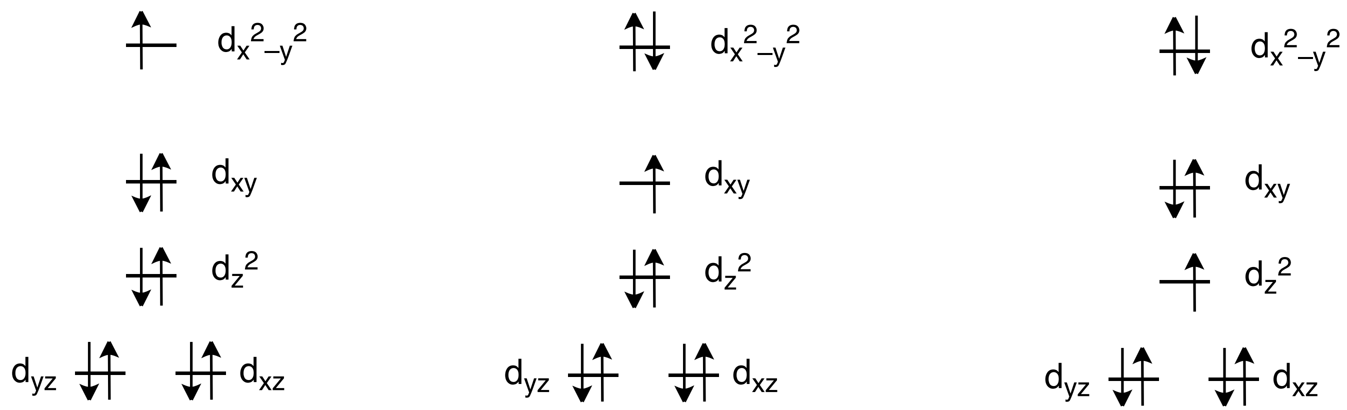

ground state

coupling excited state

d_{z^2} does not couple

orbitals have incorrect symmetry

$$g_{obs} = g_e - \frac{x\lambda}{\Delta E}$$

g_{obs}: empirical value from spectrum

g_e: energy of free electron (2.00023)

x: modification factor of the free electron based on orbital mixing

λ: spin orbit coupling constant

ΔE: energy between two orbitals

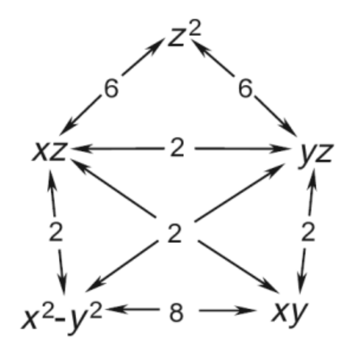

'Magic pentagon'

Chan-Evans-Lam Coupling

initial rates experiment reveals turnover-limiting step

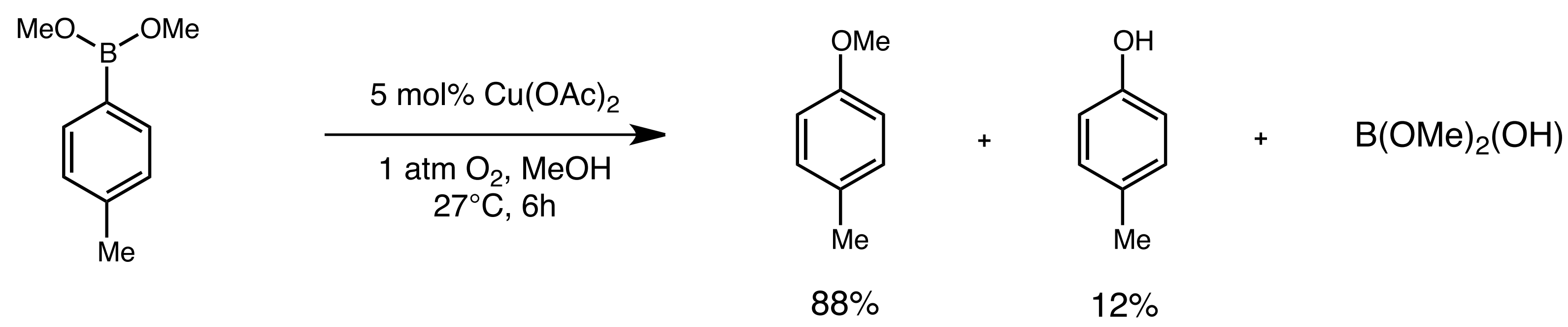

EPR spectroscopy shows catalyst resting state as Cu^{II}

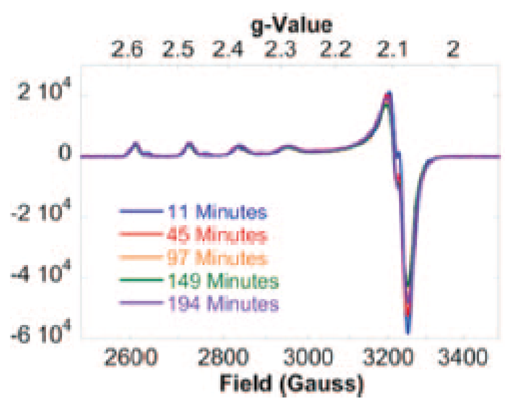

no strong field aryl ligand evident consistent with transmetalation being as turnover-limiting

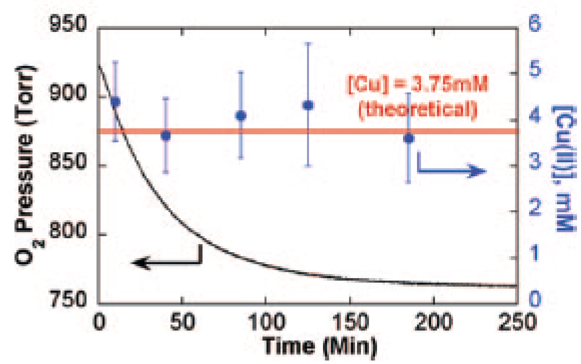

reaction progress correlated with EPR spectra

King, A. E.; Brunold, T. C.; Stahl. S. S. *J. Am. Chem. Soc.* **2009**, *131*, 5044–5045

Chan-Evans-Lam Coupling

equilibrium prior to transmetalation

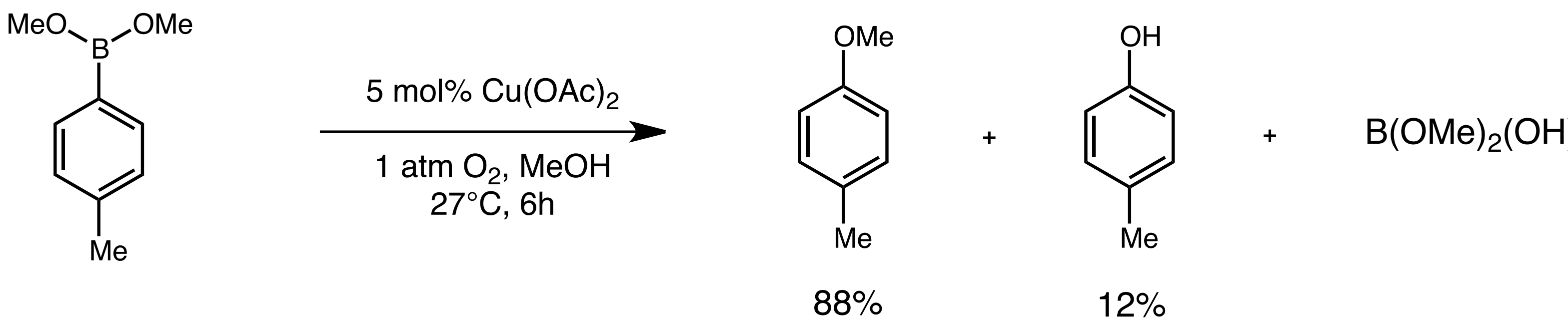

King, A. E.; Ryland, B. L.; Brunold, T. C.; Stahl, S. S. *Organometallics,* **2012**, *31*, 7948.

Chan-Evans-Lam Coupling

equilibrium prior to transmetalation

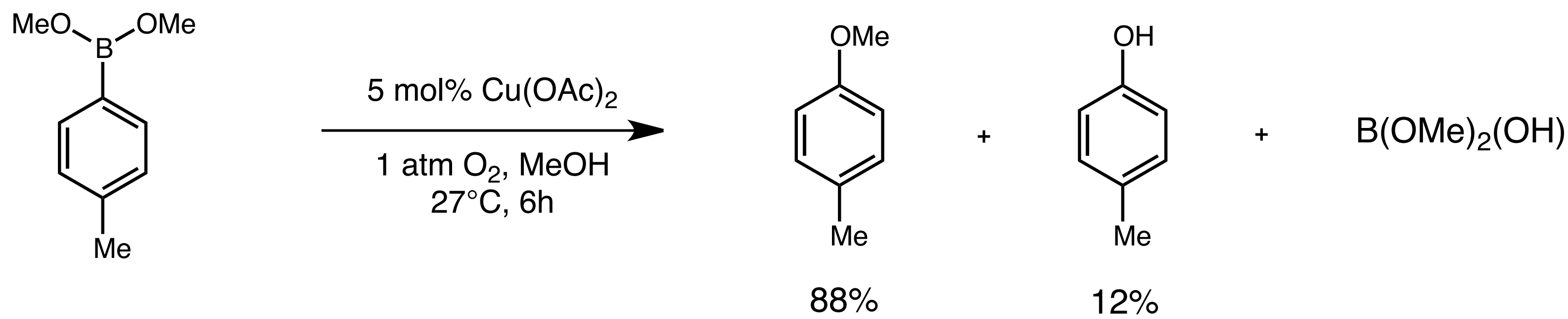

deviation from standard conditions	effect on efficiency
added acetate	inhibition
added acetic acid	inhibition
$Cu(ClO_4)_2$ instead of $Cu(OAc)_2$	no reactivity

King, A. E.; Ryland, B. L.; Brunold, T. C.; Stahl, S. S. *Organometallics,* **2012**, *31*, 7948.

Chan-Evans-Lam Coupling

equilibrium prior to transmetalation

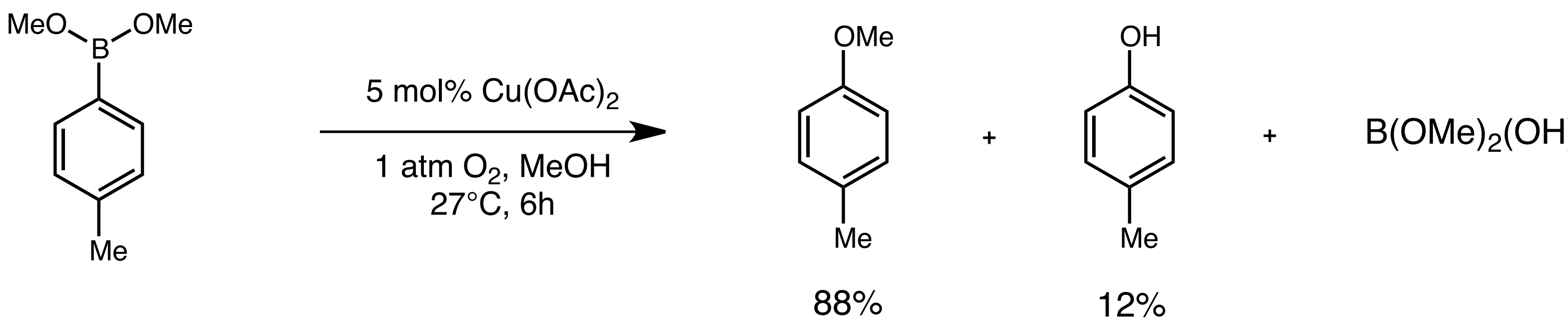

deviation from standard conditions	effect on efficiency
added acetate	inhibition
added acetic acid	inhibition
$Cu(ClO_4)_2$ instead of $Cu(OAc)_2$	no reactivity
$Cu(ClO_4)_2$ + 1 equiv NaOAc	rate acceleration
$Cu(ClO_4)_2$ + 1 equiv NaOMe	rate acceleration

King, A. E.; Ryland, B. L.; Brunold, T. C.; Stahl, S. S. *Organometallics,* **2012**, *31*, 7948.

Chan-Evans-Lam Coupling

EPR spectroscopy

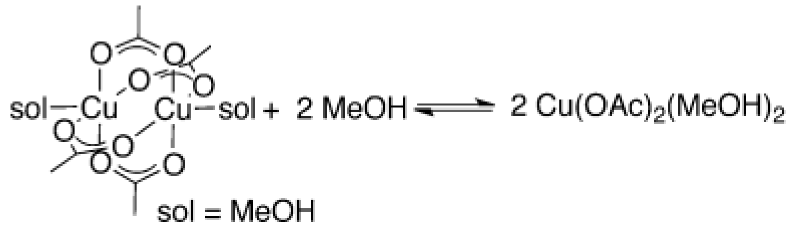

King, A. E.; Ryland, B. L.; Brunold, T. C.; Stahl, S. S. *Organometallics,* **2012**, *31*, 7948.

Chan-Evans-Lam Coupling

EPR spectroscopy

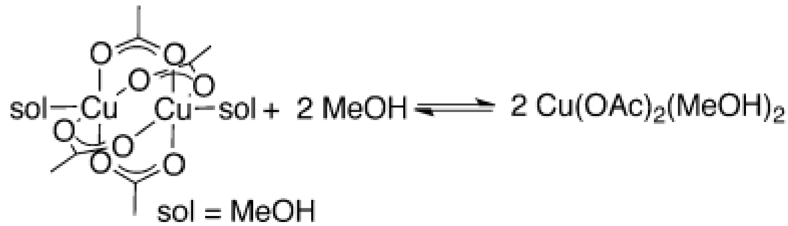

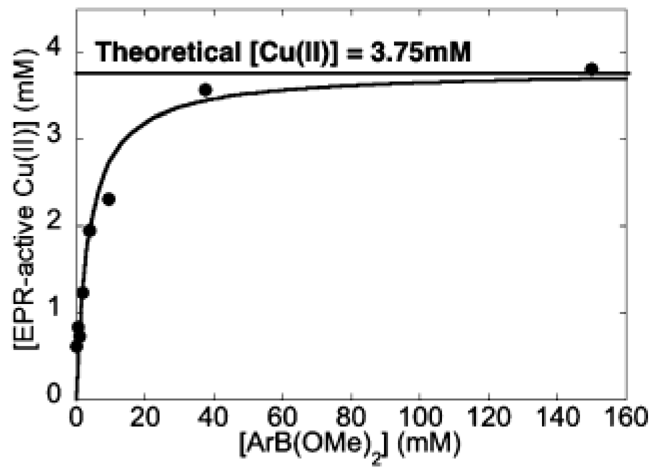

EPR signals appears after addition of boronic ester

King, A. E.; Ryland, B. L.; Brunold, T. C.; Stahl, S. S. *Organometallics,* **2012**, *31*, 7948.

Chan-Evans-Lam Coupling

EPR spectroscopy

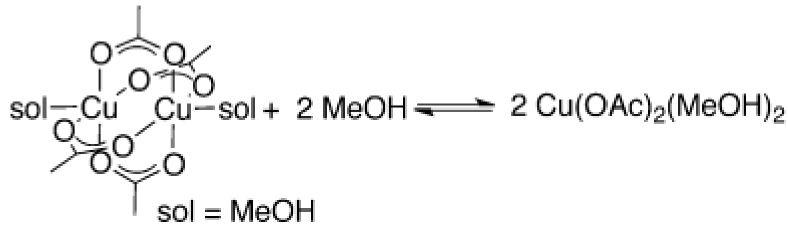

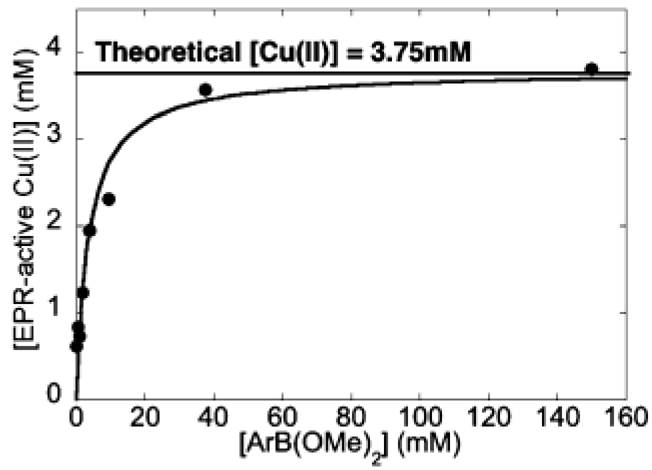

EPR signals appears after addition of boronic ester

exhibits a saturation depedence on concentration of ester

King, A. E.; Ryland, B. L.; Brunold, T. C.; Stahl, S. S. *Organometallics,* **2012**, *31*, 7948.

Chan-Evans-Lam Coupling

EPR spectroscopy

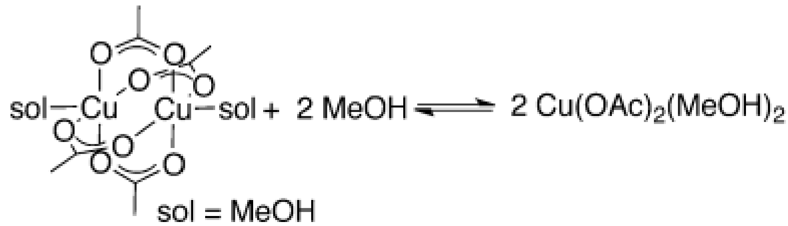

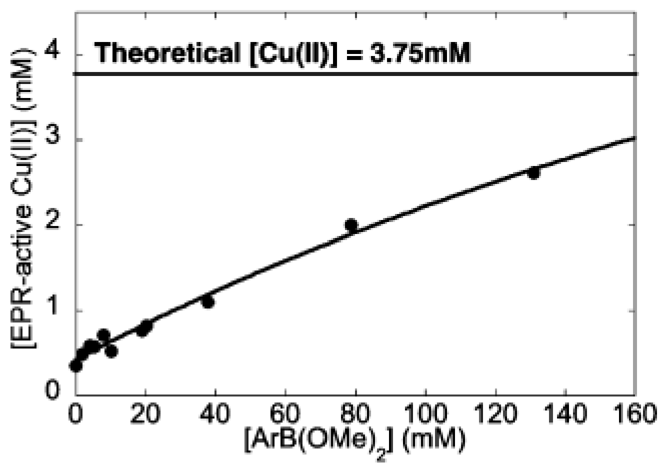

acetic acid additive

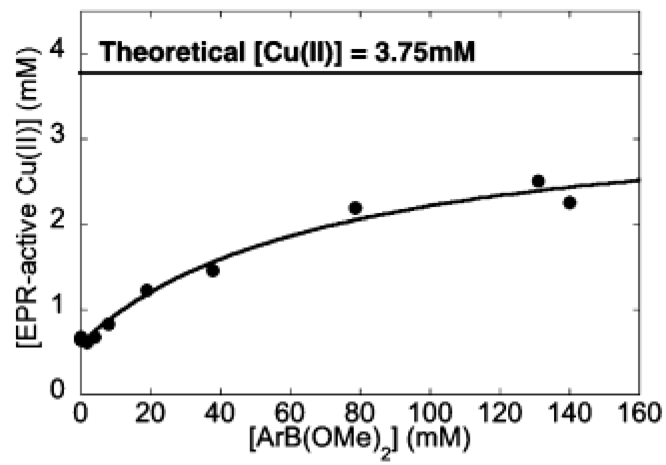

sodium acetate additive

both display an inhibitory effect on EPR signal

suggesting that paddlewheel structure is stabilized

King, A. E.; Ryland, B. L.; Brunold, T. C.; Stahl, S. S. *Organometallics,* **2012**, *31*, 7948.

Chan-Evans-Lam Coupling

EPR spectroscopy

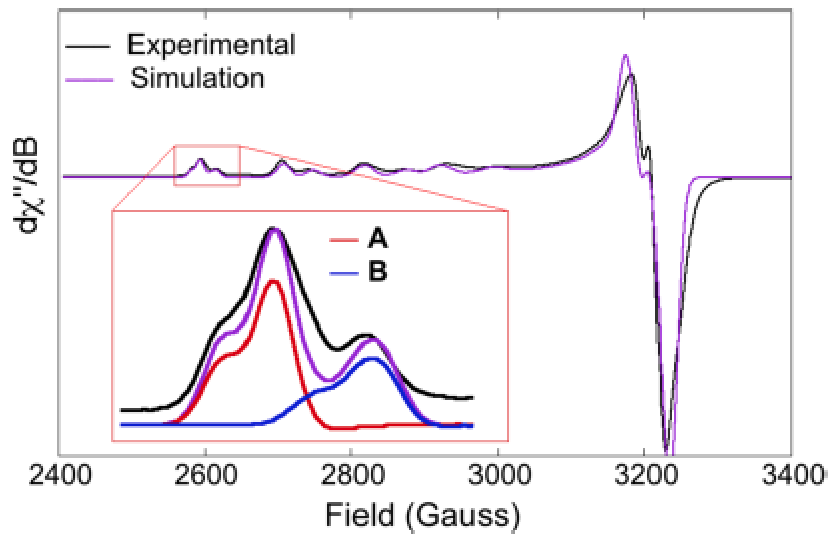

EPR signal obtained immediately after mixing $Cu(OAc)_2$ and boronic ester displays two species

King, A. E.; Ryland, B. L.; Brunold, T. C.; Stahl, S. S. *Organometallics,* **2012**, *31*, 7948.

Chan-Evans-Lam Coupling

EPR spectroscopy

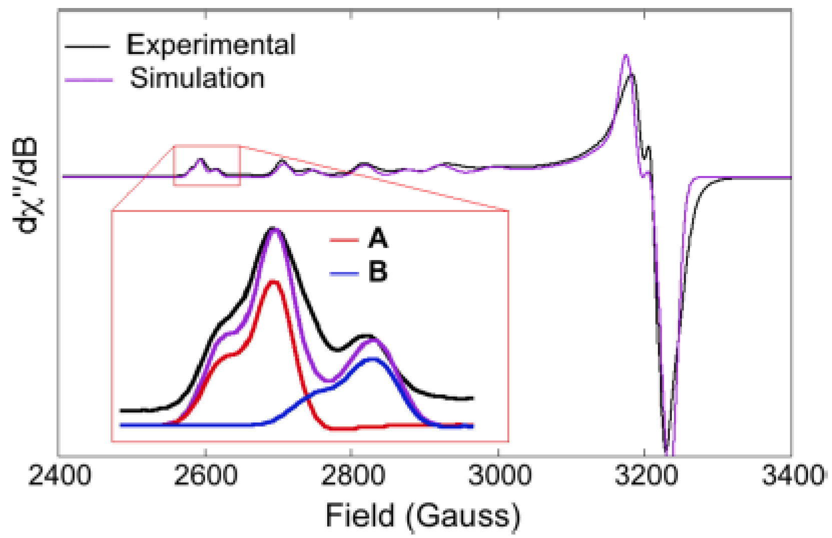

EPR signal obtained immediately after mixing $Cu(OAc)_2$ and boronic ester displays two species

relative concentrations of the two species are altered by the addition of additives

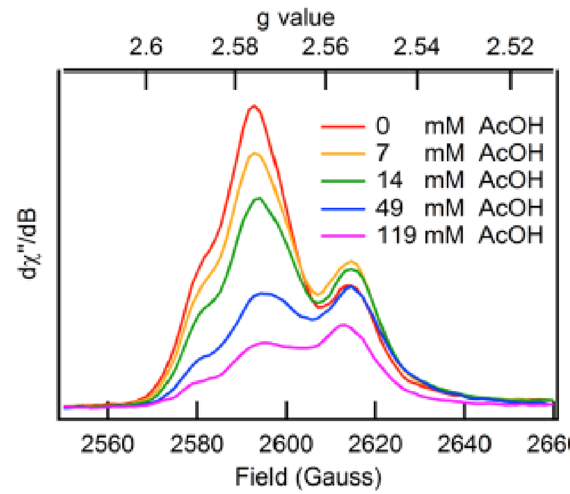

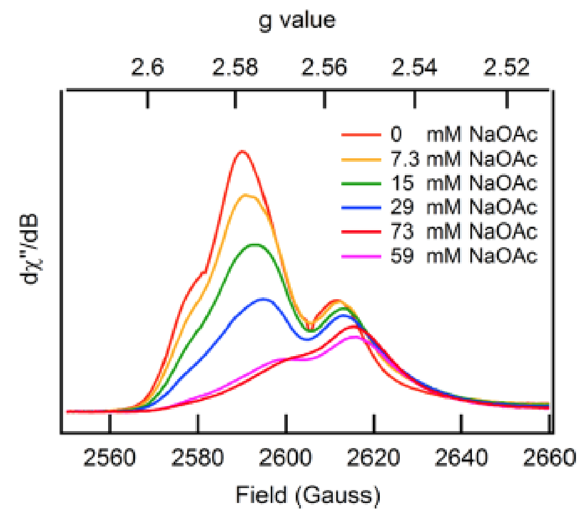

King, A. E.; Ryland, B. L.; Brunold, T. C.; Stahl, S. S. *Organometallics,* **2012**, *31*, 7948.

Chan-Evans-Lam Coupling

mechanism of transmetalation

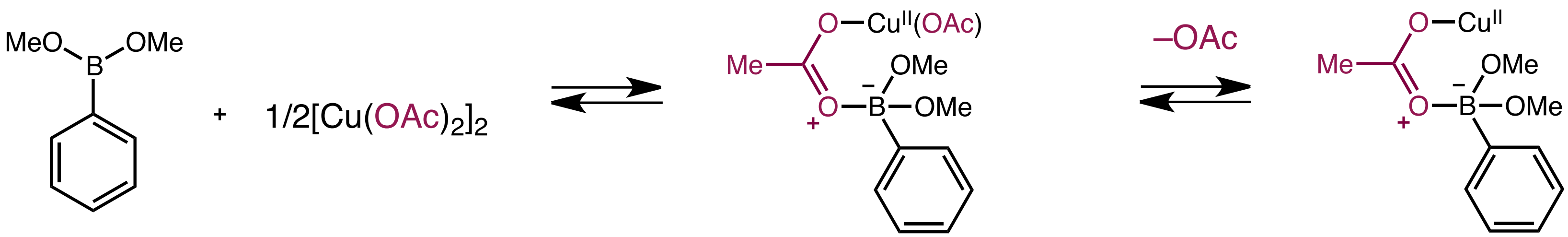

inhibitory effect of added acetate

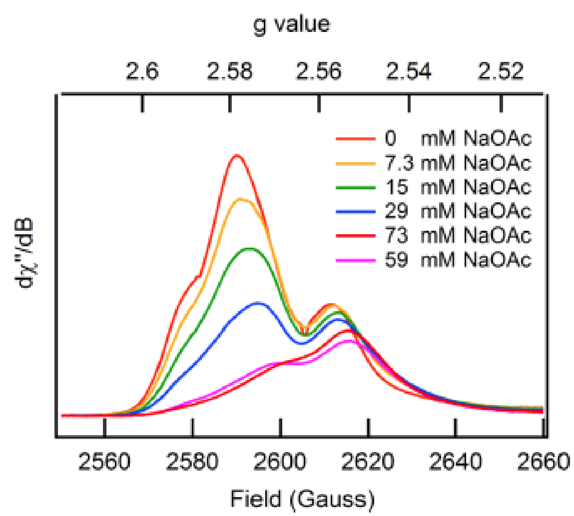

King, A. E.; Ryland, B. L.; Brunold, T. C.; Stahl, S. S. *Organometallics,* **2012**, *31*, 7948.

Chan-Evans-Lam Coupling

mechanism of transmetalation

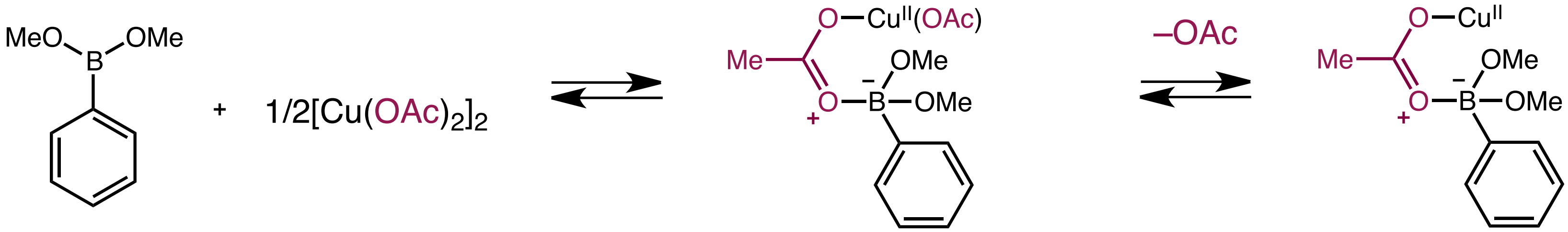

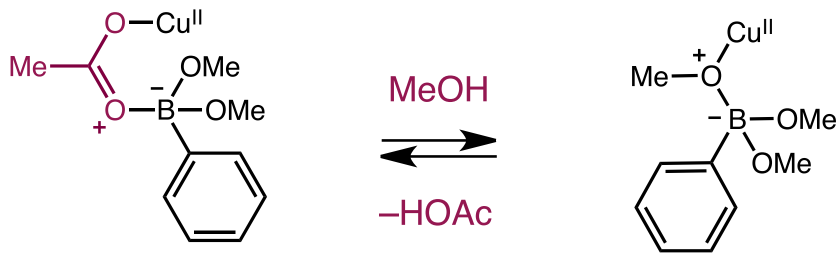

inhibitory effect of added acetic acid

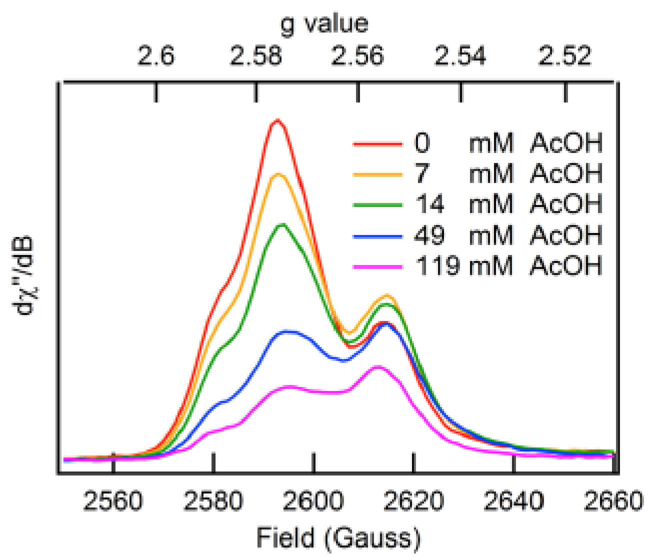

King, A. E.; Ryland, B. L.; Brunold, T. C.; Stahl, S. S. *Organometallics,* **2012**, *31*, 7948.

Chan-Evans-Lam Coupling

mechanism of transmetalation

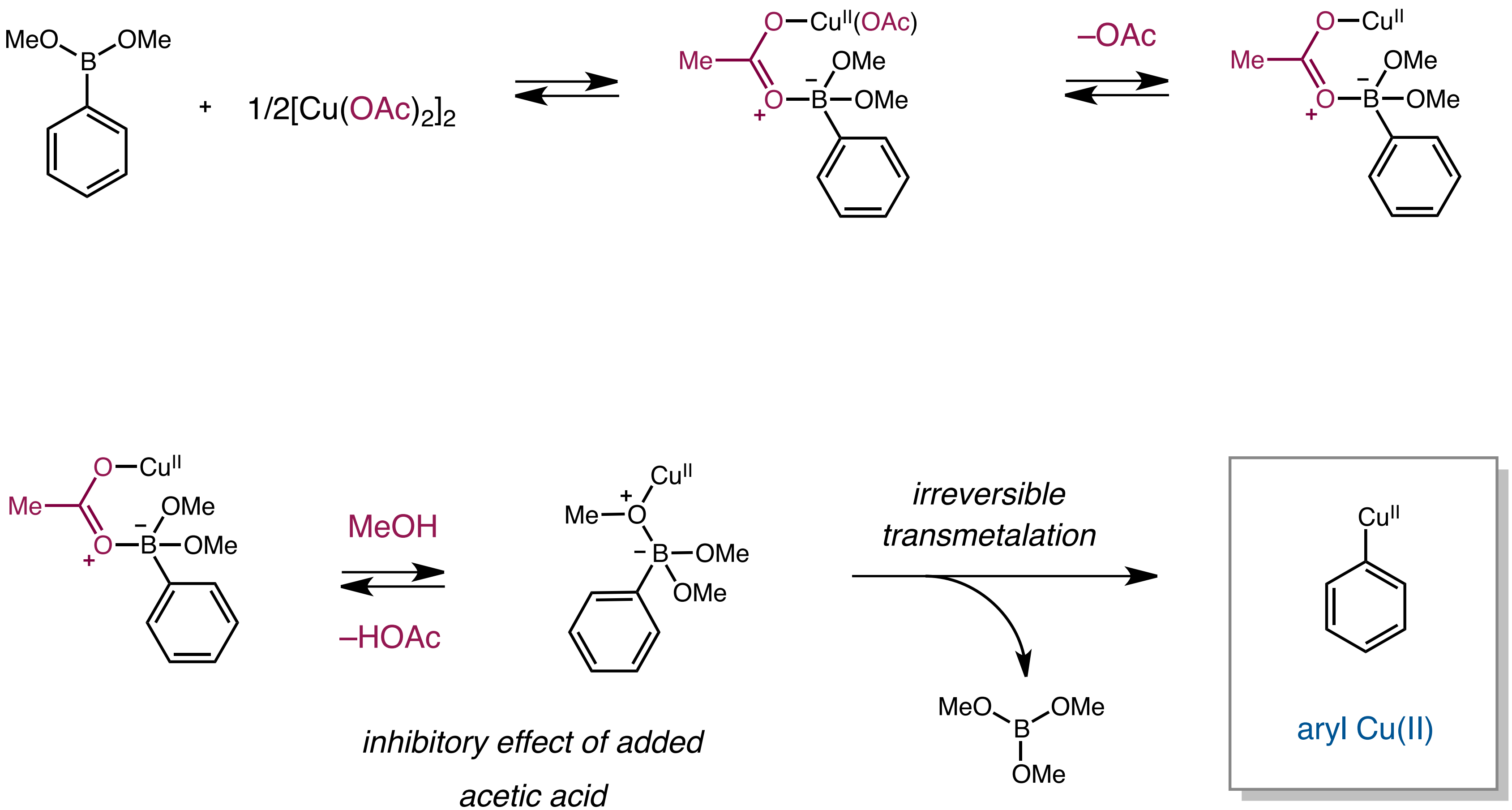

King, A. E.; Ryland, B. L.; Brunold, T. C.; Stahl, S. S. *Organometallics,* **2012**, *31*, 7948.

Chan-Evans-Lam Coupling

mechanism of oxidative coupling

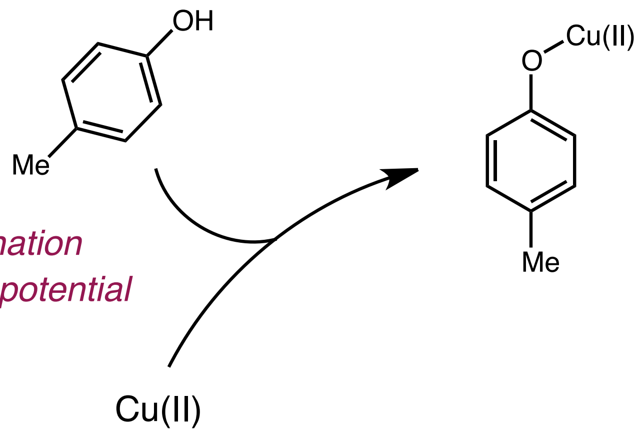

nucleophile coordination lowersCu^{II}/Cu^{III} redox potential

Copper Oxidase mechanism

King, A. E.; Ryland, B. L.; Brunold, T. C.; Stahl, S. S. *Organometallics,* **2012**, *31*, 7948.

Chan-Evans-Lam Coupling

mechanism of oxidative coupling

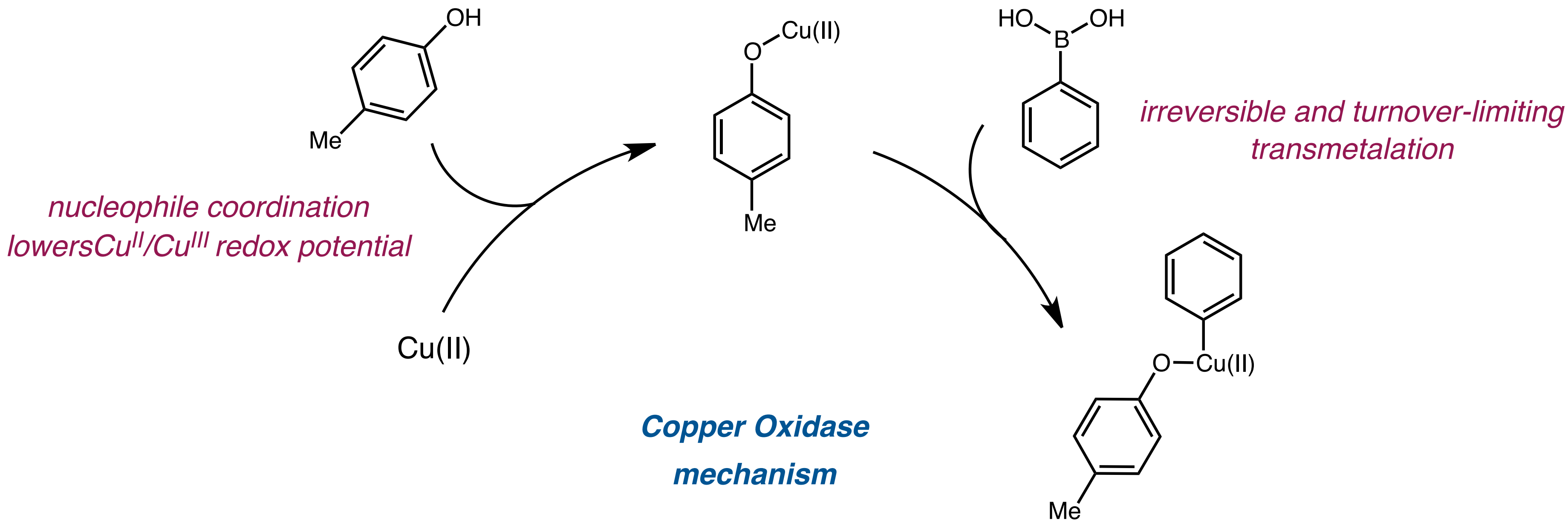

King, A. E.; Ryland, B. L.; Brunold, T. C.; Stahl, S. S. *Organometallics,* **2012**, *31*, 7948.

Chan-Evans-Lam Coupling

mechanism of oxidative coupling

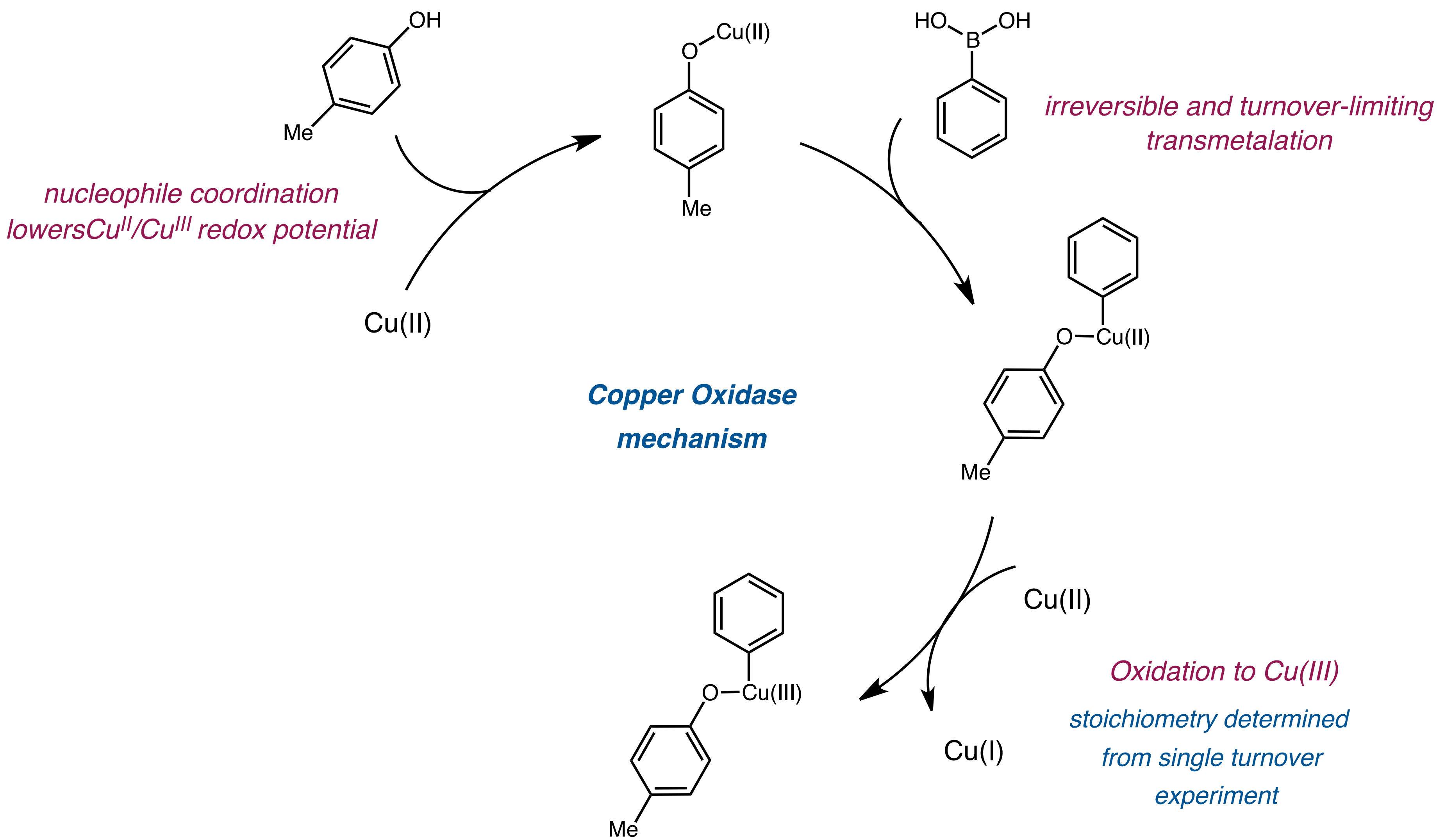

King, A. E.; Ryland, B. L.; Brunold, T. C.; Stahl, S. S. *Organometallics,* **2012**, *31*, 7948.

Chan-Evans-Lam Coupling

mechanism of oxidative coupling

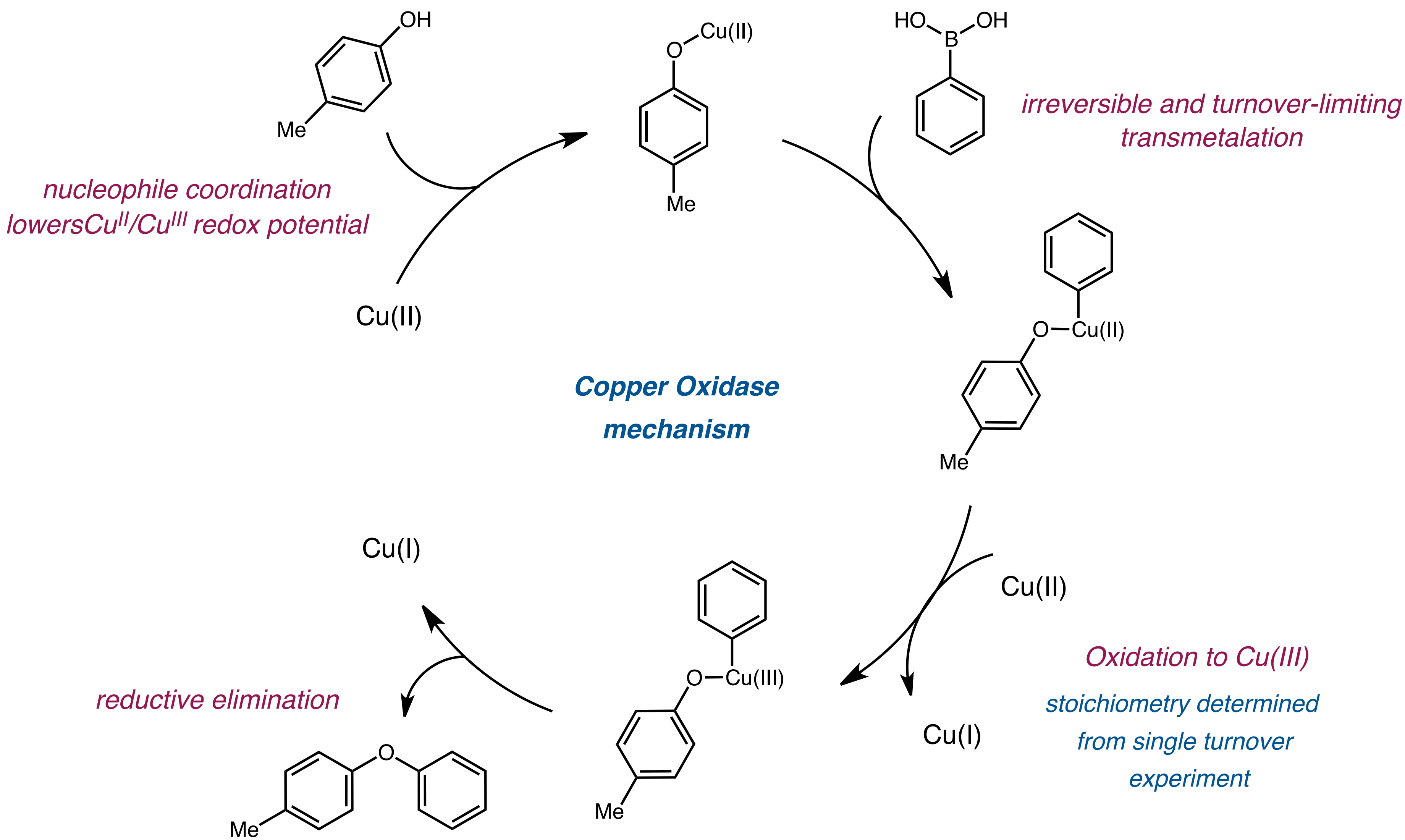

King, A. E.; Ryland, B. L.; Brunold, T. C.; Stahl, S. S. *Organometallics,* **2012**, *31*, 7948.

Chan-Evans-Lam Coupling

mechanism of oxidative coupling

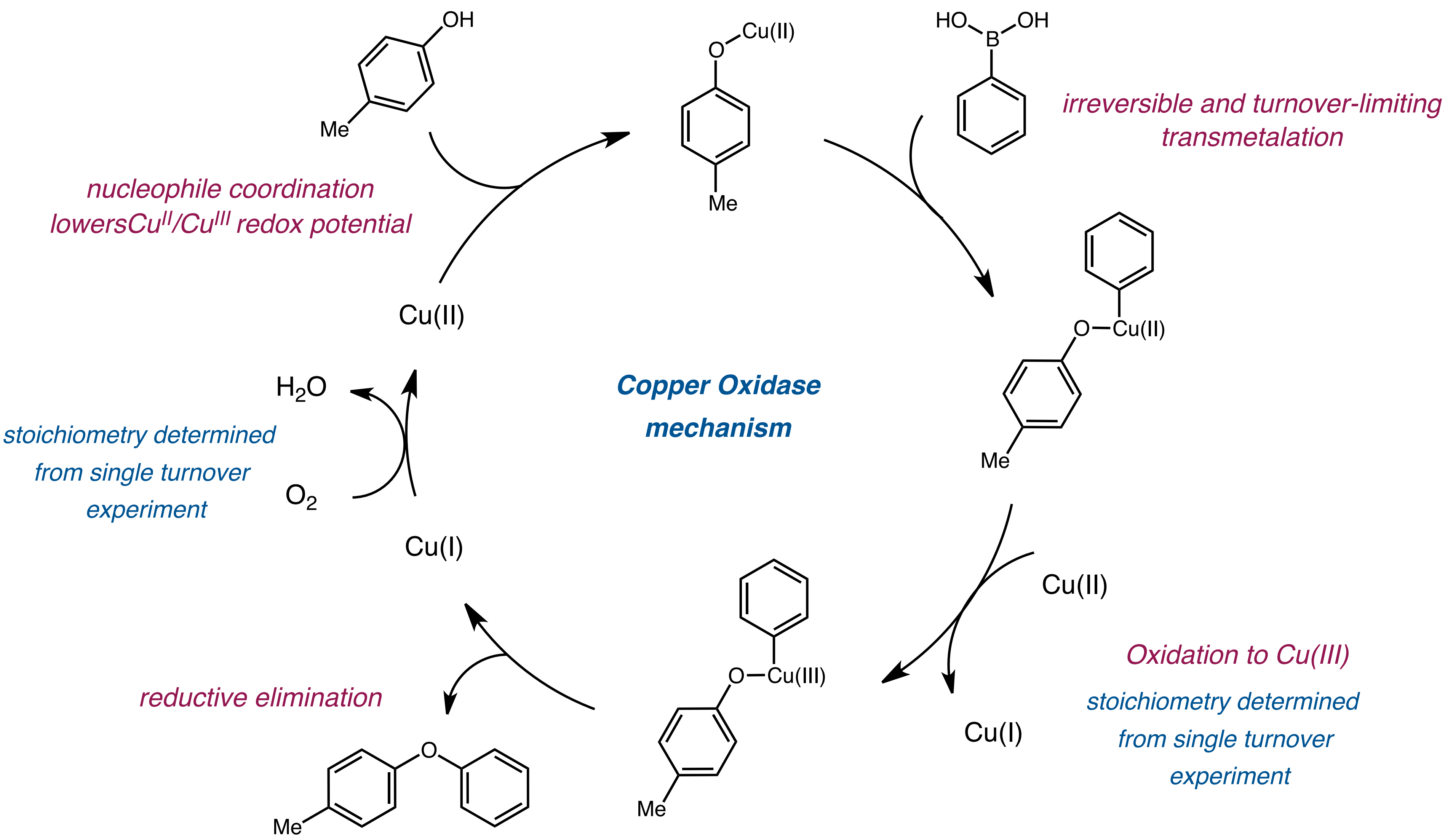

King, A. E.; Ryland, B. L.; Brunold, T. C.; Stahl, S. S. *Organometallics,* **2012**, *31*, 7948.

Copper in Cross-Coupling Reactions

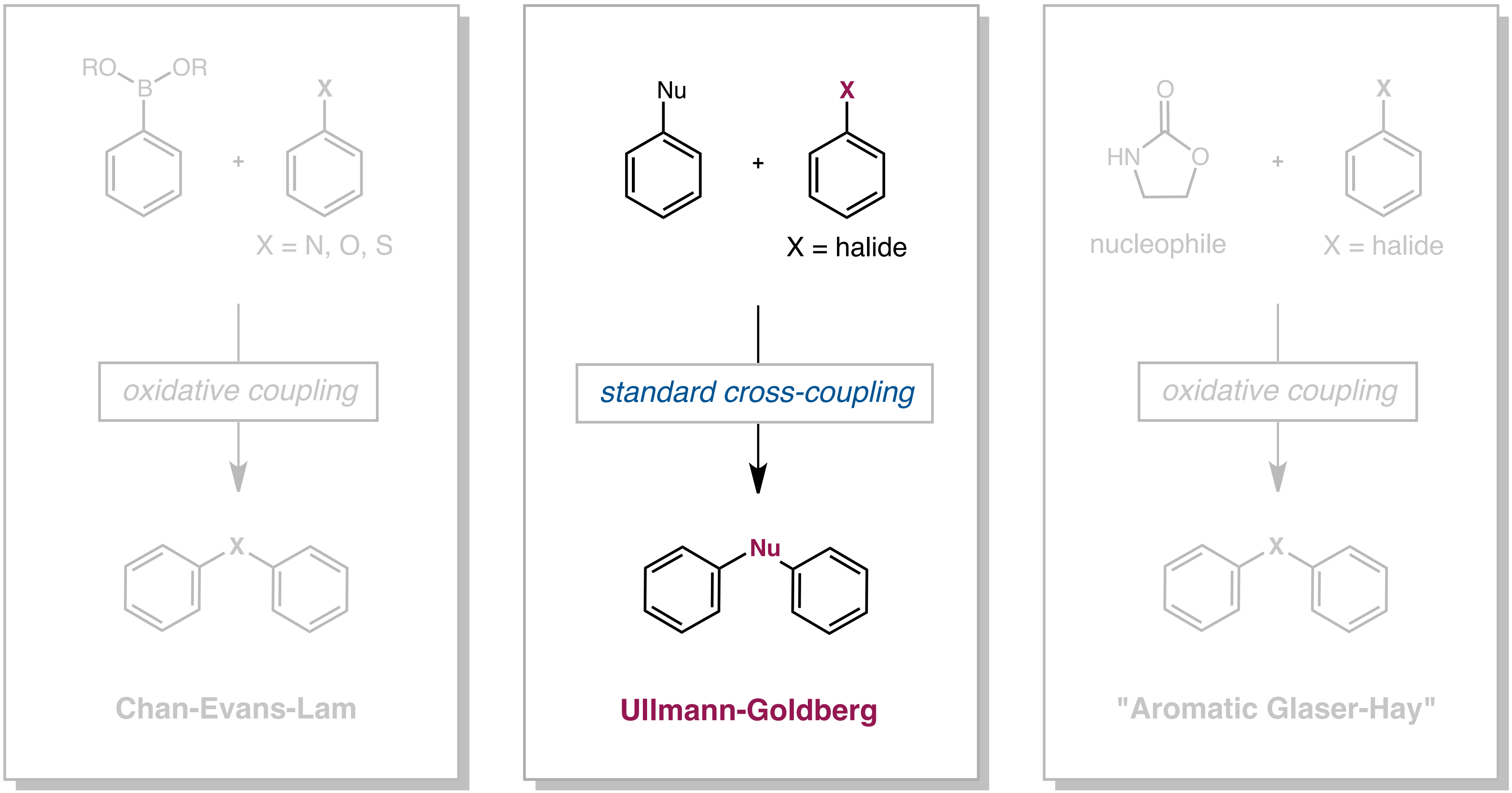

Ullmann-Goldberg Reaction

cross-coupling reaction mediated by Cu^{I}/Cu^{III} redox cycle

Classic Ullmann-Goldberg reaction

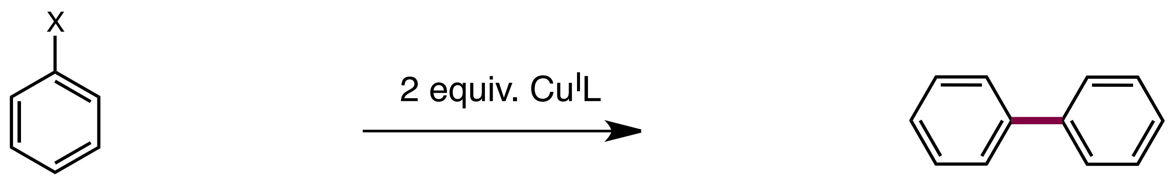

2 equiv.

X = Br, Cl, I

symmetric biaryl bond

Ullmann-Goldberg Reaction

cross-coupling reaction mediated by Cu^{I}/Cu^{III} redox cycle

Classic Ullmann-Goldberg reaction

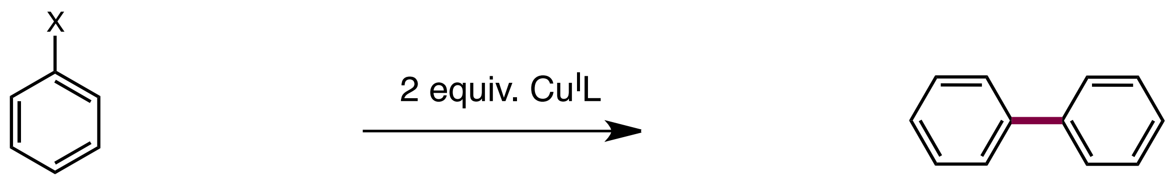

2 equiv.

X = Br, Cl, I

symmetric biaryl bond

Ullmann-type coupling

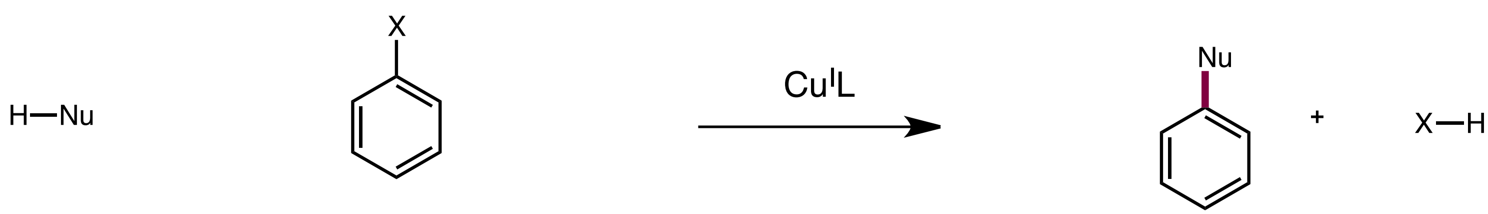

X = Br, Cl, I

C–heteroatom bond

Ullmann-Goldberg Reaction

cross-coupling reaction mediated by Cu^{I}/Cu^{III} redox cycle

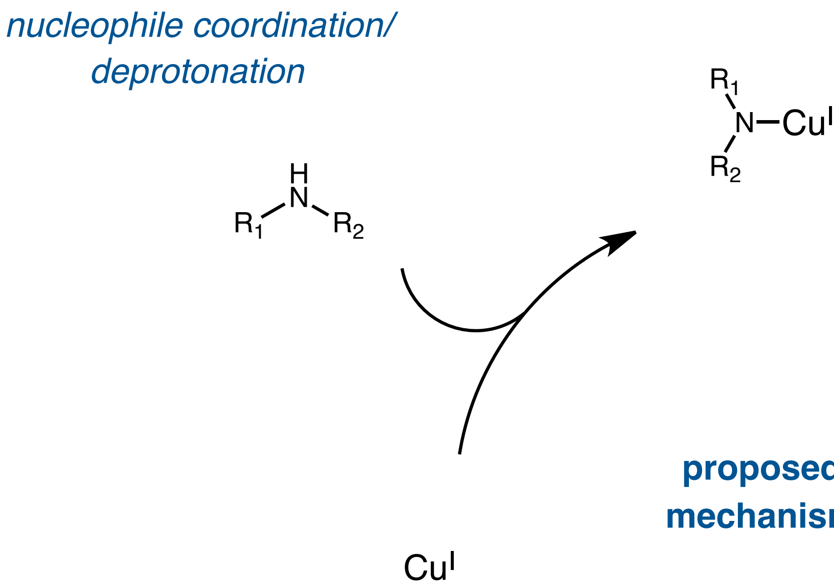

proposed mechanism

Ullmann-Goldberg Reaction

cross-coupling reaction mediated by Cu^{I}/Cu^{III} redox cycle

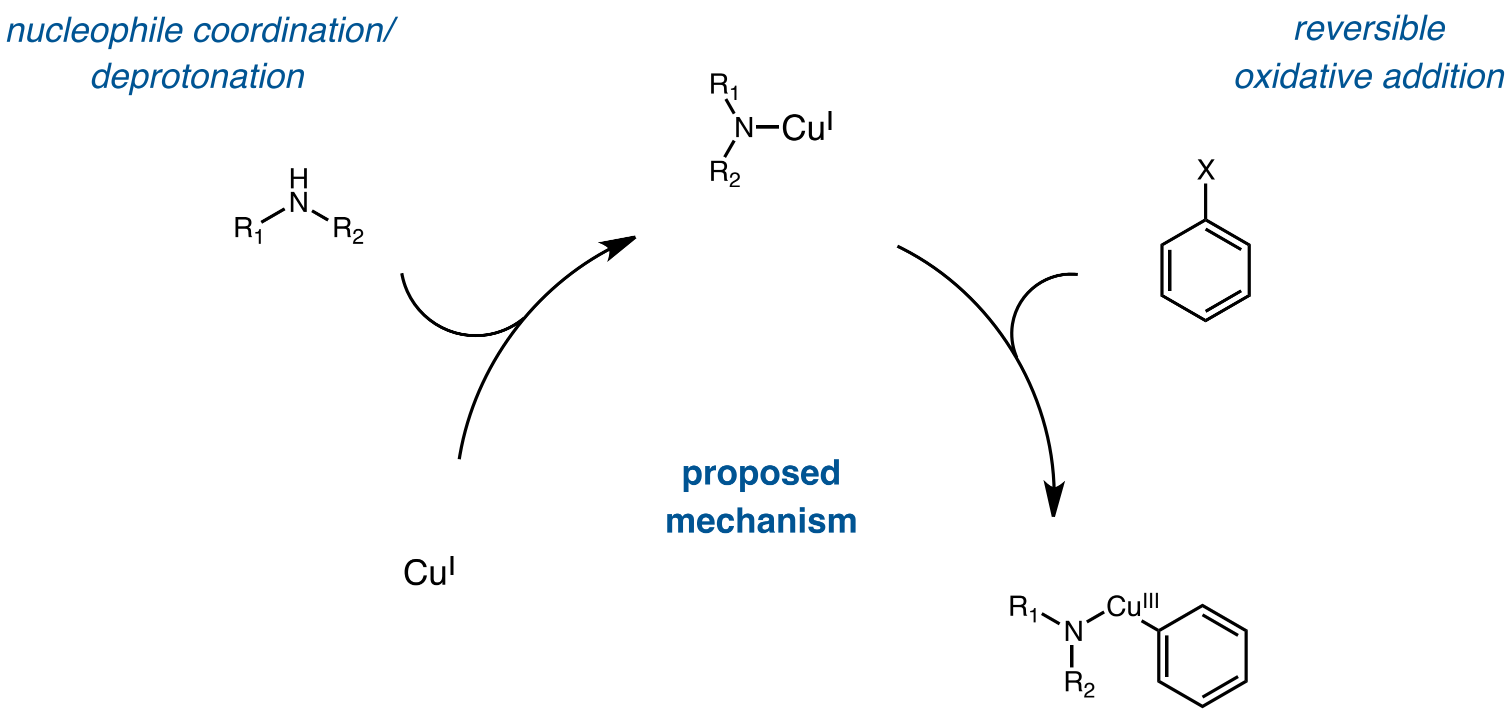

Ullmann-Goldberg Reaction

cross-coupling reaction mediated by Cu^{I}/Cu^{III} redox cycle

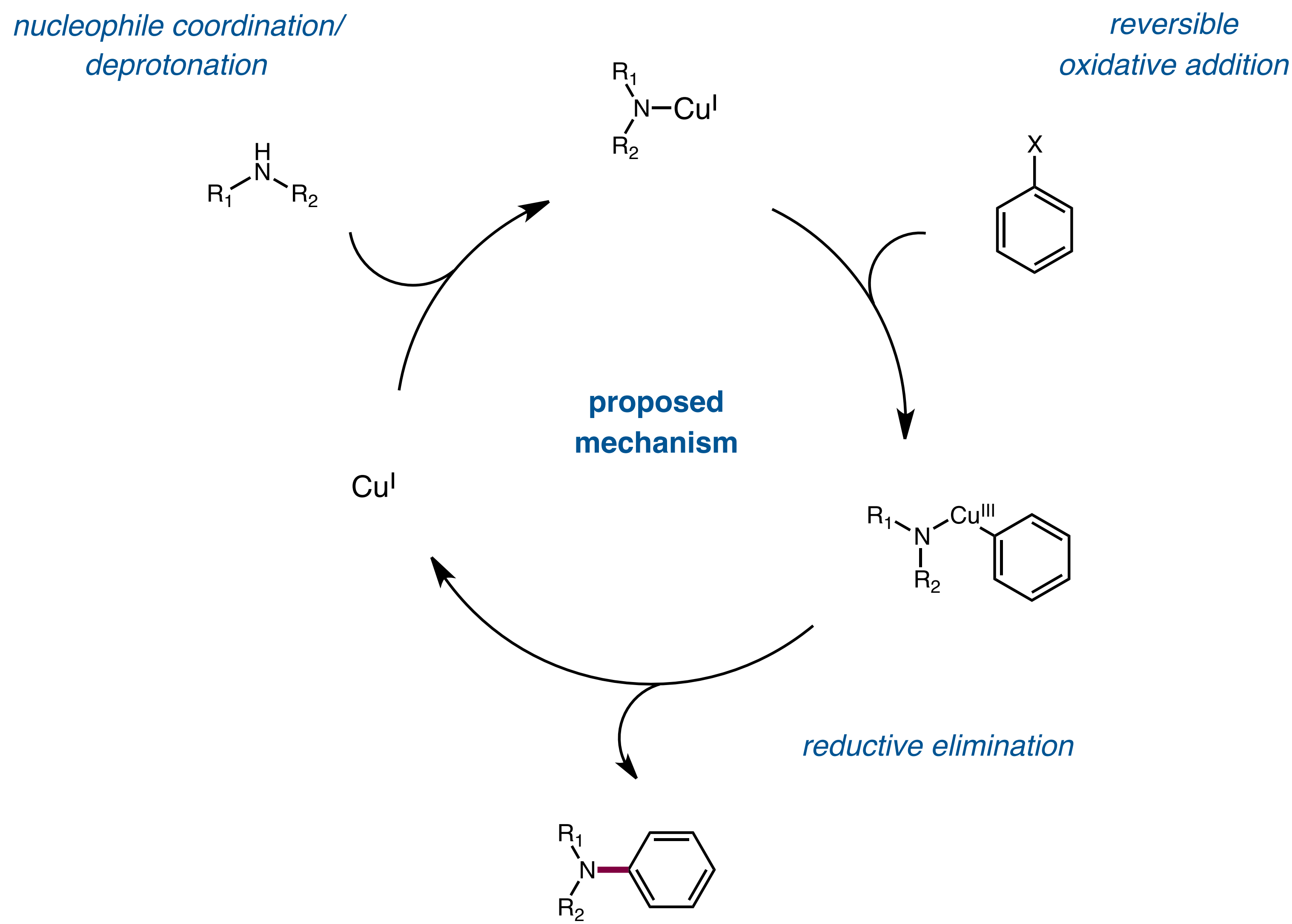

Ullmann-Goldberg Reaction

cross-coupling reaction mediated by Cu^{I}/Cu^{III} redox cycle

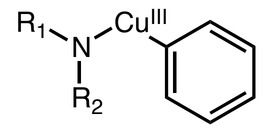

putative aryl Cu^{III}

- Cu^{III} has been widely proposed as an intermediate
- oxidative addition product has never been observed
- oxidative addition to Cu has no precedent

Ullmann-Goldberg Reaction

cross-coupling reaction mediated by Cu^{I}/Cu^{III} redox cycle

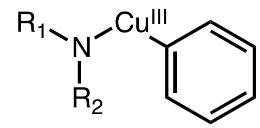

putative aryl Cu^{III}

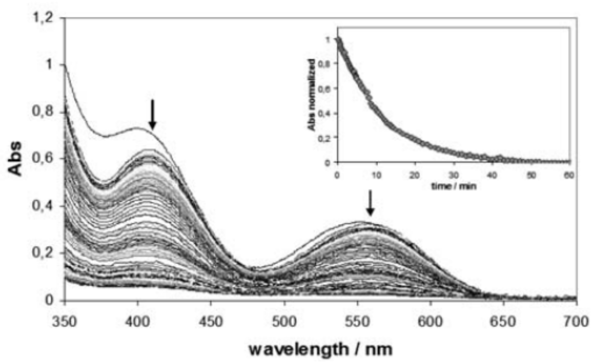

UV-Vis spectroscopy

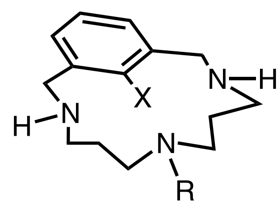

utilization of constraining macrocyclic ligands

(NMR, CV, X-ray)

$$d[Ar_2]/dt = k_{Ar_2}[ArBr]^2[Cu^{I}]$$

$$d[ArH]/dt = k_{H}[ArBr][Cu^{I}]$$

kinetics

Ullmann-Goldberg Reaction

kinetics reveal reversible oxidative addition

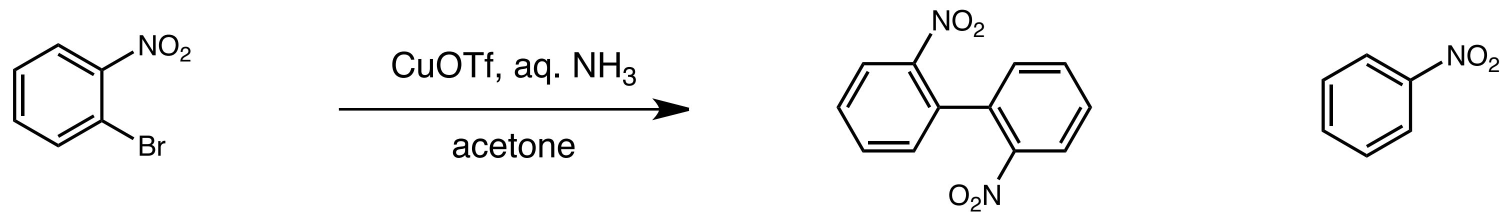

Cohen, T.; Cristea, I. *J. Am. Chem. Soc.* **1976**, *98*, 748–753

Ullmann-Goldberg Reaction

kinetics reveal reversible oxidative addition

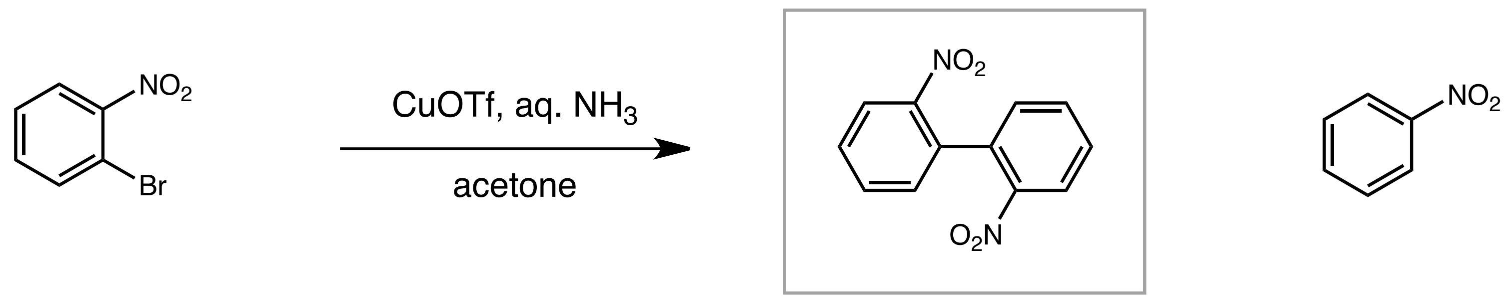

formation of 2, 2'-dinitro-biphenyl:

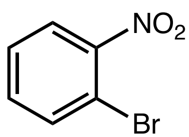

2^{nd} order dependence

CuOTf

1^{st} order

formation of nitrobenzene:

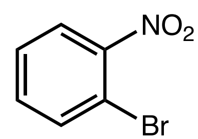

1^{st} order

CuOTf

1^{st} order

Cohen, T.; Cristea, I. *J. Am. Chem. Soc.* **1976**, *98*, 748–753

Ullmann-Goldberg Reaction

kinetics reveal reversible oxidative addition

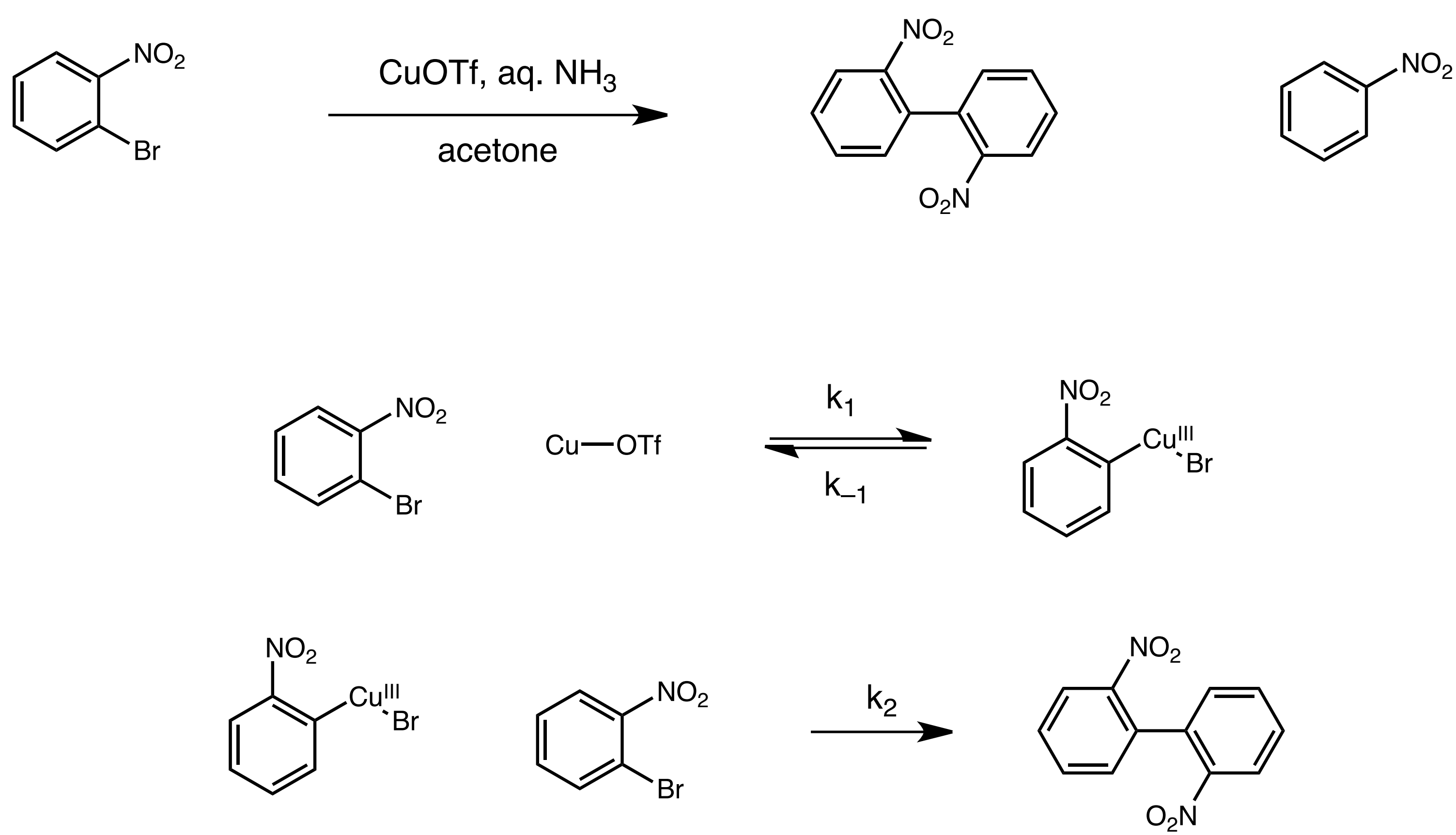

Cohen, T.; Cristea, I. *J. Am. Chem. Soc.* **1976**, *98*, 748–753

Ullmann-type Coupling Reaction

direction observation of Cu^{I}/Cu^{III} redox steps

Ribas and Stahl's strategy:

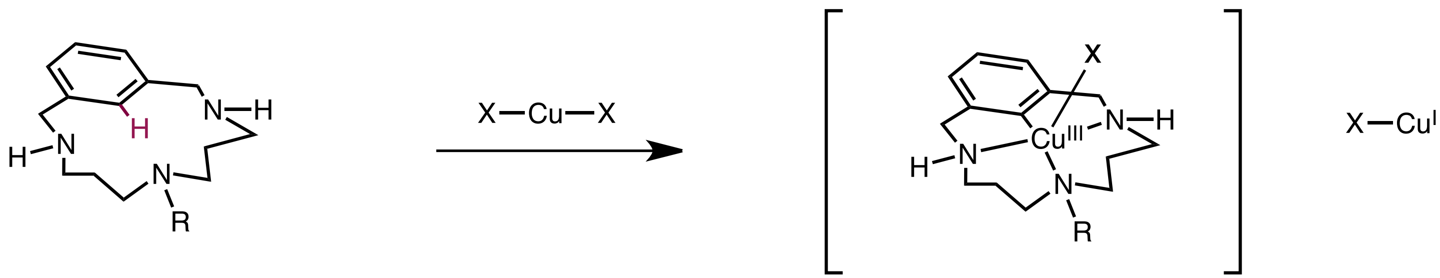

macrocyclic ligand shown to undergo C–H insertion with Cu

highly constrained and stabilized aryl Cu^{III} species

Casitas, A.; King, A. E.; Parella, T.; Costas, M.; Stahl, S. S.; Ribas, X. *Chem Sci.* **2010**, *1*, 326–330

Ullmann-type Coupling Reaction

direction observation of Cu^{I}/Cu^{III} redox steps

Ribas and Stahl's strategy:

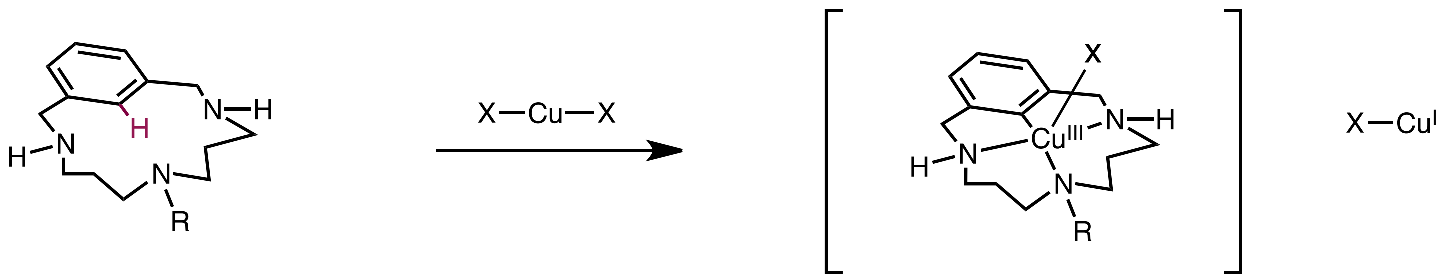

macrocyclic ligand shown to undergo C–H insertion with Cu

highly constrained and stabilized aryl Cu^{III} species

- allows for characterization by ^{1}H NMR, CV and UV-Vis
- allows for study of reductive elmination

Casitas, A.; King, A. E.; Parella, T.; Costas, M.; Stahl, S. S.; Ribas, X. *Chem Sci.* **2010**, *1*, 326–330

Ullmann-type Coupling Reaction

direction observation of Cu^{I}/Cu^{III} redox steps

Ribas and Stahl's strategy:

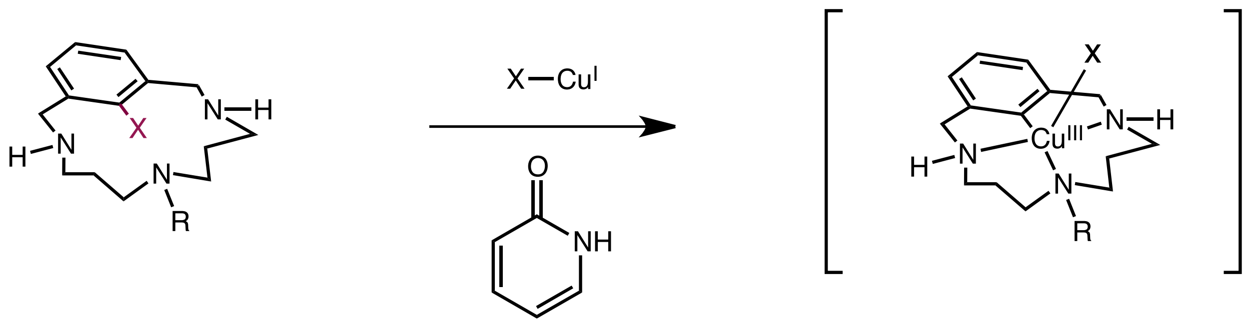

Casitas, A.; King, A. E.; Parella, T.; Costas, M.; Stahl, S. S.; Ribas, X. *Chem Sci.* **2010**, *1*, 326–330

Ullmann-type Coupling Reaction

direction observation of Cu^{I}/Cu^{III} redox steps

Ribas and Stahl's strategy:

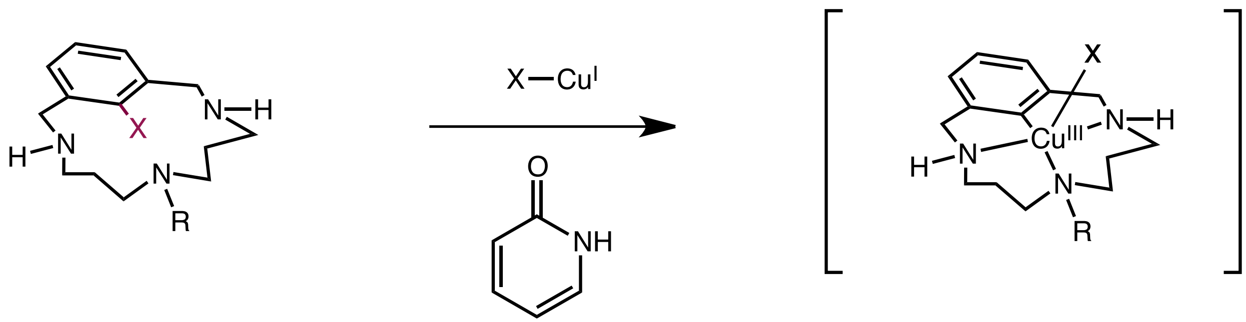

- allows for study of oxidative addition
- allows for study of mechanism of C–N bond formation

Casitas, A.; King, A. E.; Parella, T.; Costas, M.; Stahl, S. S.; Ribas, X. *Chem Sci.* **2010**, *1*, 326–330

Ullmann-type Coupling Reaction

characterization of aryl-Cu^{III} complex

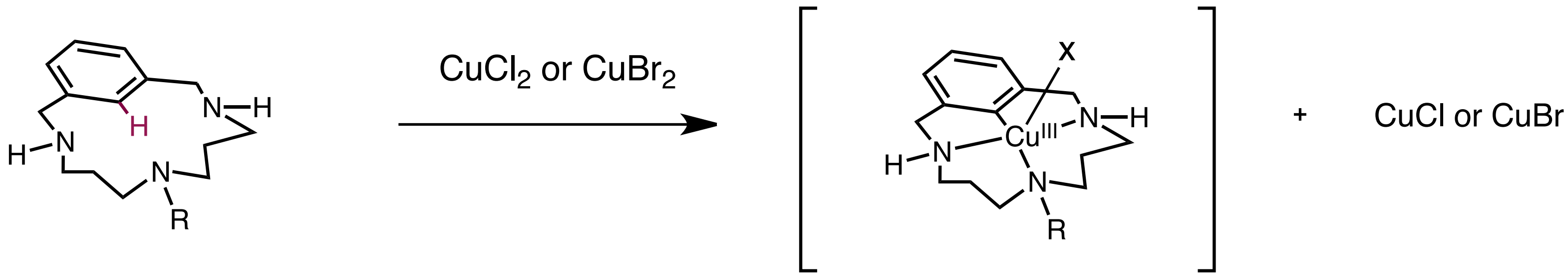

Casitas, A.; King, A. E.; Parella, T.; Costas, M.; Stahl, S. S.; Ribas, X. *Chem Sci.* **2010**, *1*, 326–330

Ullmann-type Coupling Reaction

characterization of aryl-Cu^{III} complex

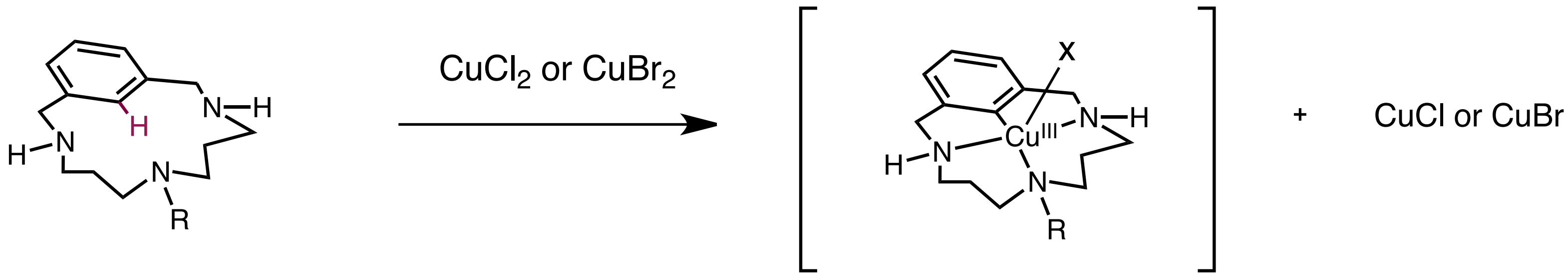

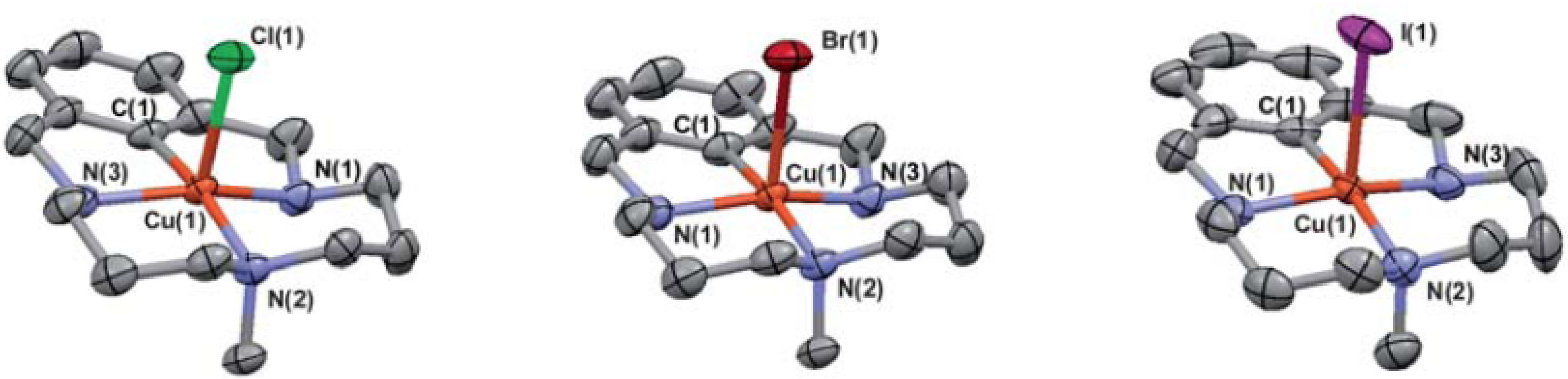

Casitas, A.; King, A. E.; Parella, T.; Costas, M.; Stahl, S. S.; Ribas, X. *Chem Sci.* **2010**, *1*, 326–330

Ullmann-type Coupling Reaction

characterization of aryl-Cu^{III} complex

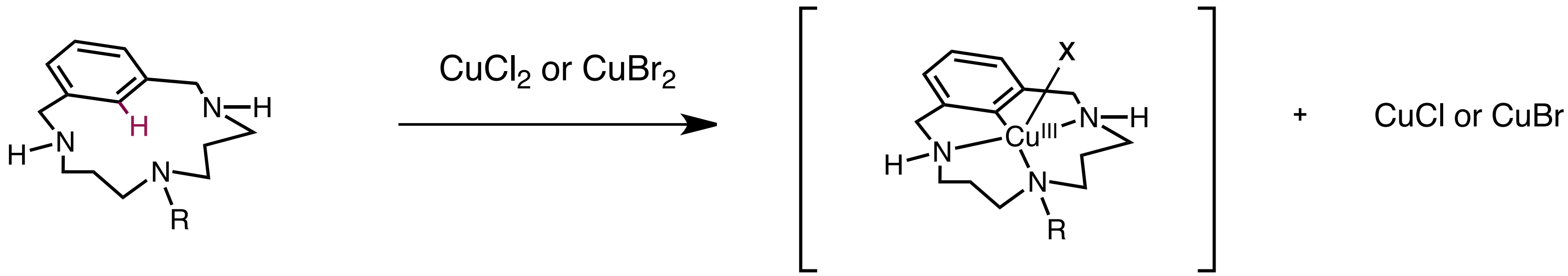

electronic spectra (LMCT): agrees with ligand field strengths of the halides

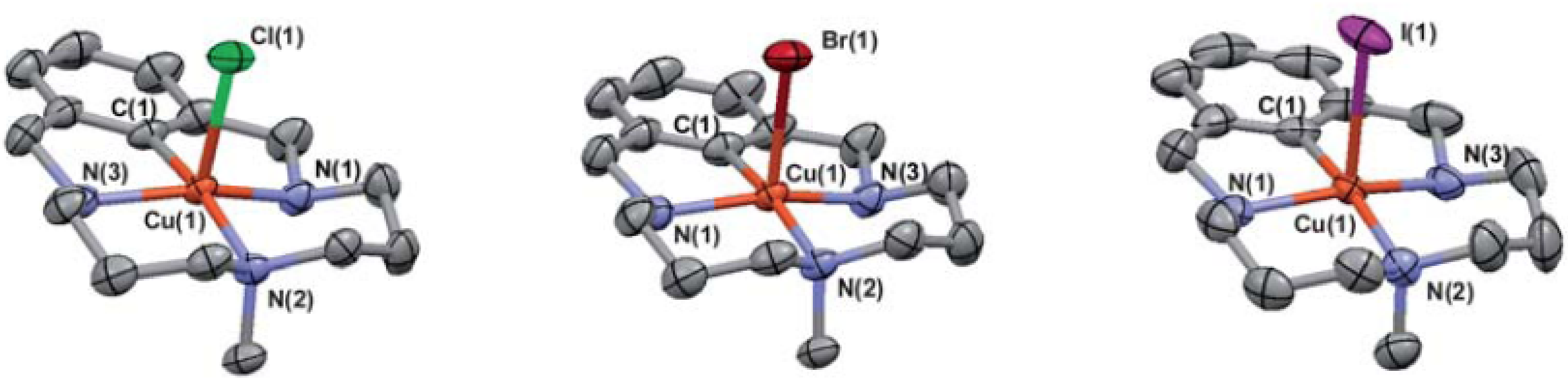

369 and 521 nm | 399 and 550 nm | 422 and 635 nm

Casitas, A.; King, A. E.; Parella, T.; Costas, M.; Stahl, S. S.; Ribas, X. *Chem Sci.* **2010**, *1*, 326–330

Ullmann-type Coupling Reaction

characterization of aryl-Cu^{III} complex

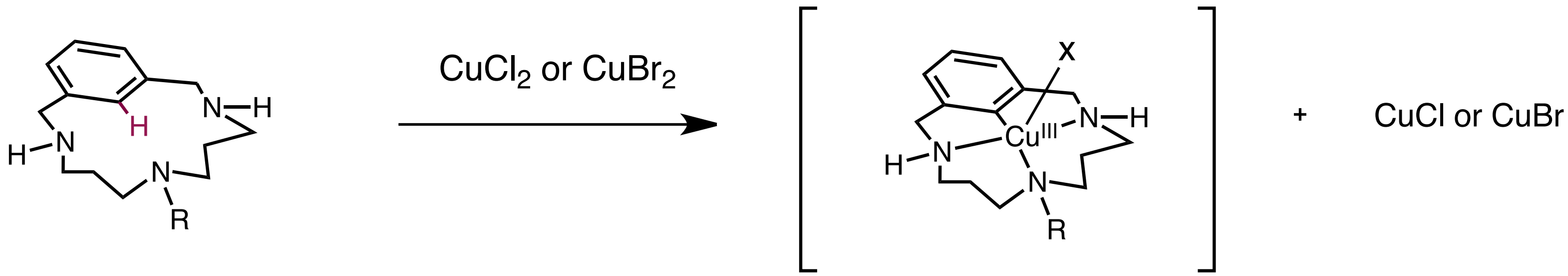

cyclic voltammetry: values for Cu^{III}/Cu^{II} redox couple

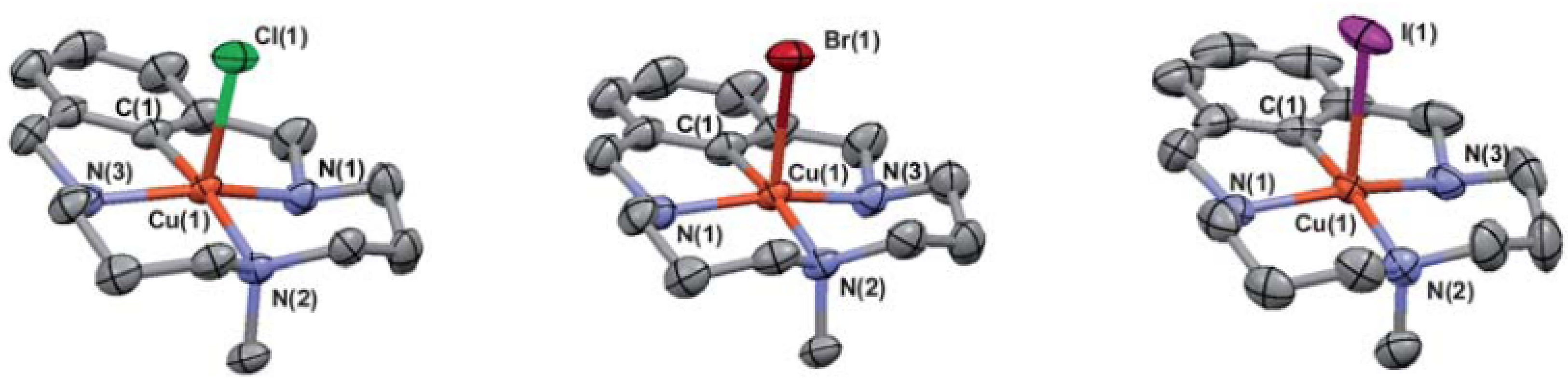

–330mV

–310mV

–300mV

Casitas, A.; King, A. E.; Parella, T.; Costas, M.; Stahl, S. S.; Ribas, X. *Chem Sci.* **2010**, *1*, 326–330

Ullmann-type Coupling Reaction

reductive elimination

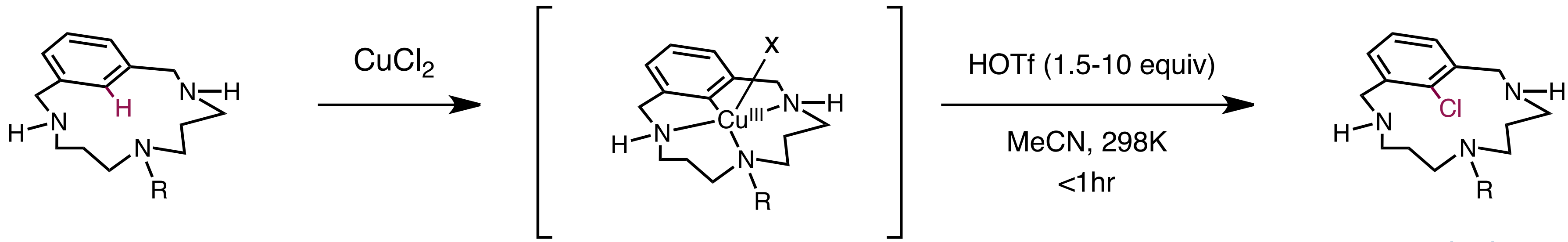

quantitative

Casitas, A.; King, A. E.; Parella, T.; Costas, M.; Stahl, S. S.; Ribas, X. *Chem Sci.* **2010**, *1*, 326–330

Ullmann-type Coupling Reaction

reductive elimination

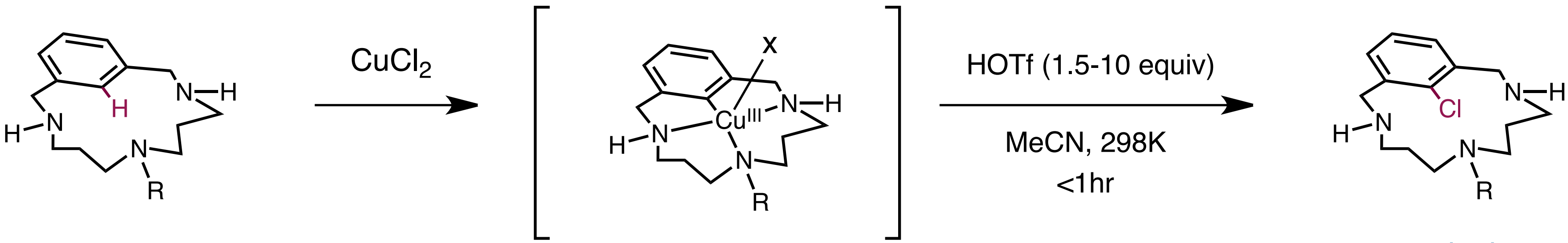

quantitative

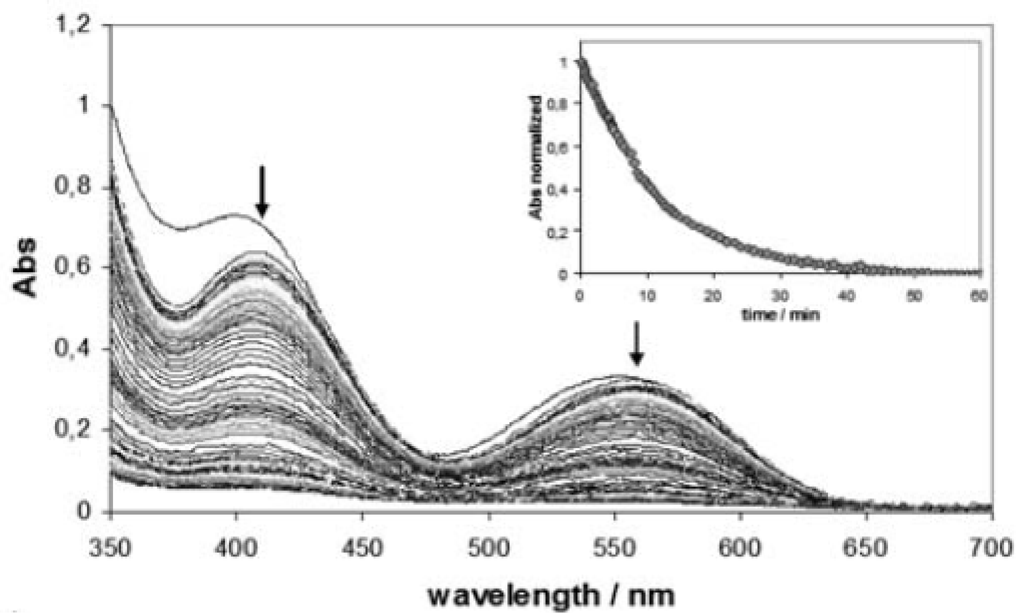

Casitas, A.; King, A. E.; Parella, T.; Costas, M.; Stahl, S. S.; Ribas, X. *Chem Sci.* **2010**, *1*, 326–330

Ullmann-type Coupling Reaction

reductive elimination

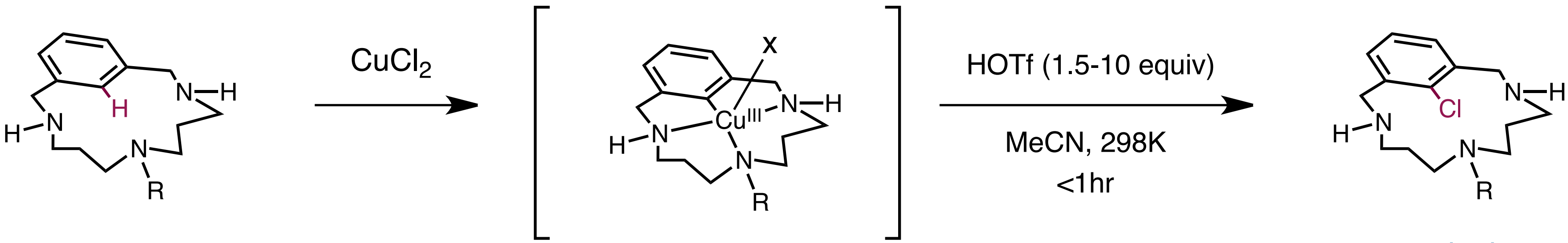

quantitative

complex

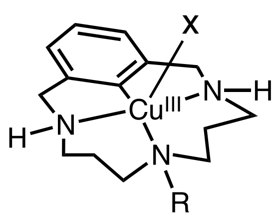

X	**R**	**$E_{1/2}$ (mV)**	**k_{obs}(S^{-1}) (298K)**
Cl	H	–330	$7.12(6)\times10^{-2}$
Br	H	–300	$4.08(5)\times10^{-4}$
Cl	Me	–400	$5.05(5)\times10^{-3}$

rate of reductive elimination controlled by C–halogen bond strength

C–X reductive elimination rates do not correlate with $E_{1/2}$ values

Casitas, A.; King, A. E.; Parella, T.; Costas, M.; Stahl, S. S.; Ribas, X. *Chem Sci.* **2010**, *1*, 326–330

Ullmann-type Coupling Reaction

reductive elimination

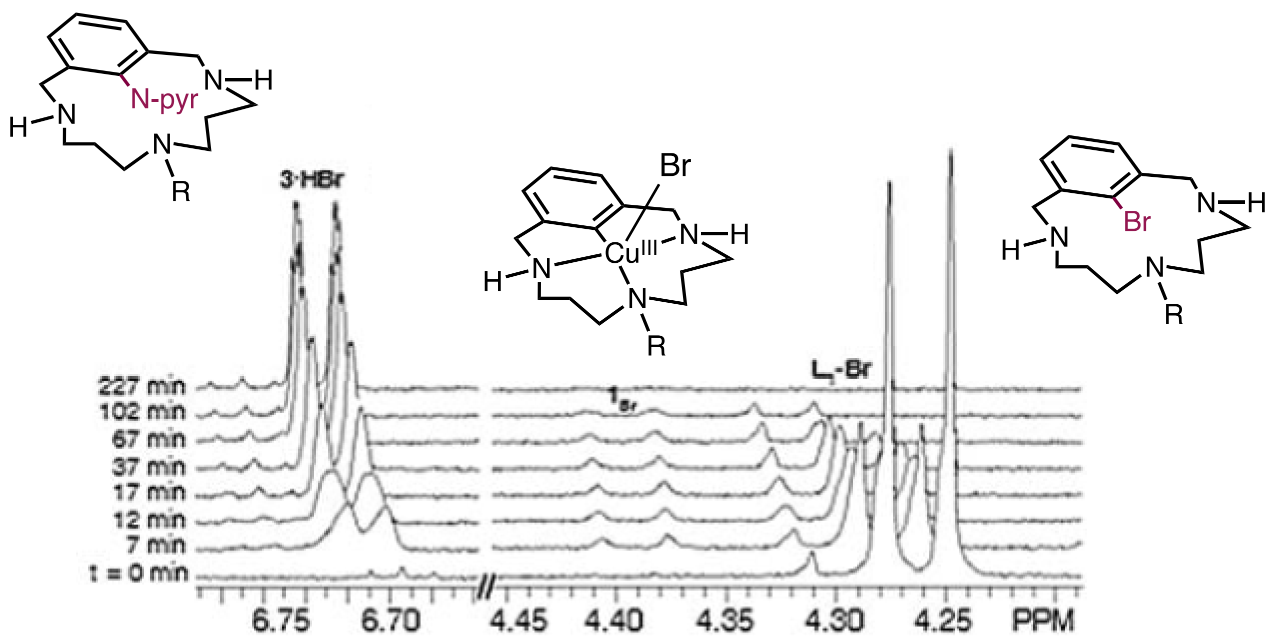

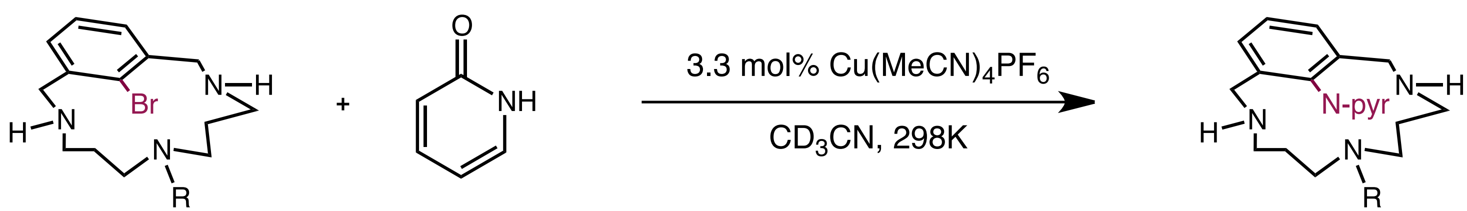

Casitas, A.; King, A. E.; Parella, T.; Costas, M.; Stahl, S. S.; Ribas, X. *Chem Sci.* **2010**, *1*, 326–330

Ullmann-type Coupling Reaction

relationship of this study to the Ullmann reaction

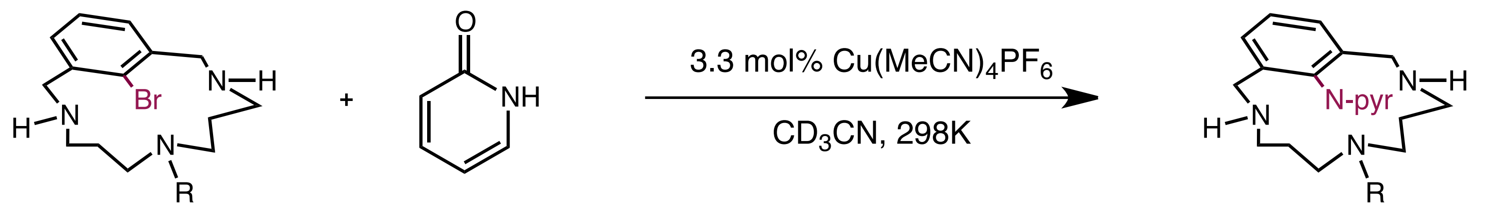

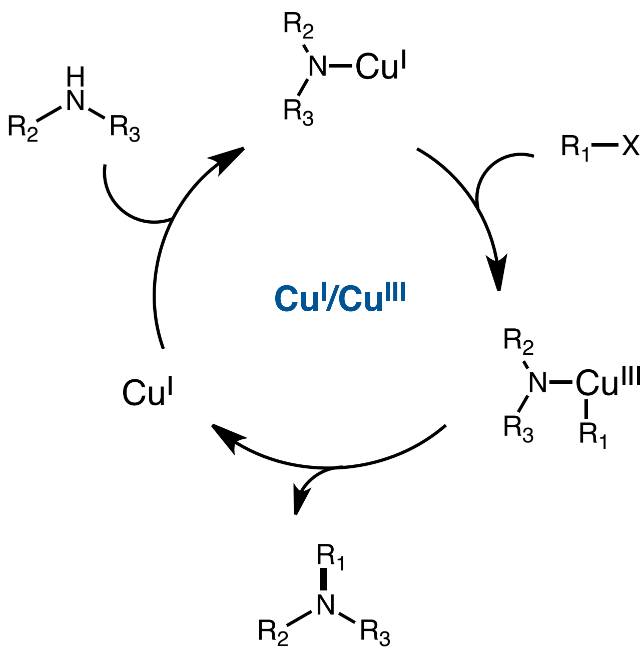

Casitas, A.; King, A. E.; Parella, T.; Costas, M.; Stahl, S. S.; Ribas, X. *Chem Sci.* **2010**, *1*, 326–330

Ullmann-type Coupling Reaction

relationship of this study to the Ullmann reaction

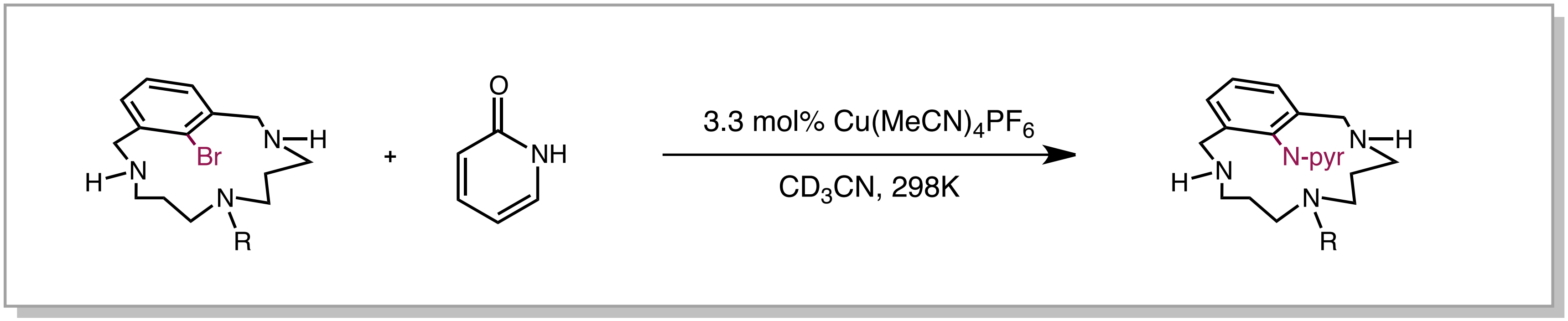

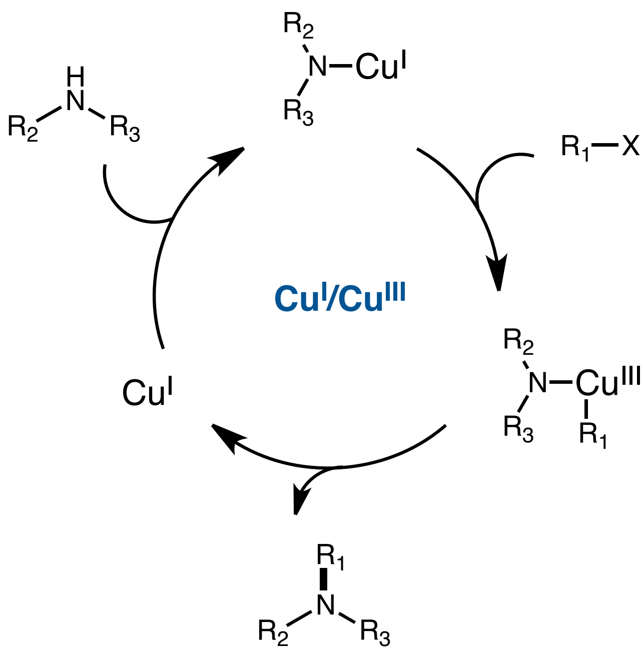

- macrocyclic ligand lowers barrier to oxidative addition
- macrocyclic ligand stabilizes Cu^{III}

**effectively inverts the relative rates of both redox steps*

Casitas, A.; King, A. E.; Parella, T.; Costas, M.; Stahl, S. S.; Ribas, X. *Chem Sci.* **2010**, *1*, 326–330

Ullmann-type Coupling Reaction

relationship of this study to the Ullmann reaction

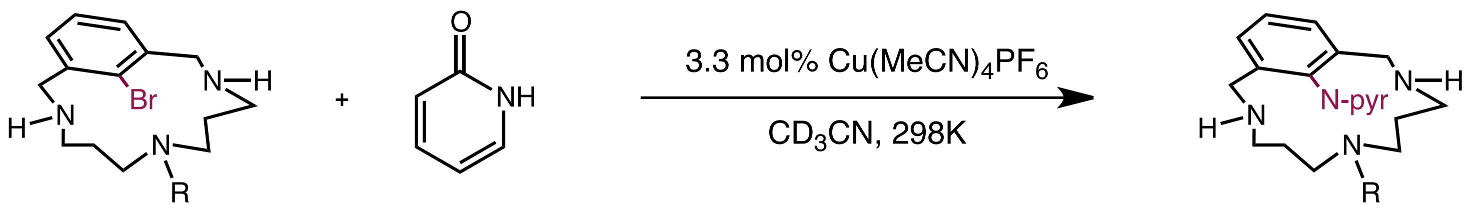

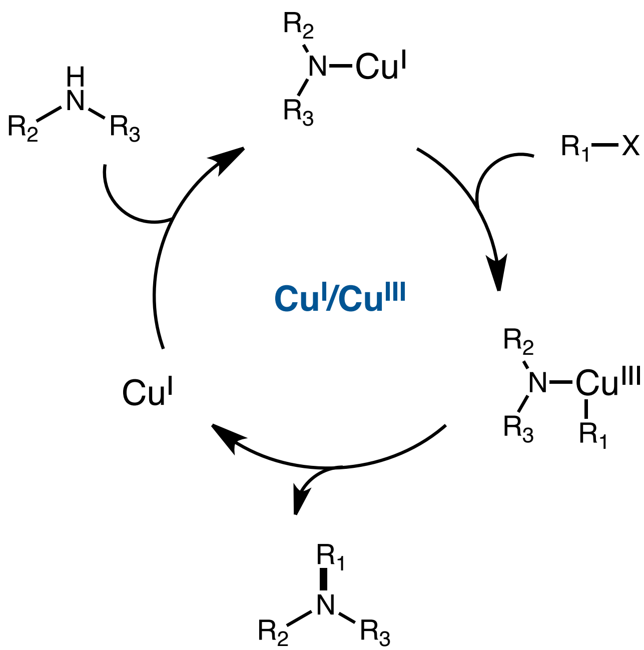

- macrocyclic ligand lowers barrier to oxidative addition
- macrocyclic ligand stabilizes Cu^{III}

  **effectively inverts the relative rates of both redox steps*

- mechanism of Ullmann-Goldberg can vary

  **use of less coordinating nucleophiles or higher coordinate ligands can affect key redox steps*

Casitas, A.; King, A. E.; Parella, T.; Costas, M.; Stahl, S. S.; Ribas, X. *Chem Sci.* **2010**, *1*, 326–330

Copper in Cross-Coupling Reactions

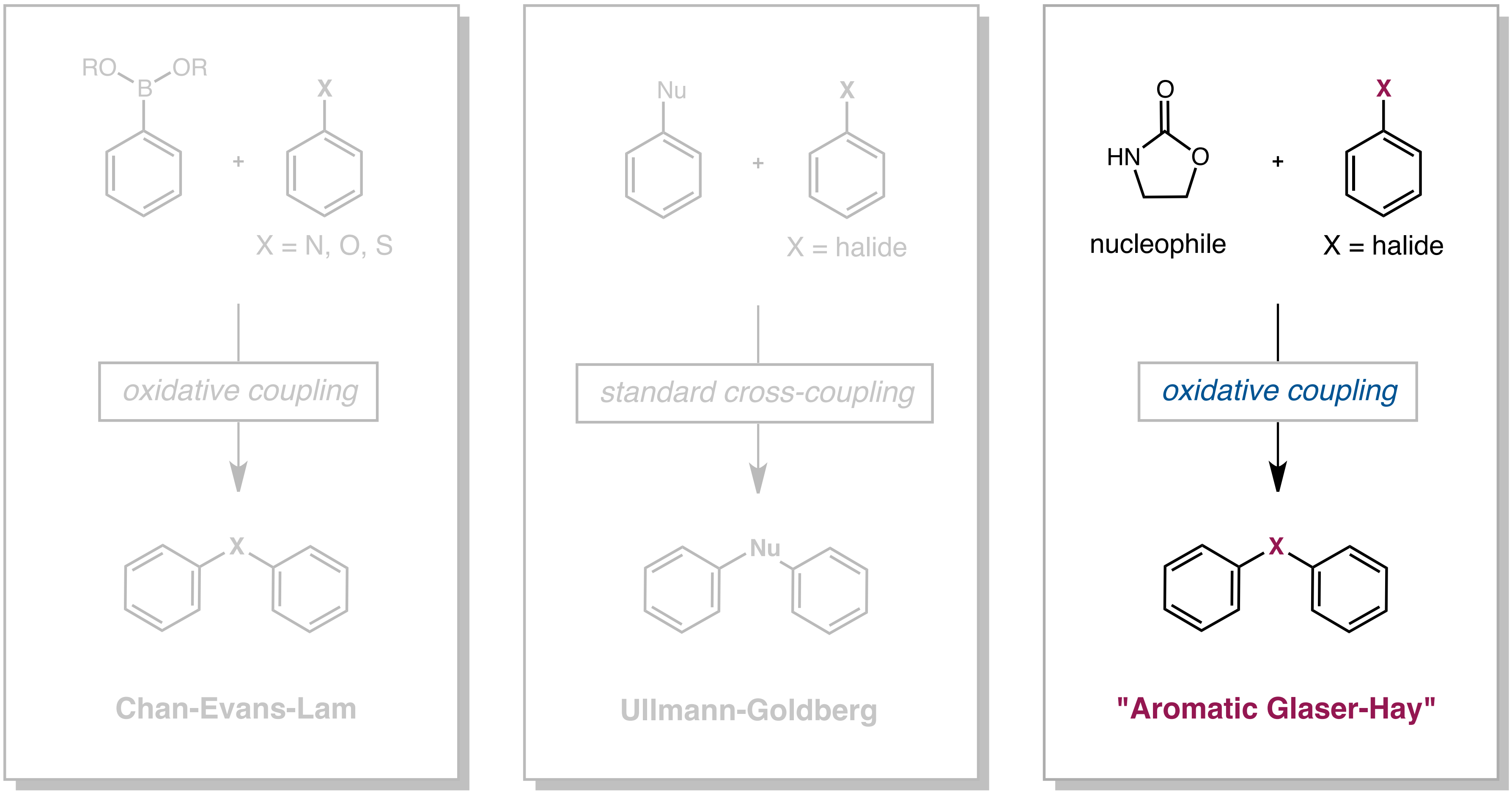

Glaser-Hay Type Couplings

oxidative cross-coupling

Oxidative coupling of a Cu-bound nucleophile and a C–H bond

Hamada, T; Ye, X.; Stahl, S. S. *J. Am. Chem. Soc.* **2008**, *130*, 833–835

Glaser-Hay Type Couplings

oxidative cross-coupling

Oxidative coupling of a Cu-bound nucleophile and a C–H bond

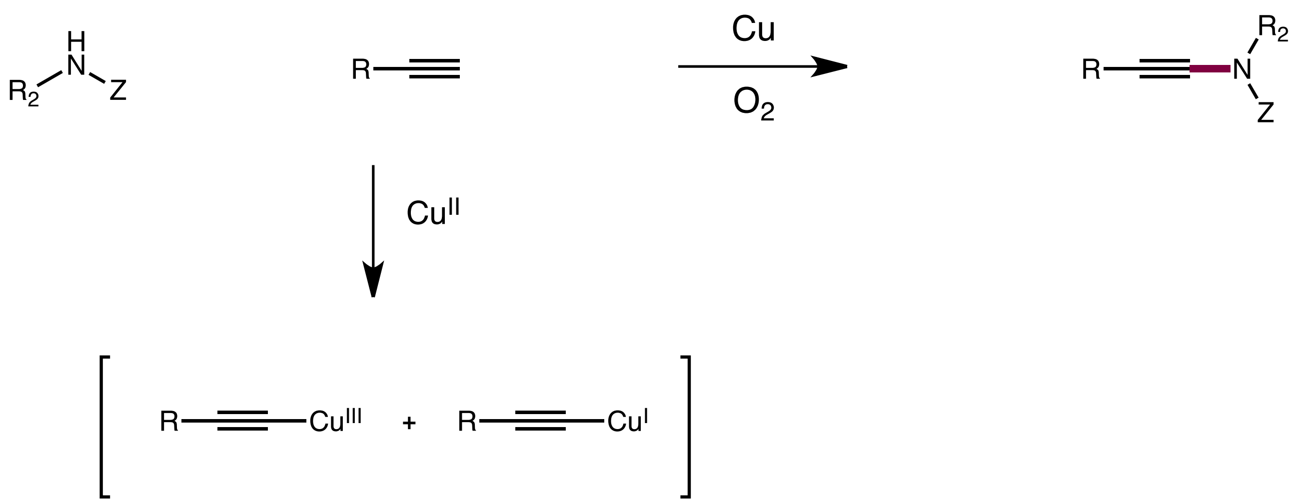

Hamada, T; Ye, X.; Stahl, S. S. *J. Am. Chem. Soc.* **2008**, *130*, 833–835

Brasche, G.; Buchwald, S. L. *Angew. Chem. Int. Ed.* **2008**, *47*, 1932–1934

Yang, L.; Lu, Z.; Stahl, S. S. *Chem Commun*, **2009**, 6460–6462

Glaser-Hay Type Couplings

oxidative cross-coupling

Oxidative coupling of a Cu-bound nucleophile and a C–H bond

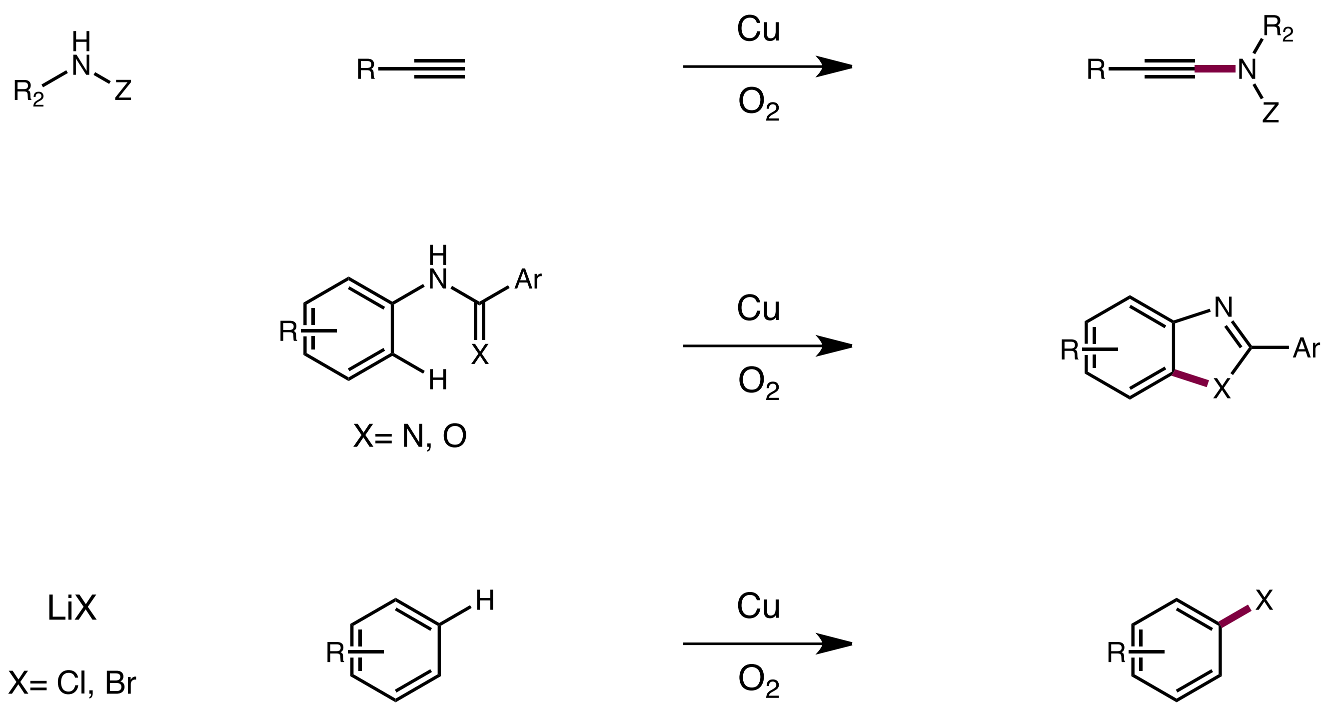

Hamada, T; Ye, X.; Stahl, S. S. *J. Am. Chem. Soc.* **2008**, *130*, 833–835

Brasche, G.; Buchwald, S. L. *Angew. Chem. Int. Ed.* **2008**, *47*, 1932–1934

Yang, L.; Lu, Z.; Stahl, S. S. *Chem Commun*, **2009**, 6460–6462

Glaser-Hay Type Couplings

oxidative cross-coupling

Oxidative coupling of a Cu-bound nucleophile and a C–H bond

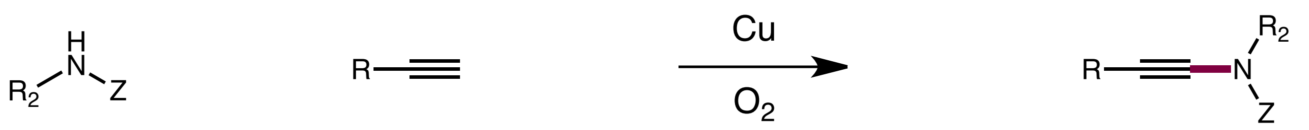

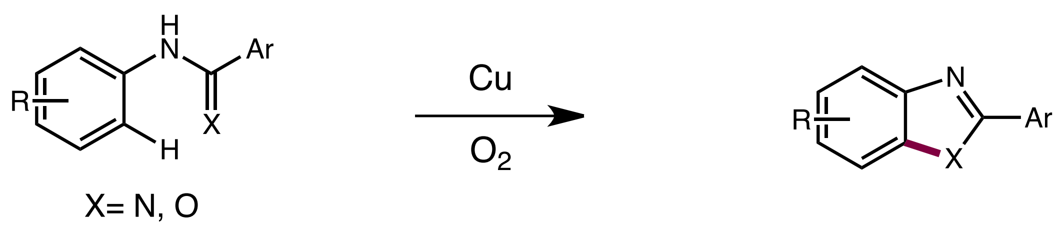

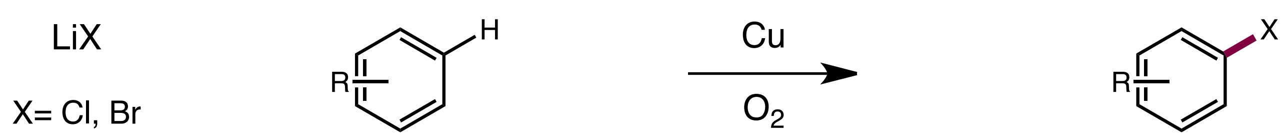

Hamada, T; Ye, X.; Stahl, S. S. *J. Am. Chem. Soc.* **2008**, *130*, 833–835

Brasche, G.; Buchwald, S. L. *Angew. Chem. Int. Ed.* **2008**, *47*, 1932–1934

Yang, L.; Lu, Z.; Stahl, S. S. *Chem Commun*, **2009**, 6460–6462

Glaser-Hay Type Couplings

oxidative cross-coupling

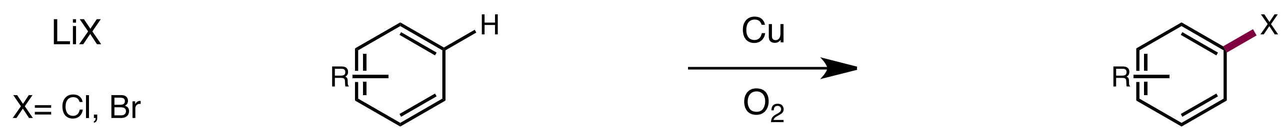

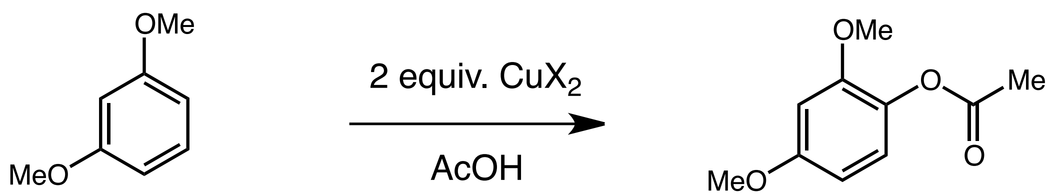

Yang, L.; Lu, Z.; Stahl, S. S. *Chem Commun*, **2009**, 6460–6462

Glaser-Hay Type Couplings

oxidative cross-coupling

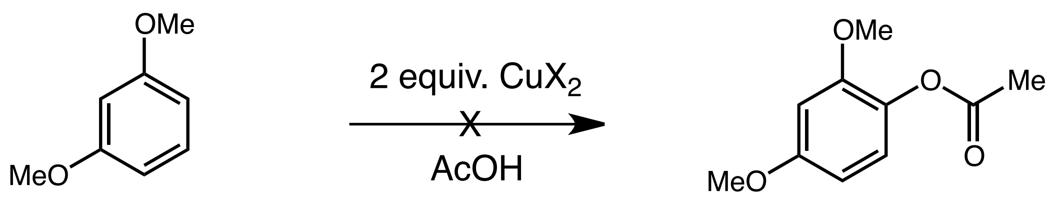

$Cu(OAc)_2$

$Cu(OTf)_2$

$Cu(ClO_4)_2$

CuF_2

$CuCl_2$

$CuBr_2$

Yang, L.; Lu, Z.; Stahl, S. S. *Chem Commun*, **2009**, 6460–6462

Glaser-Hay Type Couplings

oxidative cross-coupling

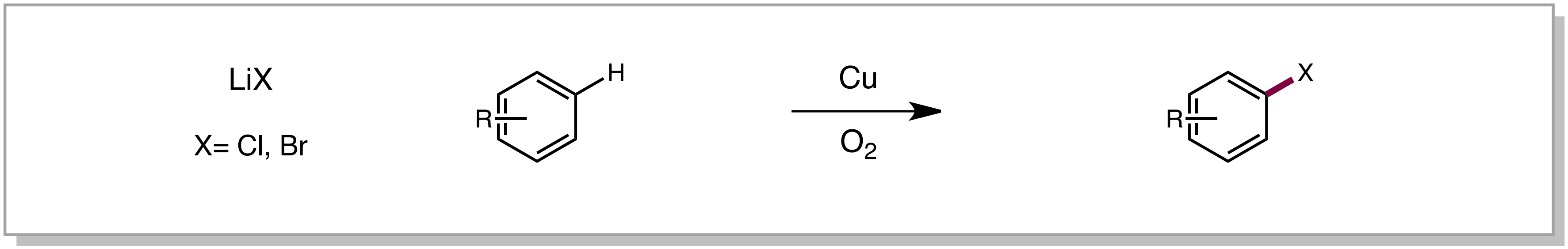

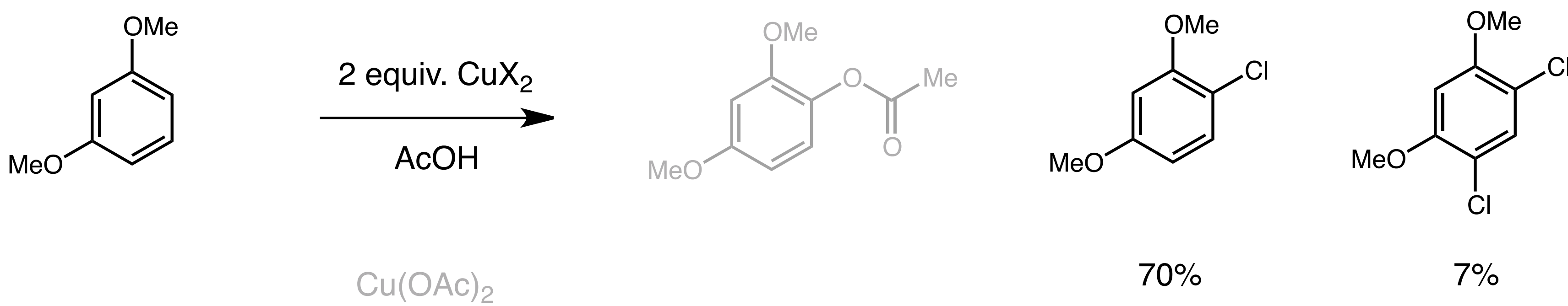

$Cu(OAc)_2$

$Cu(OTf)_2$

$Cu(ClO_4)_2$

CuF_2

$CuCl_2$

$CuBr_2$

Yang, L.; Lu, Z.; Stahl, S. S. *Chem Commun*, **2009**, 6460–6462

Glaser-Hay Type Couplings

preliminary investigations

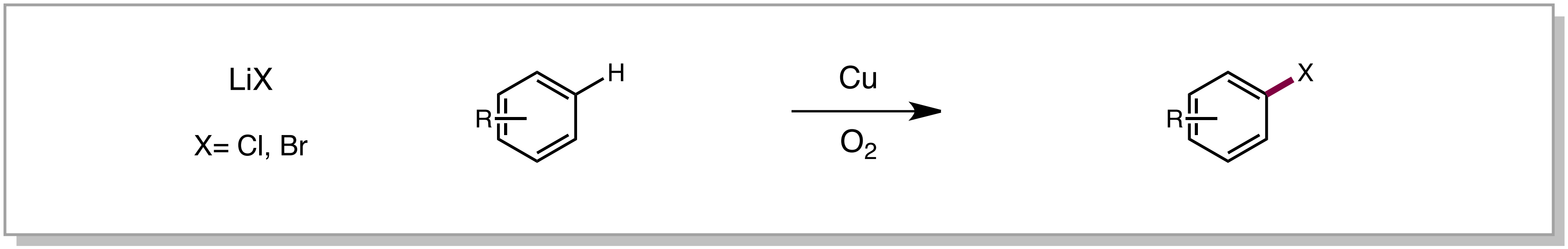

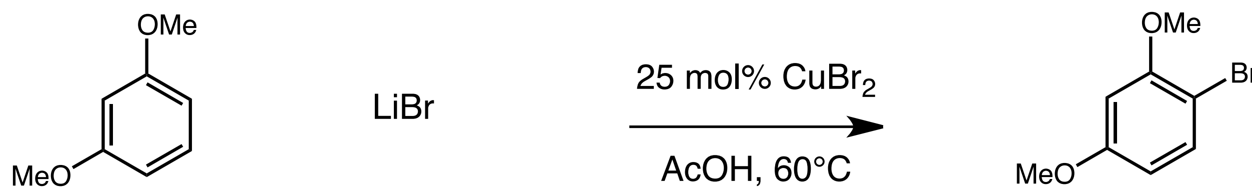

Yang, L.; Lu, Z.; Stahl, S. S. *Chem Commun*, **2009**, 6460–6462

Glaser-Hay Type Couplings

preliminary investigations

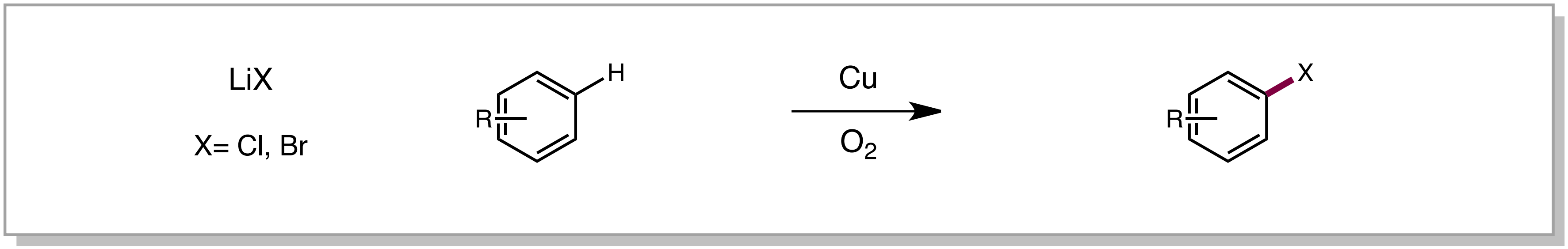

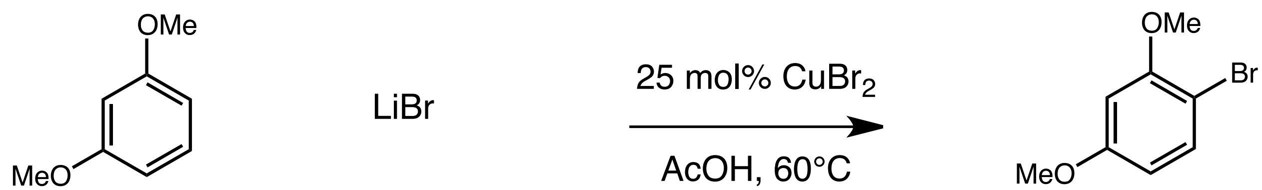

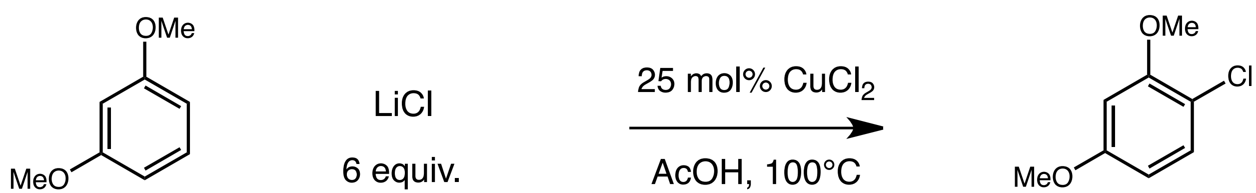

Yang, L.; Lu, Z.; Stahl, S. S. *Chem Commun*, **2009**, 6460–6462

Glaser-Hay Type Couplings

preliminary investigations

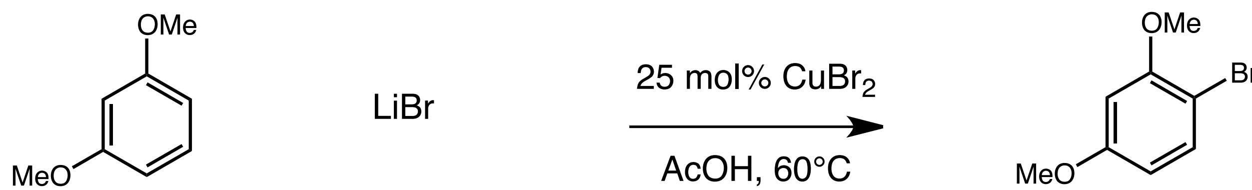

$$CuBr_2 \xrightarrow{\Delta} 2\ CuBr + Br_2$$

regioselectivity follows that of electrophilic aromatic bromination

Barnes, J. C.; Hume, D. N. *Inorg. Chem.* **1963**, *2*, 445–448

Yang, L.; Lu, Z.; Stahl, S. S. *Chem Commun*, **2009**, 6460–6462

Glaser-Hay Type Couplings

preliminary investigations

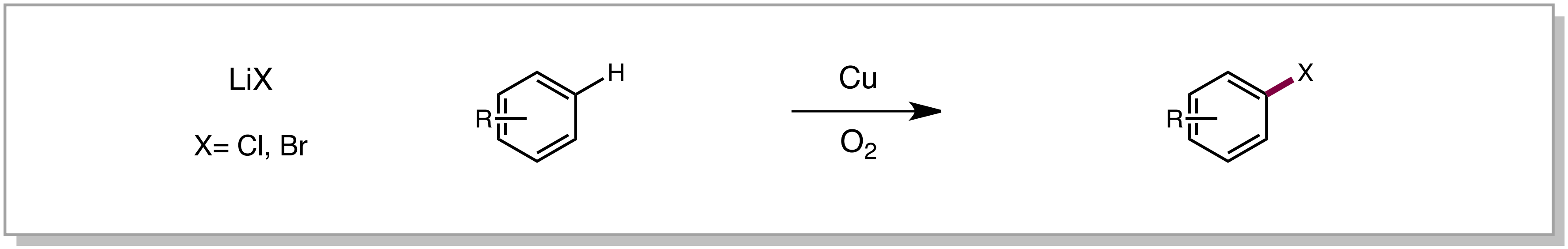

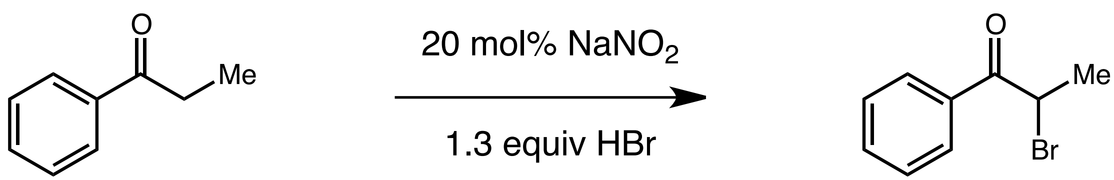

$$CuBr_2 \xrightarrow{\Delta} 2\ CuBr + Br_2$$

regioselectivity follows that of electrophilic aromatic bromination

Zhang, G.; Liu, R.; Xu, Q.; Ma, L.; Liang, X. *Adv. Synth. Catal.* **2006**, *346*, 862–866

Barnes, J. C.; Hume, D. N. *Inorg. Chem.* **1963**, *2*, 445–448

Yang, L.; Lu, Z.; Stahl, S. S. *Chem Commun*, **2009**, 6460–6462

Glaser-Hay Type Couplings

preliminary investigations

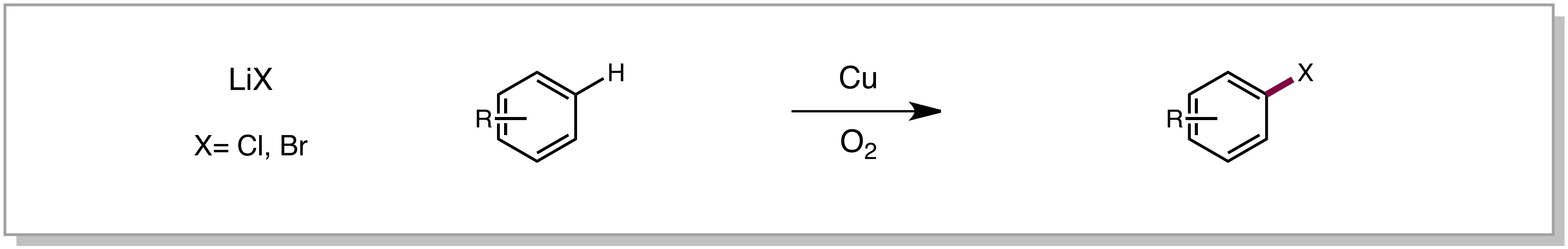

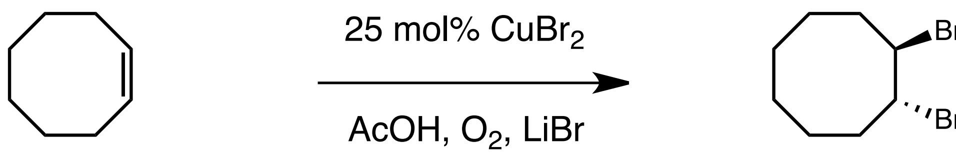

75%

$$CuBr_2 \xrightarrow{\Delta} 2\ CuBr + Br_2$$

regioselectivity follows that of electrophilic aromatic bromination

Zhang, G.; Liu, R.; Xu, Q.; Ma, L.; Liang, X. *Adv. Synth. Catal.* **2006**, *346*, 862–866

Barnes, J. C.; Hume, D. N. *Inorg. Chem.* **1963**, *2*, 445–448

Yang, L.; Lu, Z.; Stahl, S. S. *Chem Commun*, **2009**, 6460–6462

Glaser-Hay Type Couplings

oxidative cross-coupling

Oxidative coupling of a Cu-bound nucleophile and a C–H bond

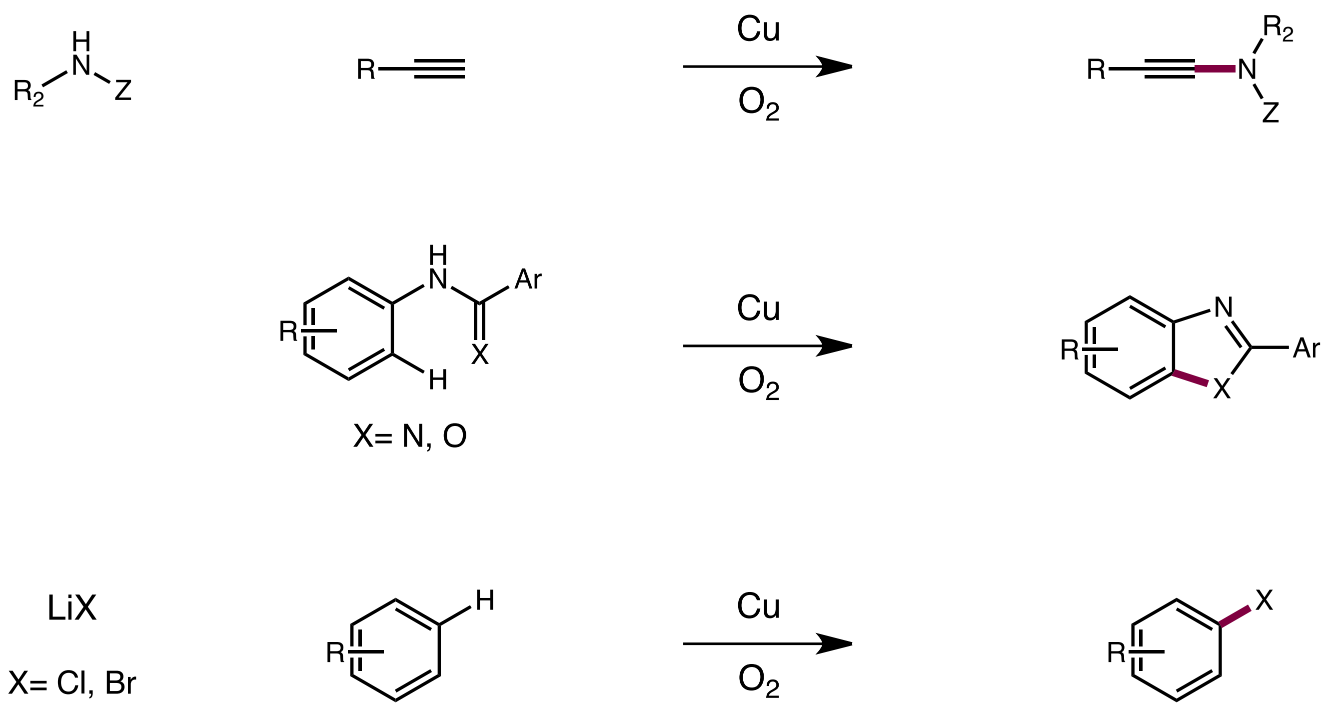

Hamada, T; Ye, X.; Stahl, S. S. *J. Am. Chem. Soc.* **2008**, *130*, 833–835
Brasche, G.; Buchwald, S. L. *Angew. Chem. Int. Ed.* **2008**, *47*, 1932–1934
Yang, L.; Lu, Z.; Stahl, S. S. *Chem Commun*, **2009**, 6460–6462

Glaser-Hay Type Couplings

oxidative cross-coupling

Oxidative coupling of a Cu-bound nucleophile and a C–H bond

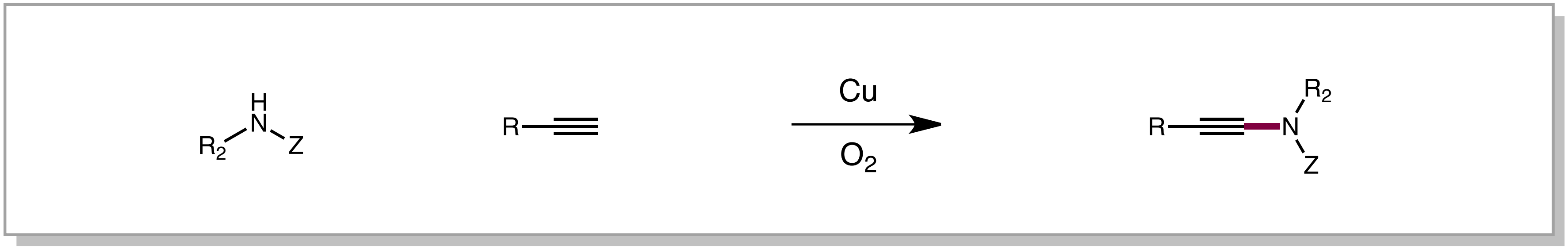

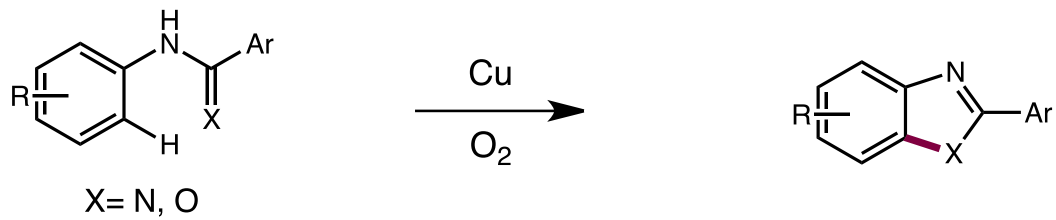

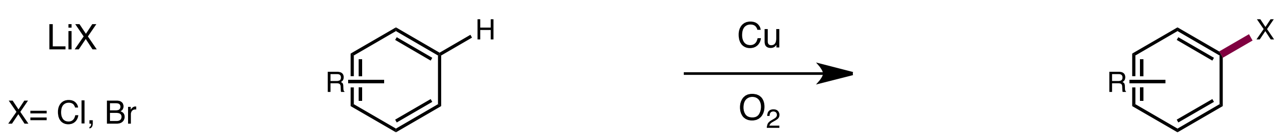

Hamada, T; Ye, X.; Stahl, S. S. *J. Am. Chem. Soc.* **2008**, *130*, 833–835

Brasche, G.; Buchwald, S. L. *Angew. Chem. Int. Ed.* **2008**, *47*, 1932–1934

Yang, L.; Lu, Z.; Stahl, S. S. *Chem Commun*, **2009**, 6460–6462

Glaser-Hay Type Couplings

evidence for an aryl-Cu^{III}

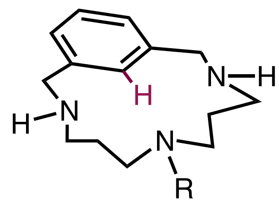

King, A. E.; Huffman, L. M.; Casitas, A.; Costas, M.; Ribas, X.; Stahl, S. S. *J. Am Chem. Soc*, **2010**, 1147–1169

Glaser-Hay Type Couplings

evidence for an aryl-Cu^{III}

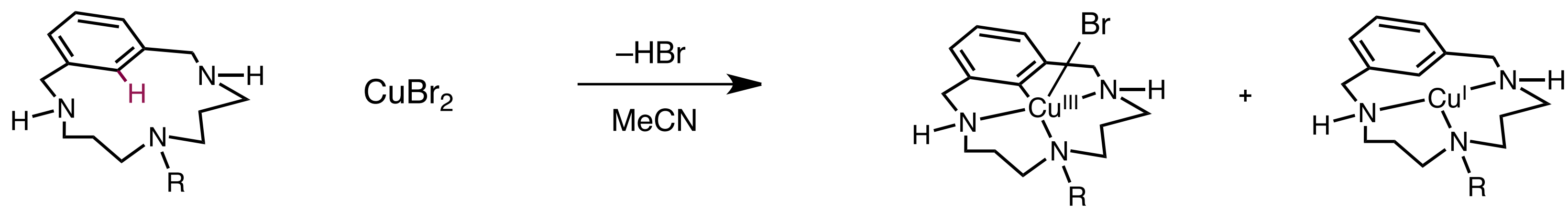

King, A. E.; Huffman, L. M.; Casitas, A.; Costas, M.; Ribas, X.; Stahl, S. S. *J. Am Chem. Soc*, **2010**, 1147–1169

Glaser-Hay Type Couplings

evidence for an aryl-Cu^{III}

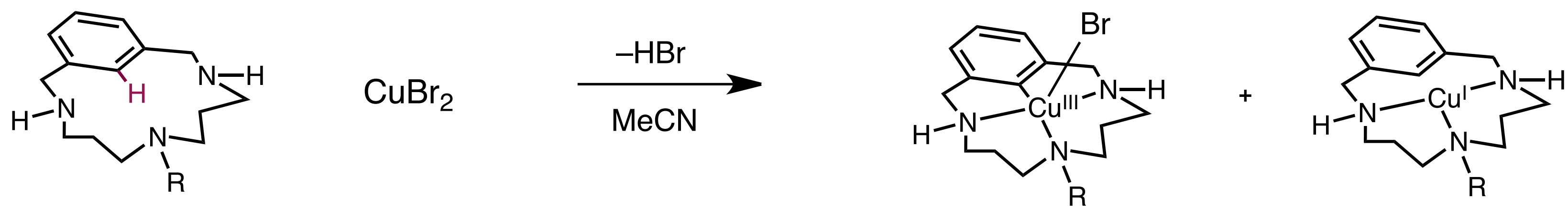

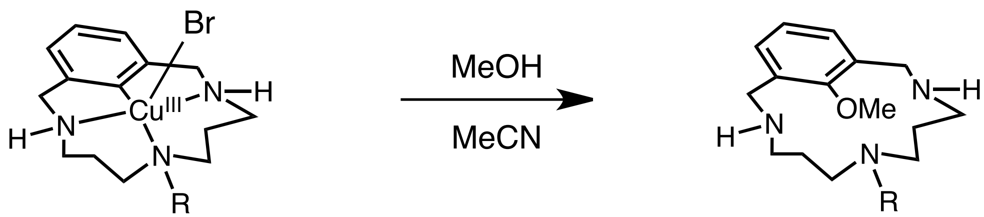

King, A. E.; Huffman, L. M.; Casitas, A.; Costas, M.; Ribas, X.; Stahl, S. S. *J. Am Chem. Soc*, **2010**, 1147–1169

Glaser-Hay Type Couplings

evidence for an aryl-Cu^{III}

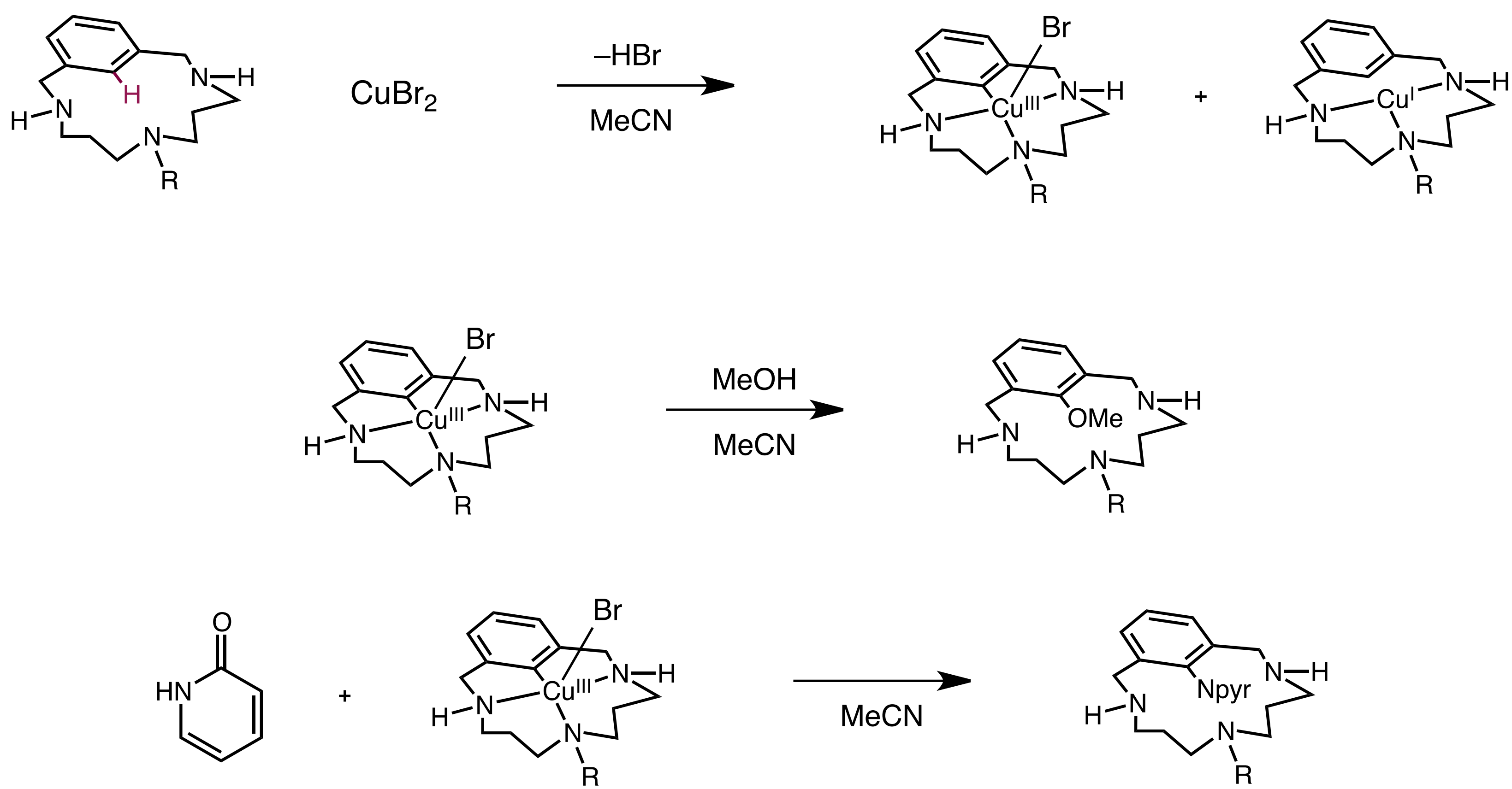

King, A. E.; Huffman, L. M.; Casitas, A.; Costas, M.; Ribas, X.; Stahl, S. S. *J. Am Chem. Soc*, **2010**, 1147–1169

Glaser-Hay Type Couplings

kinetics of methoxylation reaction using the method of intial rates

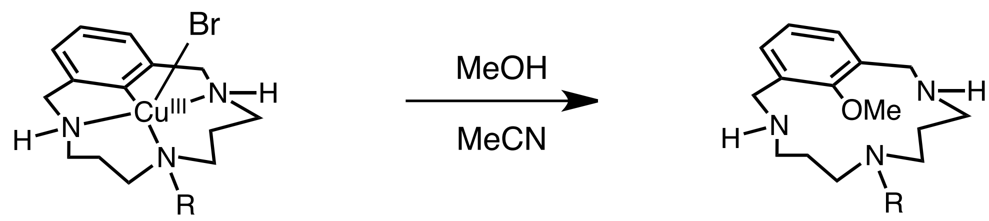

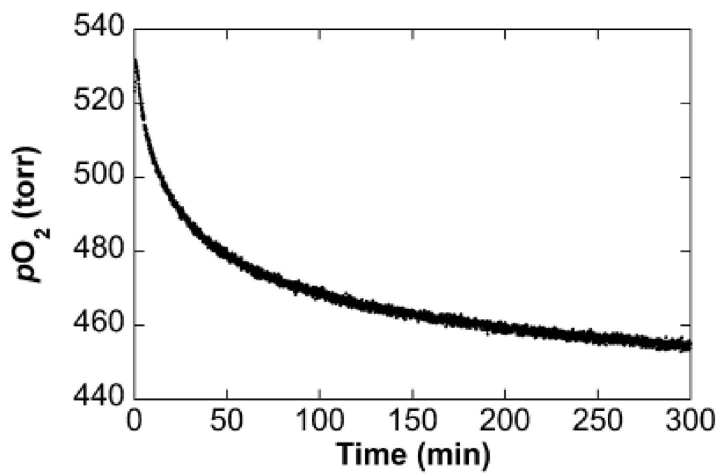

kinetics determined by O_2 consumption

King, A. E.; Huffman, L. M.; Casitas, A.; Costas, M.; Ribas, X.; Stahl, S. S. *J. Am Chem. Soc*, **2010**, 1147–1169

Glaser-Hay Type Couplings

kinetics of methoxylation reaction using the method of intial rates

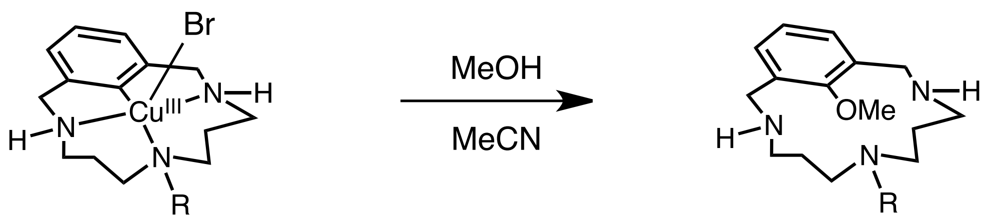

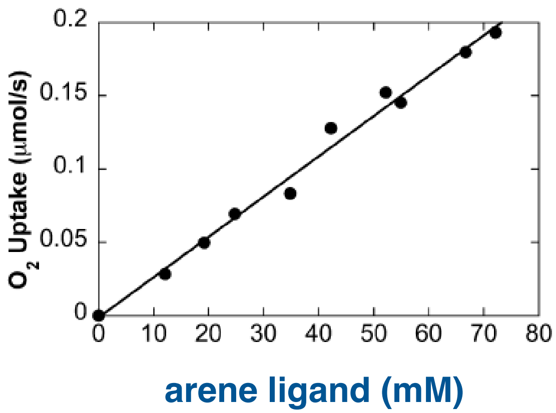

1st order dependence

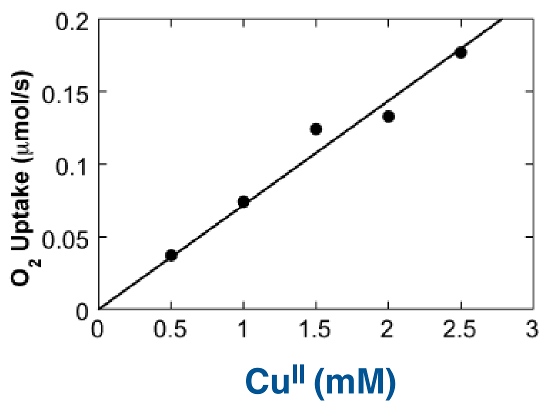

1st order dependence

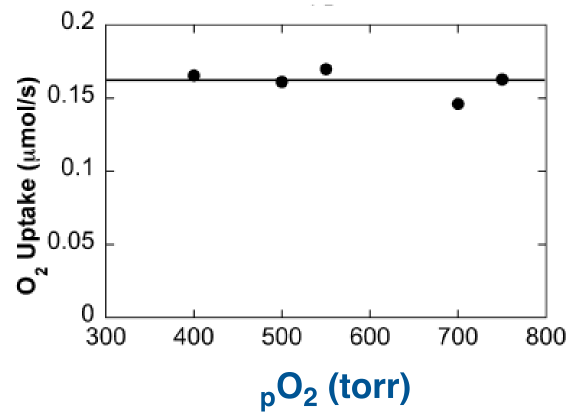

0 order dependence

King, A. E.; Huffman, L. M.; Casitas, A.; Costas, M.; Ribas, X.; Stahl, S. S. *J. Am Chem. Soc*, **2010**, 1147–1169

Glaser-Hay Type Couplings

kinetics of methoxylation reaction using the method of intial rates

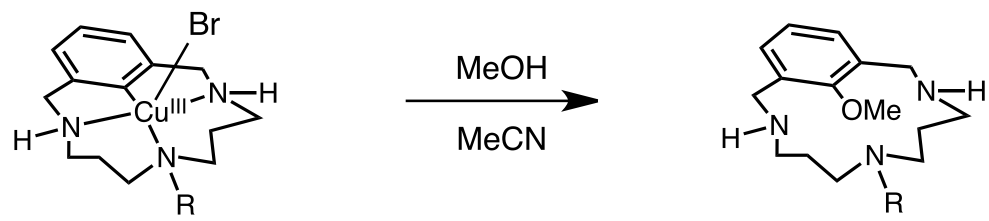

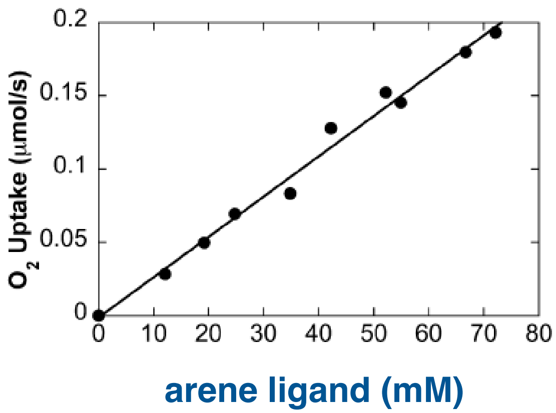

1st order dependence

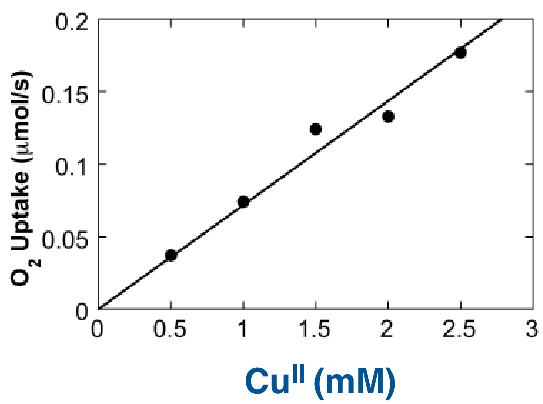

1st order dependence

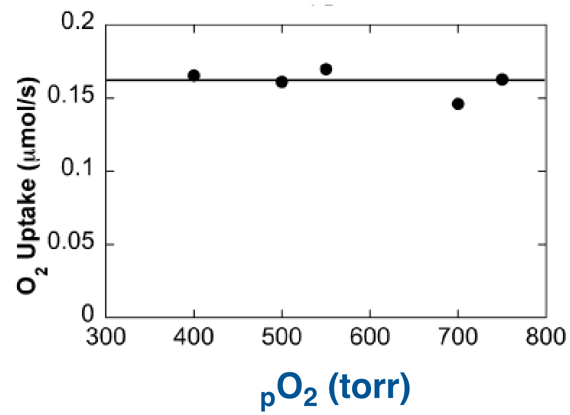

0 order dependence

catalytic steps involving O_2 are comparatively fast

Cu reoxidation is not rate-determining

King, A. E.; Huffman, L. M.; Casitas, A.; Costas, M.; Ribas, X.; Stahl, S. S. *J. Am Chem. Soc*, **2010**, 1147–1169

Glaser-Hay Type Couplings

kinetics of methoxylation reaction using the method of intial rates

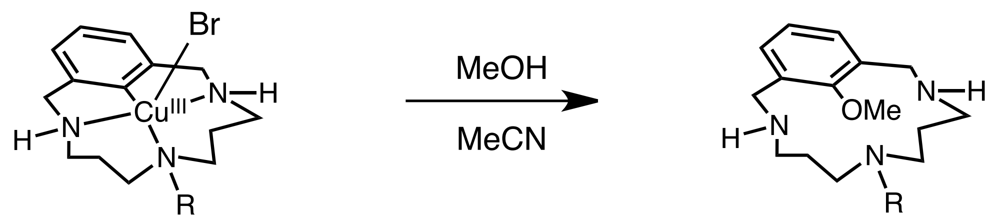

[1]H NMR complicated due to paramagnetic line broadening

indicates that Cu^{II} is formed during reaction

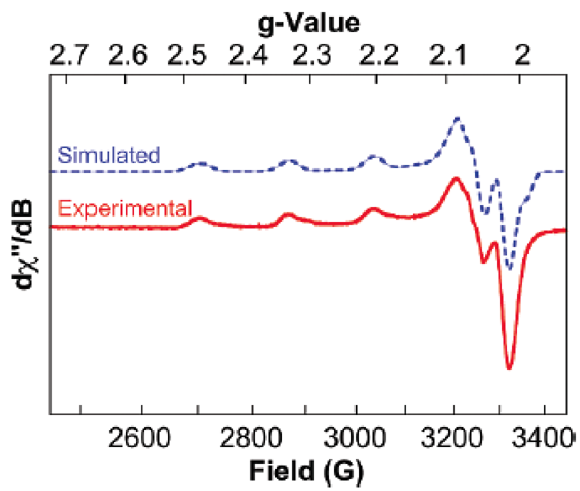

King, A. E.; Huffman, L. M.; Casitas, A.; Costas, M.; Ribas, X.; Stahl, S. S. *J. Am Chem. Soc*, **2010**, 1147–1169

Glaser-Hay Type Couplings

kinetics of methoxylation reaction using the method of intial rates

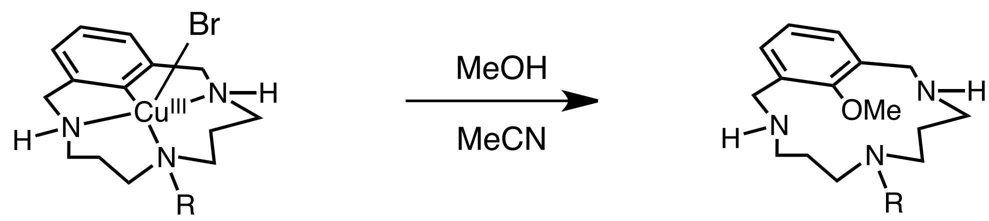

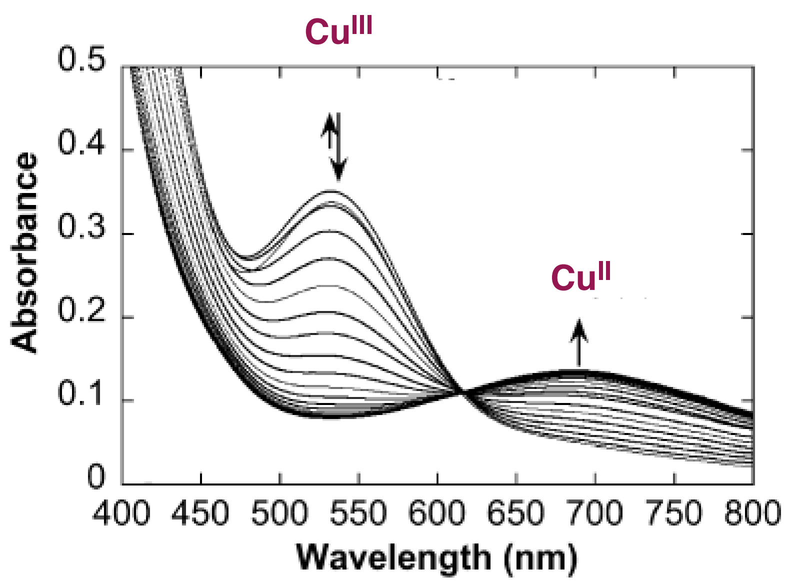

King, A. E.; Huffman, L. M.; Casitas, A.; Costas, M.; Ribas, X.; Stahl, S. S. *J. Am Chem. Soc*, **2010**, 1147–1169

Glaser-Hay Type Couplings

kinetics of methoxylation reaction using the method of intial rates

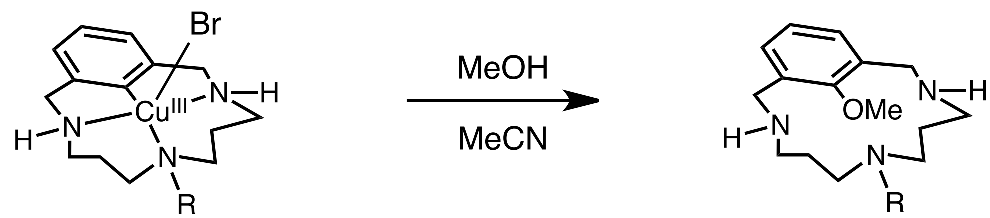

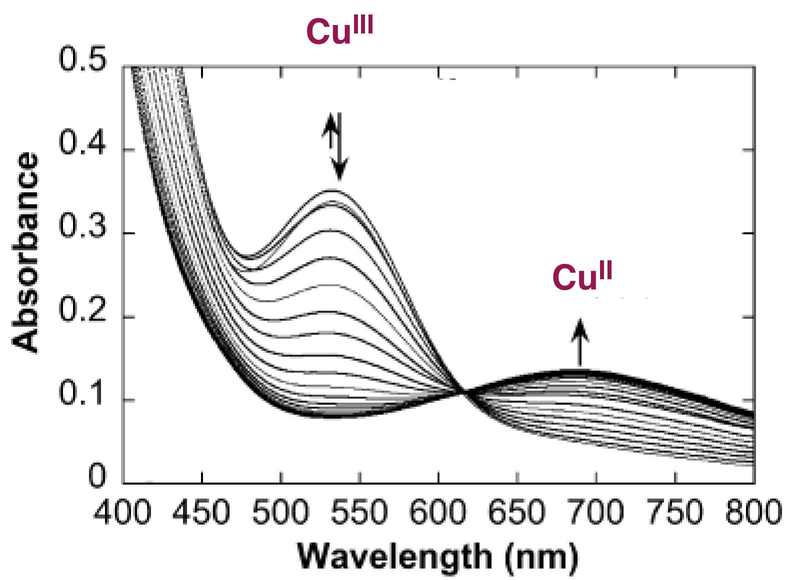

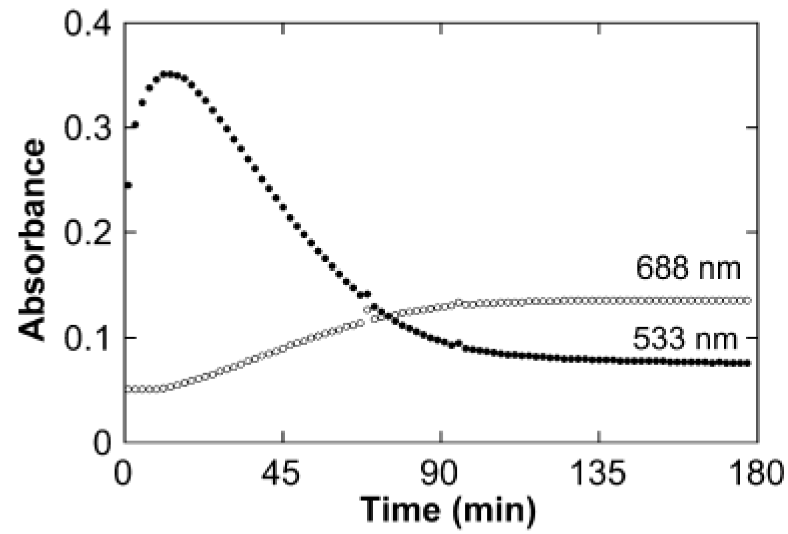

King, A. E.; Huffman, L. M.; Casitas, A.; Costas, M.; Ribas, X.; Stahl, S. S. *J. Am Chem. Soc*, **2010**, 1147–1169

Glaser-Hay Type Couplings

proposed mechanism of Aromatic Glaser-Hay coupling

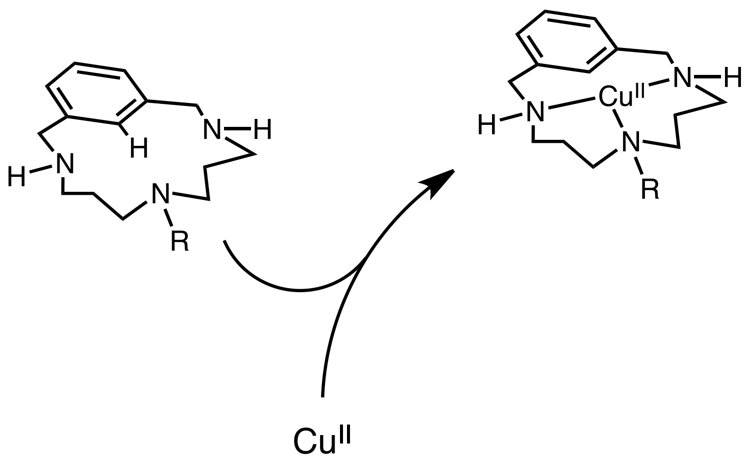

King, A. E.; Huffman, L. M.; Casitas, A.; Costas, M.; Ribas, X.; Stahl, S. S. *J. Am Chem. Soc*, **2010**, 1147–1169

Glaser-Hay Type Couplings

proposed mechanism of Aromatic Glaser-Hay coupling

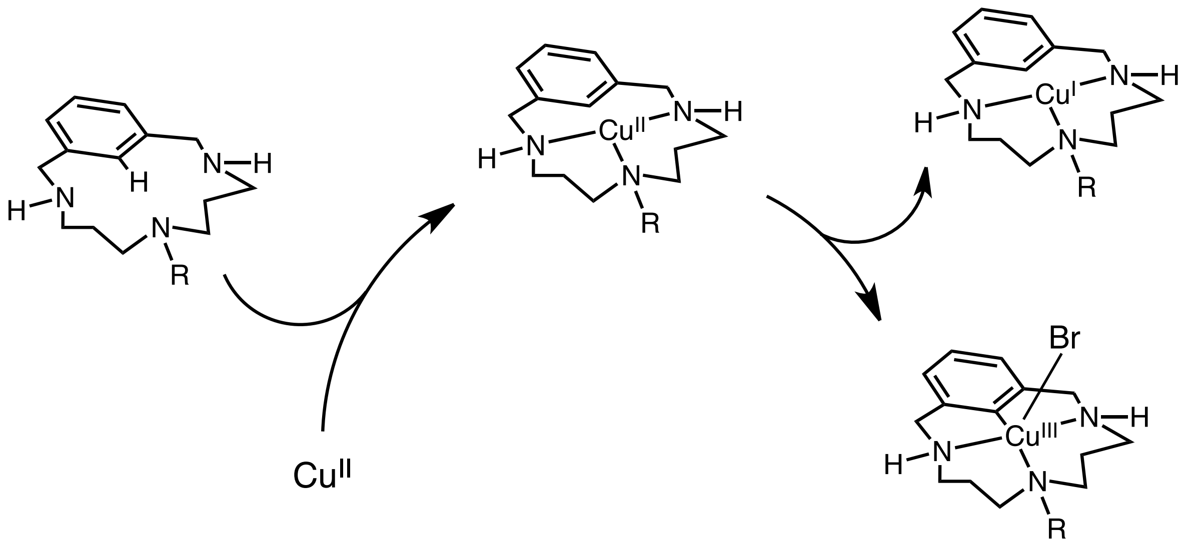

King, A. E.; Huffman, L. M.; Casitas, A.; Costas, M.; Ribas, X.; Stahl, S. S. *J. Am Chem. Soc*, **2010**, 1147–1169

Glaser-Hay Type Couplings

proposed mechanism of Aromatic Glaser-Hay coupling

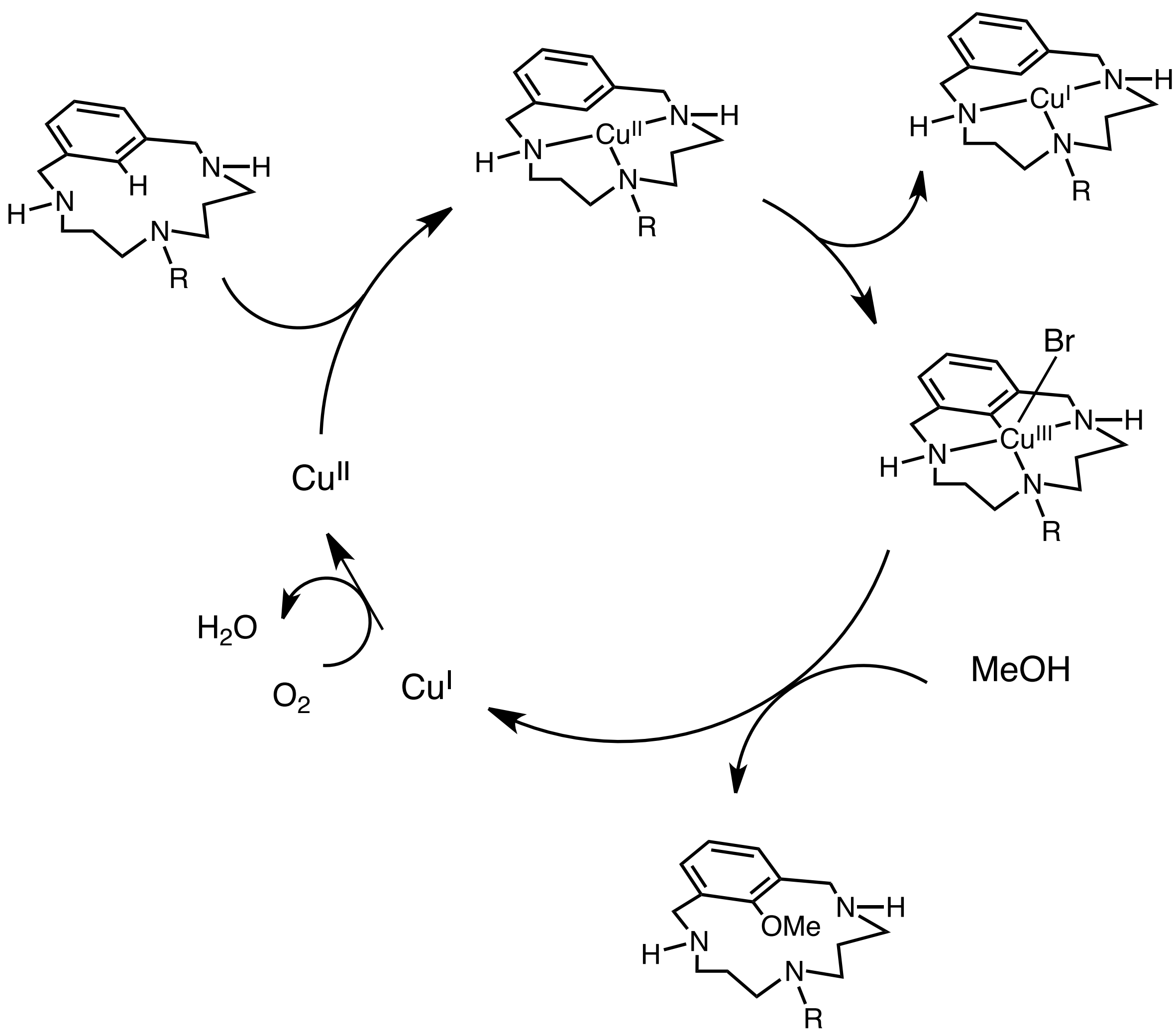

King, A. E.; Huffman, L. M.; Casitas, A.; Costas, M.; Ribas, X.; Stahl, S. S. *J. Am Chem. Soc*, **2010**, 1147–1169

Glaser-Hay Type Couplings

proposed mechanism of Aromatic Glaser-Hay coupling

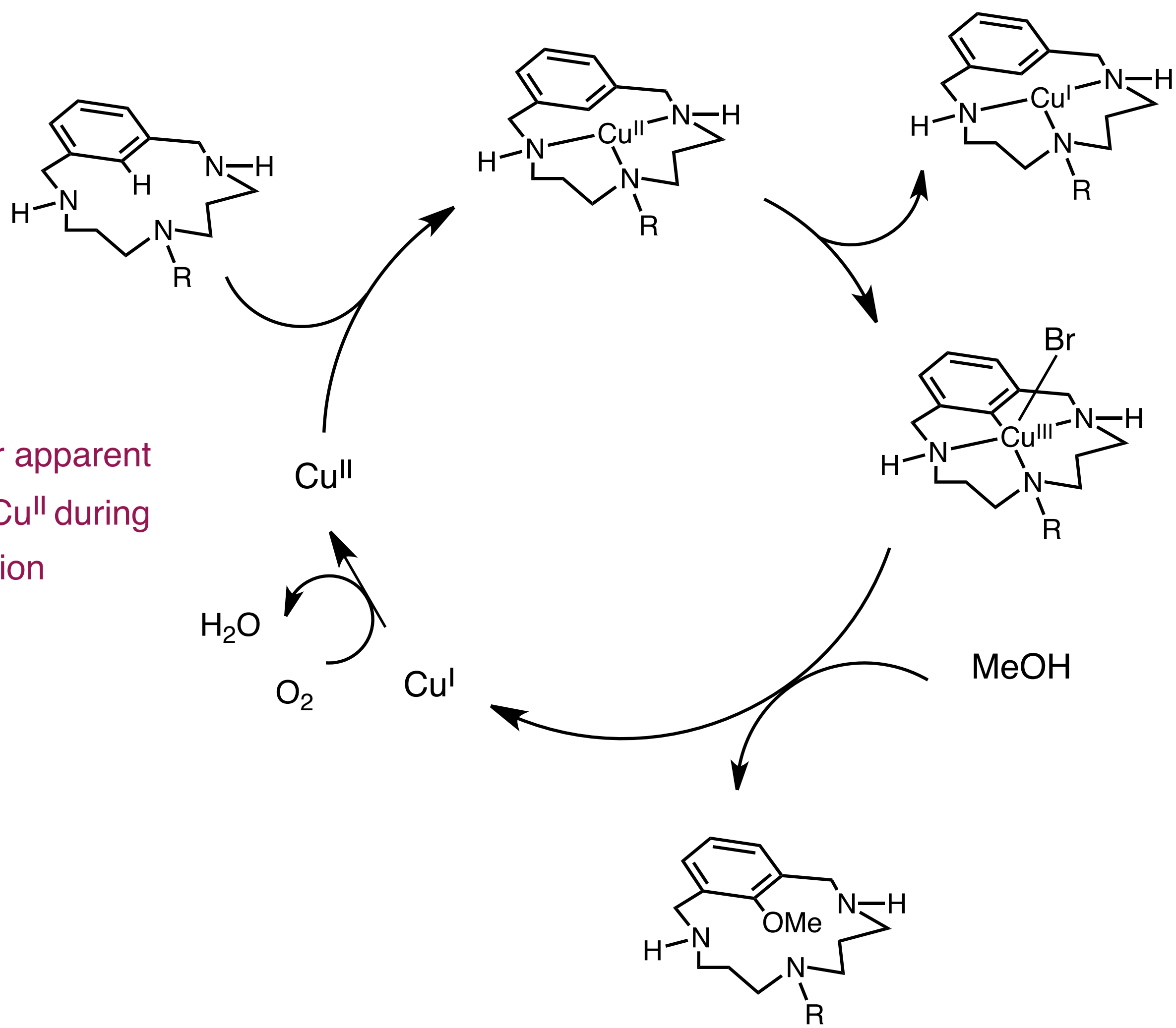

accounts for apparent build-up of Cu^{II} during reaction

King, A. E.; Huffman, L. M.; Casitas, A.; Costas, M.; Ribas, X.; Stahl, S. S. *J. Am Chem. Soc*, **2010**, 1147–1169

Copper in Cross-Coupling Reactions

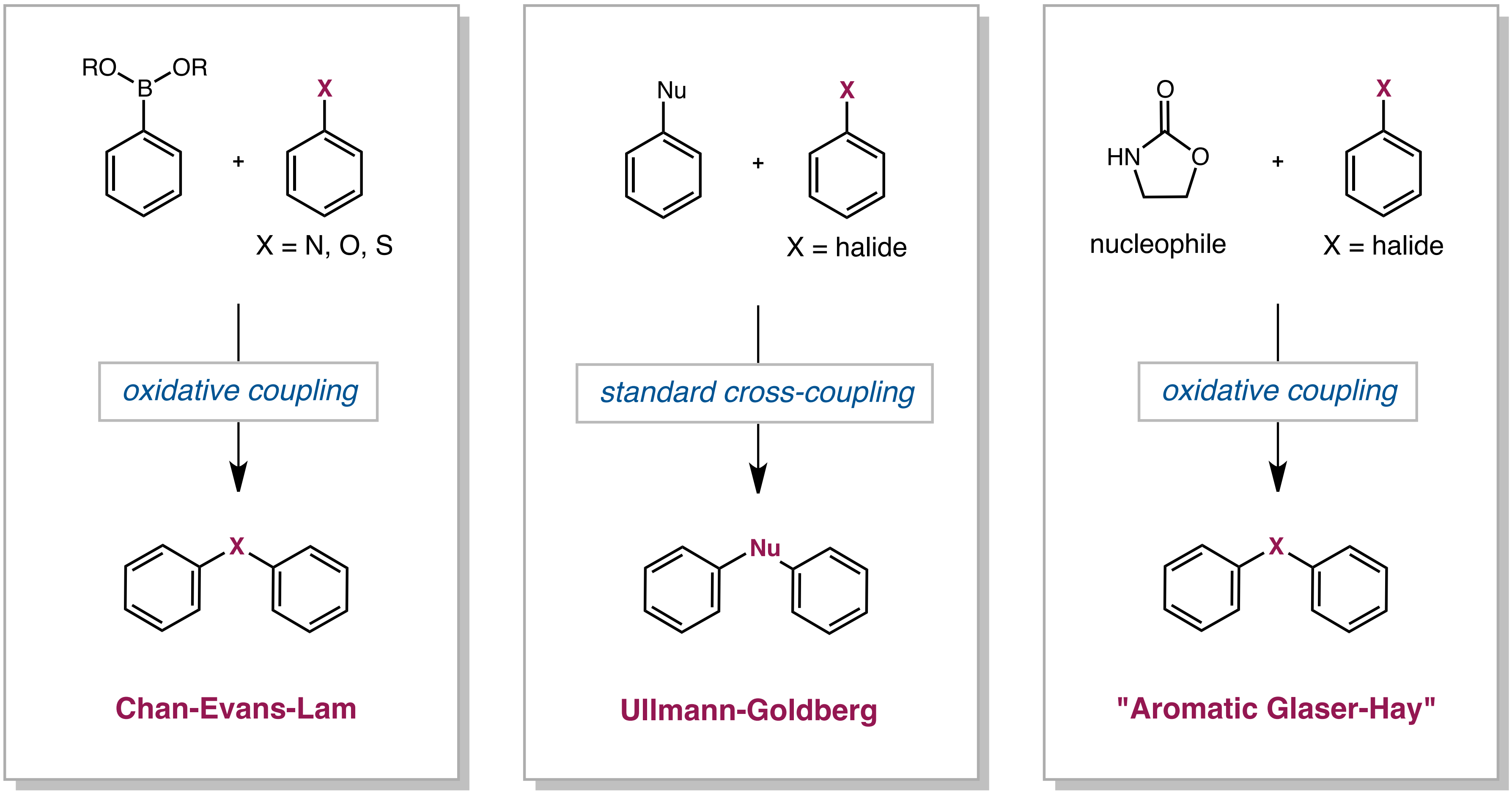

Copper in Cross-Coupling Reactions

pubs.acs.org/organometallics

NOVEMBER 26, 2012 VOL. 31 • ISSUE 22

ORGANOMETALLICS

ACS Publications
MOST TRUSTED. MOST CITED. MOST READ.

www.acs.org